DFO - Library / MPO - Bibliothèque
10028693

Dept. of Mines and Technical Surveys
LIBRARY
Date
Bedford Institute of Oceanography

CANADA

INSTITUT OCÉANOGRAPHIQUE DE BEDFORD

INSTITUTE OF OCEANOGRAPHY

DARTMOUTH, N. S.

A THREE COMPONENT THRUST ANEMOMETER FOR STUDIES OF VERTICAL TRANSPORTS ABOVE THE SEA SURFACE

by

L. A. E. Doe

REPORT B.I.O. 63-1

APRIL 1963

PROGRAMMED BY

THE CANADIAN COMMITTEE ON OCEANOGRAPHY

B E D F O R D I N S T I T U T E O F O C E A N O G R A P H Y

D A R T M O U T H, N. S. - C A N A D A

The material in this report was submitted as a dissertation in the Department of Meteorology and Oceanography of New York University.

This is a technical report to our Headquarters which has received only limited circulation. On citing this report in a bibliography, the title should be followed by the words "UNPUBLISHED MANUSCRIPT" which is in accordance with accepted bibliographic custom.

A THREE COMPONENT THRUST ANEMOMETER FOR STUDIES OF VERTICAL TRANSPORTS ABOVE THE SEA SURFACE

by

L. A. E. Doe

REPORT B.I.O. 63-1

APRIL 1963

CONTENTS

ABSTRACT

A THREE COMPONENT THRUST ANEMOMETER FOR STUDIES OF VERTICAL TRANSPORTS ABOVE THE SEA SURFACE

There is urgent need for good measurements of the energy exchanges across the sea surface, since these exchanges are among the principal factors in the dynamics of both the ocean and the atmosphere. The most direct means of determining the exchanges of momentum, heat, and water vapor at present is by the measurement of turbulent flux in the atmosphere, which involves correlating the vertical component of wind velocity with the variable in question. Modern high speed computers make the data processing relatively easy, leaving instrumentation as the primary requirement for good determinations.

The three component thrust anemometer measures the x, y, and z components of thrust exerted by the wind on a light spherical shell 3 inches (7.6 cm.) in diameter. The shell is made of styrofoam, 3/16 inch thick, and is densely perforated with holes 3/32 inch in diameter. Inside the shell are three transducers set orthogonally and attached to the shell by three pairs of flexible ties, so that each transducer responds to only one component of thrust on the sphere. Response is flat to at least 10 c.p.s.

The outputs of the three transducers are fed to three differential amplifiers which emit DC voltages proportional to the respective components of thrust. These voltages are applied to three voltage controlled oscillators whose outputs, which are on different frequency bands, are multiplexed and recorded on magnetic tape. Data processing starts with separating the three frequency

bands, demodulating each to obtain a DC voltage again proportional to one component of thrust, then digitizing these voltages and feeding the digital data to a computer. The computer derives the components of velocity corresponding to the three components of thrust, and may be programmed to operate upon these as required.

Calibration and verification tests in the laboratory, and with speed up to 20 m/sec. in a wind tunnel, indicate a response that is linear to applied thrust and to the square of wind speed. There is no critical wind speed within the range tested, but the noise level of the transverse components is somewhat higher at three m/sec. than at higher speeds. Also, there is a slight non-linearity in the resolution of small angles. It seems virtually certain, however, that both of these defects can be eliminated by more precise fabrication and assembly, and by modification of the shell.

A consideration of the errors introduced into the stress determination by an apparent mean vertical component of wind indicates that precise plumbing of the instrument is important, and derives a correction for the residual mean z component in any such stress measurement. Spectra and cross spectra computed from the data of a single field test made in a wind of 9.25 m/sec. at 2 m. height under strongly unstable conditions indicate a stress of 2.3 dynes, or a drag coefficient of .0022. The energy of each component and of the cospectrum decreased approximately according to n^{-2} at frequencies above about 2 c.p.s. Contribution to the stress ceased to be significant at about 5 c.p.s., corresponding to $nz/\bar{u} = 1.1$. At higher frequencies the indicated energy of the transverse components was greater than that of the axial component, but it

is doubtful if the data are good enough to consider quantitative ratios.

An interesting consequence of the quadratic response to wind speed is the theoretical possibility of measuring stress merely by integrating the z component of force on the sphere. This is limited as a practical technique, however, by the necessity for very precise erection of the instrument.

INTRODUCTION

The exchanges of energy between air and sea are major factors in the dynamics of both the ocean and the atmosphere. The ocean, in addition to its role as a moderator of climate, plays a part of major importance as the source of most of the water vapor and therefore of most of the fresh water in the world. The liberation of the latent heat of vaporization in turn is a principal source of energy in weather of all kinds, spectacularly released in thunderstorms, hurricanes and tornadoes. The influence of these exchanges on the ocean is equally profound, affecting to some degree every oceanographic parameter. The stress of the wind on the sea surface obviously causes waves and the wind driven circulation, but what about its role in the exchange of gases across the interface? It seems safe to guess that if all friction between the two media were to cease, aeration of the water would be drastically reduced and most of the ocean would become anaerobic through the decomposition of organic materials which in turn would cease in large part to be produced.* Evaporation is a sink for energy in the sea to the same extent that it is a source in the atmosphere. As such it is one of the principal terms in both the energy budget and the water budget, and therefore also one of the major factors in the thermohaline circulation.

---

*Shortly after these sentences were written, Dr. John Kanwisher, of Woods Hole Oceanographic Institution, told the writer that he has recently completed a series of observations which indicate that the rate of exchange of gases across the liquid-air interface is approximately proportional to the square of wind speed.

In view of the general recognition which statements such as these have received, it seems remarkable that more effort has not been devoted to the direct study of the exchange processes and the measurement of the quantities exchanged, even when due allowance is made for the difficulties involved.

Measurements of the vertical transports of heat, water vapor, and momentum in the atmosphere over land have received increasing attention in recent years. While the major efforts have been by meteorologists, the results are of direct interest to microclimatologists, glaciologists, engineers, in fact to all who are concerned with either the transfer of these quantities across the interface or their dissipation in the atmosphere. Observations of this type over the land are usually accepted to be the most satisfactory means of measuring the rates of transfer across the surface beneath, although other more direct measures may be feasible in some cases. Such direct measures would include the determination of stress by the measurement of thrust on a suitable plate (Vehrencamp, 1952), the determination of evaporation by measuring the loss of weight of a container of earth suitably vegetated (Mather, 1954), the determination of heat loss by suitable soil thermometry (Portman, 1957), and so on.

Over the oceans, however, such direct approaches are usually not feasible, and the most practical way of measuring exchanges across the sea surface is through the vertical transports in the atmosphere near the surface. There is no doubt that the reason why these measurements have received less attention than their counterparts over the land is simply a matter of the relative efforts involved.

Of the two general procedures that have been used, the profile method has the advantage, usually, of simpler instrumentation and easier computation, and the disadvantage of being an indirect measurement, based upon assumed mixing processes. The turbulent flux method, on the other hand, has the advantage of being a direct measure of transport, and the disadvantage of involving more exacting instrumentation and the manipulation of great quantities of data. With the advent of modern electronic computers and recording techniques, data processing has become relatively easy, leaving instrumentation as the first requirement for good vertical transport determinations by the turbulent flux method.

For this purpose we need the horizontal and vertical components of "instantaneous" wind velocity, usually defined in terms of a coordinate system with the x axis horizontal and pointed in the mean wind direction, the y axis horizontal and transverse to the wind, and the z axis vertical. Then, in the usual notation, ρuw is the instantaneous rate at which horizontal momentum, ρu, is being moved vertically across a unit section of the horizontal plane through the point of observation. The net transport of momentum in time T will be given by $\int_0^T \rho uw.dt$ and the average rate of transport by $\frac{1}{T}\int_0^T \rho uw.dt$ or $\overline{\rho uw}$. If ρ be treated as a constant this can be written $\rho\overline{uw}$.

Now,

$u = \bar{u} + u'$ and

$w = \bar{w} + w'$, so that

$$\rho\overline{uw} = \rho(\bar{u}\bar{w} + \bar{u}\overline{w'} + \overline{u'}\bar{w} + \overline{u'w'})$$

$$= \rho\bar{u}\bar{w} + \rho\overline{u'w'}$$

since $\overline{u'}$ and $\overline{w'}$ are zero by definition. The first of the remaining terms, $\rho \bar{u} \bar{w}$ is the vertical transport of horizontal momentum by the mean vertical component of motion, which Swinbank (1951) for example has called the vertical mass transfer of momentum. The other term, $\rho \overline{u'w'}$, is the Reynolds stress, or the vertical transport of momentum by the turbulent fluctuations of velocity, which can be written equivalently as $\rho \overline{(u-\bar{u})(w-\bar{w})}$.

In the computation of the stress, therefore, either we may first obtain $u' = u - \bar{u}$ and $w' = w - \bar{w}$, and then multiply and integrate to get $\overline{u'w'}$, or we may multiply uw directly, integrate to get $\overline{uw}$, and then subtract $\bar{u}.\bar{w}$. In theory at least, $\overline{u'w'}$ can also be simply equated with $\overline{uw}$ if $\bar{w}$ can be made precisely zero. In practice, however, this last is usually not feasible since even a very slight error in plumbing the instrument or establishing a reference vertical will introduce an apparent $\bar{w}$ which, when multiplied by $\bar{u}$, will mask the relatively small stress term. In the usual case, therefore, it is necessary to determine $\bar{u}$ and $\bar{w}$ and to eliminate the term due to vertical mass transport, either real or apparent. This is an integral part of the computation which will be done by the electronic computer.

The procedure which at present appears most promising for handling data such as these is the computation of the spectra and cross spectra of the three components of velocity. In general terms this yields the contributions to the variance of an individual component, or to the covariance of two components, by turbulent

elements whose "frequencies" or "wave lengths" occur within predetermined bands. The result is a set of spectra and cross spectra showing the energies of turbulent motion as functions of frequency (or wave length, according to the presentation.) This form of computing and presenting results is in general use at the present time (see, for example, Panofsky and Deland, 1959; Cramer et al, 1962, etc.), and is the most complete and adequate method currently available for studying the statistical properties of the turbulence, as well as evaluating the vertical transport. It is also an excellent example of the sort of analysis that could be undertaken only in virtually token amounts before the advent of modern computers, but which can now be handled with relative ease.

In deriving the spectra the computer will normally obtain first the mean of each variable over the sampling interval, then the turbulent fluctuations about the mean, and finally the spectra and cross spectra of these fluctuations. This procedure automatically eliminates the effect of any real or apparent net value of the vertical component $\overline{w}$, but it does not remove the error in the stress term itself introduced by faulty alignment of the instrument. This will be shown more explicitly with reference to the present instrument in the section FIELD TEST AND COMPUTED RESULTS. Bunker (1955), using data obtained with an airplane, has found it desirable to define his turbulent fluctuations with reference to a regression line rather than a single mean value. He thus eliminates "trends", or in other words periods (or wave lengths) significantly greater than the duration (or track length) of the sample. This is analogous, for example, to subtracting the variation of sea level due to tide

from a record of surface waves. The desirability of using such a technique would appear to depend upon the length of interval which shall define the mean condition, as compared with the length of sample to be analyzed. This in turn should presumably depend upon the scale of the largest turbulent element which contributes significantly to the phenomenon under investigation - in this case the vertical transport of momentum. The decision whether to use a trend line or a single mean for the definition of turbulent fluctuations therefore would depend upon the particular case to be studied. The trend line was not used in the example which will be considered later in this paper.

The three-component thrust anemometer to be described here is an attempted solution of the requirement for a simple, reliable device of fast response to measure the turbulent fluctuations of wind velocity. The main requirements for such an instrument are that:

(1) its operational range include all the velocities that it is required to measure, and its sensitivity and signal to noise ratio be sufficient to distinguish turbulent fluctuations of small amplitude;

(2) there be a consistent one-to-one relation between velocity and response;

(3) the sensing head be small compared to any turbulent element which it is to measure, so that it may respond virtually to the velocity at a "point";

(4) its total bulk not interfere significantly with the air flow, so that it may respond essentially to the velocity which

would occur if the instrument were not there; and

(5) its time of response should be short enough to observe all spectral components which contribute significantly to the transport.

Much of the work that has been done over land has been with instruments whose linear dimensions and time constants were of the order of one foot (25 cm) and one second, respectively (for example, Deland and Panofsky, 1957; Cramer, Record and Tillman, 1962). These dimensions and times appear adequate for work on towers at heights of twenty, or perhaps ten, metres or more as will be shown below, but at heights of the order of one or two metres a time constant of the order of 0.1 second is required. Working at low levels is particularly desirable over the ocean at low wind speeds both because of the difficulty of building a floating support which extends to great heights and yet is steady enough for this type of observation and because of the need to understand more fully the effects of the moving sea surface on the motions and fluxes in the atmosphere directly above it. For work at higher wind speed, of course, the required height will be greater to avoid the zone of splash and spray.

Hot wire anemometry is perhaps the most promising technique for measuring turbulent fluctuations of wind velocity over the land, and may prove to be equally useful over the sea. It remains to be proved, however, that the impingement of hydroscopic nuclei with their associated water will not cause significant errors in the apparent velocity when operating near the sea surface. The finer the wire, the more efficient it is as a collector of minute

aerosol droplets. Bivanes involve a different set of problems, including the spacial separation of speed and direction sensors, and the necessity of compromising between small size to minimize the scale and time constant, adequate damping to prevent flutter, and the development of sufficient torque to actuate the indicating mechanism. Moreover, with a bivane one still has the problem of measuring speed changes with a sufficiently short time constant, which involves the use of hot wires or some other device of small size and fast response. Therefore, while any one of these or other familiar devices may be adaptable for the turbulent flux measurements over the sea, it seemed worth while to try to develop an entirely new type of instrument with the necessary small size and speed of response which would measure the magnitude and direction of the wind vector with a single sensing head.*

---

*The general principle of the present instrument was worked out in 1957, and some preliminary designs were tested during the following two years using RCA type 5734 mechanoelectronic transducers. Systematic development and design work, however, were begun again in 1960 at the Woods Hole Oceanographic Institution using differential transformers as transducers. In 1961, when wind tunnel tests were started, a paper was brought to the writer's attention which described a similar type of instrument that had been built and tested by Glyndon L. Lynde and Francis W. Stapor as a thesis project for the degree of Master of Science at Massachusetts Institute of Technology in 1952. Their instrument employed a system of internal linkages somewhat similar to the one to be described in the present paper, but used strain gauges instead of differential transformers as the transducers. Their sphere was of smooth plastic, nine inches in diameter, and weighing approximately 220 grams, as compared with a perforated rough sphere, three inches in diameter and weighing approximately 12 grams in the present instrument. For reasons that will be apparent, their instrument in that form could not have fulfilled the requirements for a study of turbulent flux in the atmosphere, but it did serve to show that the system of internal linkages was a practical way to resolve an applied force into three orthogonal components.

In principle the three component thrust anemometer consists of a light spherical shell three inches (7.5 cm.) in diameter which is exposed to the wind (Figure 1) and a system of transducers which measures the thrust of the wind on the sphere.

Three transducers are mounted orthogonally on a rigid frame inside the sphere (Figure 3). The frame is supported by radial wires which pass through holes in the shell without touching it and attach to an outer support ring, like the spokes of a wheel. These wires also serve as electrical leads to the transducers. The spherical shell is linked to the transducers in such a way that any force impressed upon it is resolved into three components in the directions of the axes of the transducers. The instrument will usually be set with the support ring normal to the mean wind direction so that the x, y and z axes will be oriented in the conventional manner in relation to the wind. The outputs of the three transducers will then be the components of the thrust of the wind on the sphere resolved along these three axes.

(Cont'd) In 1962 the writer was introduced to another instrument of the same general type recently developed by Flow Corporation of Cambridge, Massachusetts. This one uses a metal sphere twelve inches in diameter with a "tripping" wire welded to its surface in a scroll-like pattern to ensure turbulence in the boundary layer. This anemometer uses a somewhat different system of linkages to resolve the thrust into three components, and is intended primarily for use at high speeds (up to one hundred miles per hour). The designers had not, however, eliminated the very high "noise level" in the transverse components due to the detachment of eddies in the wake, which, with its large size makes it rather unsuitable for the type of work envisaged here. With these exceptions, however, it appeared to be a well designed rugged device, which may lend itself readily to modification for this purpose.

The outputs of the three transducers are suitably amplified and rectified and fed to three voltage controlled oscillators whose outputs in turn are multiplexed and recorded on magnetic tape. Data processing in the laboratory is intended to start with the playing of the tape on the ADDReSOR system of the Woods Hole Oceanographic Institution (Ketchum and Stevens, 1962) or an equivalent device. This system separates the three frequency bands of the record, samples each at selected intervals, digitizes the sample according to its position in its own frequency band, and feeds the resulting data directly to a digital computer which can be programmed to compute the velocity components and operate on these as required.

The mechanical time constant of the sphere and transducer system, undamped, is of the order of .003 second, obtained from the free period of vibration which is approximately 0.013 second. The filter system of the ADDReSOR through which the data are passed while sampling and digitizing, however, has a cut-off at ten cycles per second, corresponding to a period of 0.1 second and a time constant of approximately 0.025 second, and this is therefore the effective time constant of the system as a whole.

Priestley (1959) has summarized the results of data obtained by various investigators and shows that the highest non-dimensional frequency, $nz/\bar{u}$, which contributes significantly to vertical fluxes is in the vicinity of 0.6 to 1.2. The response of our instrument should be at least fast enough to observe such frequencies, and preferably significantly faster.

Table 1 lists the maximum values of n which satisfy the relation

$$nz/\bar{u} = 1.2 \quad \text{or} \quad n = 1.2\bar{u}/z \qquad (1)$$

for various z and u. Values below the line are all = 10 per second and are therefore within the capabilities of the instrument and data processing system combined. At a height of two metres, for example, the relation is satisfied up to a speed of the order of 16 metres per second, obviously a greater wind speed than can be observed at this height under open sea conditions. The response time of the system as a whole is therefore adequate for studies of vertical transports over the sea, and that of the sensing head is significantly faster than adequate.

TABLE 1

Values of n at various $\bar{u}$ and z, where

$nz/\bar{u} = 1.2$

Z(m)	$\bar{u}$ (m/s) 1	2	5	10	15	20	30
1	1.2	2.4	6.0	12	18	24	36
2	.6	1.2	3.0	6	9	12	18
3	.4	.8	2.0	4	6	6.7	10
4	.3	.6	1.5	3	4.5	5	7.5
5	.2	.5	1	2	3	4	6
10	.1	.2	.5	1	1.5	2	3
20	.05	.1	.2	.5	.8	1	1.5

The linear dimensions of a turbulent element of "frequency" n must be of the order of $\bar{u}/n$, which by (1) is equal to or greater than $z/1.2$. At a height of two metres this would be at least 160 centimetres, or a good order of magnitude greater than the diameter of the sphere. It is therefore reasonable to assume that the instrument is small enough to observe the full range of frequencies which contribute significantly to vertical transports at all heights at which it is feasible to work over the sea surface.

The three component thrust anemometer, therefore, reasonably satisfies the requirements for size and speed of response. The remainder of the paper will deal with the details of its construction and functioning, and attempt to evaluate its fidelity as a means of observing the three components of the wind vector.

DESCRIPTION OF THE INSTRUMENT

Inside the Sphere

The framework inside the sphere is intended to be motionless and is supported on eight phosphor-bronze wires .020 inches (0.51 cm.) in diameter which pass through the sphere at the equator, where the two hemispheres are joined, and attach to the outer support ring. The inner structure is built up on the segments of three circles (A, B, and C in Figure 2) which are joined orthogonally and which support the three transducers. These circles are positioned so that the proximal face of each one is displaced 0.156 inches (0.40 cm.) from the center of the sphere. A mounting beam, D, is fastened to each with machine screws and serves as a support for the sliding base, E. A formica block, F, is fastened to the sliding base with machine screws and epoxy resin, and the differential transformer, G, is clamped in the formica block. The Springs, H, are cantilevered upwards from the mounting beam where they are secured in the notches at each end by means of clamping bits, J. The clamping bits are secured by screws which pass through the springs into the ends of the mounting beam. The upper ends of the springs are gripped in clamps, K, which are threaded onto the tie rod, L, and tightened with nuts. The core, M, of the differential transformer is threaded and screws onto the tie rod, which passes through the bore of the transformer to form the fourth side of the spring parallelogram. Any force applied to the clamps which has a component parallel to the tie rod will result in a displacement of the core of the transformer and a corresponding voltage output.

A transducer unit of this type is assembled for each of the three components, and the three are carefully fitted together and joined with machine screws. The axes of the three tie rods are then orthogonal to one another and each passes the center of the sphere at a distance of 0.125 inches (0.32 cm.).

Surrounding this assembly are three great circles of polyvinyl chloride (PVC) with an outer diameter of 2.625 inches (6.7 cm.), a width of 0.187 inches (0.48 cm.) and a thickness of 0.040 inches (0.10 cm.). These are set orthogonally and positioned so that opposite points of intersection are colinear with the three diameters of the sphere that are respectively parallel to the three tie rods. Three pairs of flexible ties, P, which lie on these diameters, connect the PVC rings to the clamps. Each tie is a piece of phosphor-bronze wire .008 inches (0.02 cm.) in diameter, and 0.28 inches (0.71 cm.) long, and is fastened to the clamps and to the studs, Q, with soft solder.

The radial wires, R, which support the assembly attach at the inner end to terminal strips mounted on the inside of the collar, S, (Figure 3). The collar slips over ring C and is secured in place with three screws. The terminal strips are secured in place with epoxy resin which also serves as insulation. The radial wires pass through eight holes in the collar spaced at intervals of 45 degrees and through smaller holes in the terminal strips. Their inner ends are bent and soldered to the terminal strips, which serve as connectors with the leads to the three differential transformers. Four holes in the collar allow for the passage of the flexible ties of the y and z components.

Each of the differential transformers has six leads: two for the primary and two for each half of the secondary. These are led to binding posts located on each side of the formica block, F (Figure 2). The two centre leads of the secondary are joined, and the other two are connected to two of the radial wires at the terminal strips on the inside of the collar. The secondaries of the three transducers are thus connected to six of the radial wires. The three primaries are connected in series between the remaining two.

Outside the Sphere

At the outer end, the radial wires go to small ceramic insulators, d, on bolts which pass through the support ring, e. Soldered connections are made at these points to the leads from the excitation oscillator and the amplifiers.

The support ring is of 3/8 inch steel and is one foot (30 cm.) in diameter. It is stiffened by two orthogonal semi-circles which are welded together to form a dish, U. In use, the dish stands on edge with the plane of the support ring perpendicular to the wind; the sensing head is in the center of the ring looking rather like a large white spider in the center of its web. A coupling, V, is welded to the lower side of the ring to receive the upper end of the mounting stem, while a second coupling, v, at the intersection of the two semi-circles behind the ring serves as an alternative mounting which is used in calibration and testing. Also incorporated for the purpose of testing is a universal joint, W, in the stem. This was to allow the instrument to be tilted at arbitrary angles in relation to the wind in order to test its resolution of the thrust vector. In

normal field use it will be clamped at zero angle. The mounting stem also incorporates a sleeve, f, which fits over the spindle, a, on top of the base. The sleeve, and with it the entire sensing head, can be rotated about the vertical axis of the spindle, its angle of orientation indicated by a pointer and an azimuth ring. This also was arranged primarily for use in the wind tunnel, but may be useful in the field for pointing the instrument towards the wind.

To prevent the sphere and internal assembly from being set in vibration by the wind - the spider bounding on its web - a tie-back rod is passed through one of the holes in the shell and connects mounting ring A (Figure 2) to the piston of a small dashpot mounted on the dish at the rear. In the absence of the tie-back, resonant vibrations may be set up under some wind conditions, which can cause extraneous signals to appear because of the inertia of the shell and associated moving parts.

Electrical System

The schematic arrangement of the electrical system is shown in Figure 4. The primaries of the three differential transformers are connected in series and excited by an excitation oscillator whose output is approximately 20 volts at 2700 cycles per second. A variable resistor in series with the three transformers reduces the total EMF across the three primaries to 9 volts, RMS, or 3 volts across each.

The output from the secondary winding of each differential transformer is fed to the input of a differntial amplifier which amplifies, phase detects, and rectifies the signal yielding an output on the range -2.5 to +2.5 volts D.C. An adjustable D.C.

voltage is then added to bring it to the range 0 to +5 volts. An adjustable A.C. voltage either in phase or 180 degrees out of phase with the output of the differential transformer is added at the input of the amplifier to enable a continuous selection of zero point over the linear range of the amplifier. The output of the three amplifiers is fed to three VCO's (voltage controlled oscillators) which operate on three IRIG (Intermediate Range Instrumentation Group) frequency bands. Since these bands do not overlap, they may be multiplexed and recorded on a single channel of magnetic tape. The output of a crystal controlled reference oscillator with a frequency of 14.5 kilocycles is also multiplexed with the three data frequencies and serves as a control of the tape speed when the data are being analyzed. Circuit diagrams of the two oscillators are shown in Figure 5. Figure 6 is a wiring diagram of the chassis which contains all the units shown in Figure 4 with the exception of the transducers and the tape recorder.

Figure 7 shows the circuitry of one component in greater detail. The amplifier, which is fully transistorized, consists of two cascaded D.C. operational amplifiers feeding a phase sensitive demodulator. The first amplifier has a differential input and a high common mode rejection. Its gain is fixed at 20 by the feedback loop. The feedback resistor of the booster amplifier can be selected by means of the gain switch to give a nominal gain of 5, 10, 25 or 50. Since the ratios of these values are precisely fixed, calibration in terms of any one is validated for any other simply by use of the appropriate

gain ratio. Fine adjustment of booster gain is accomplished by varying the coupling resistor with the Gain Adjust control. The gain of the two amplifiers in series is the product of their individual gains.

The output of the phase sensitive demodulator is a DC voltage proportional to the AC voltage input. Its polarity will be positive if the signal voltage and the excitation voltage are of the same phase, and negative if they are of opposite phase. The overall gain from RMS input to DC output is approximately 1800 when adjusted to maximum sensitivity.

DC Biassing Circuit

The "DC output bias" of 2.5 volts, which is added to the output of the amplifier to bring it to the range of 0.0 to 5.0 volts to match the input of the VCO, is obtained by floating the demodulator circuit on a zener-regulated voltage divider connected across the +15 and -15 volt leads from the power supply (Figure 7). The bias is adjustable over a range of approximately -3.2 to +3.2 volts, but for the present application will always be set at +2.5 volts.

AC Biassing Circuit

It usually is not feasible to set the zero point of the instrument precisely by moving the differential transformer in relation to the core. In practice it has been found preferable to make an approximate setting by this means before assembling the spherical shell, and then to make the final adjustment by means of an AC biassing circuit when the instrument is fully assembled and mounted ready to begin a set of measurements.

The primary of an audio transformer is excited by the excitation oscillator, and its secondary is connected in series with the secondary of the differential transformer (Figure 6). The two outputs will therefore be either in phase or 180 degrees out of phase according to the polarity of their connections. The output of the biassing transformer, which can be varied by means of a trim potentiometer in the primary circuit, can therefore be either added to or subtracted from that of the transducer to allow the zero point to be set anywhere on the range of the amplifier input. In practice the zero point of the x component will be set at the lower edge of the amplifier range, while those of the y and z components will be set at the center to admit of both positive and negative deviations.

Calibration Circuit

A calibration voltage is obtained from a 100 ohm potentiometer in series with a 100,000 ohm resistor across the output of the excitation oscillator (Figure 6) and is therefore precisely in phase with the excitation voltage of the differential transformers and the reference supplied to the demodulator circuit. Once the potentiometer is set, the value of the calibration voltage will be proportional to the excitation of the transducers. A three position switch applies this calibration signal to either side of the amplifier input or shorts both sides to ground. With the DC output bias set at +2.5 volts and the amplifier set to maximum gain (gain position 1), the three positions of the switch will yield outputs of 0.0, 2.5, and 5.0 volts respectively. Any change

in excitation voltage, amplifier gain, or DC bias will be indicated by a change of one or more of these outputs. If the VCO is correctly adjusted, its corresponding output frequencies will be at the lower band edge, band center, and upper band edge, respectively. The calibration circuit therefore provides a convenient means of checking the performance of the entire electrical system, exclusive of the transducers, with a single test. Moreover, since the sensitivity of the transducers is practically proportional to primary voltage, unless large temperature changes occur, the calibration check in effect also tests the sensitivity of the instrument as a whole. In order to eliminate temperature effects a constant current excitation oscillator would be preferable to the present constant voltage unit. However, during any one series of measurements, occupying perhaps an hour, temperature changes should be negligible, so that the only appreciable error introduced in this way would be a slight change in sensitivity between runs at different ambient temperatures. This can presumably be corrected by the use of a suitable temperature factor, which has not yet been determined.

MECHANICAL DESIGN CONSIDERATIONS

Sources of Error

In order that each of the three transducers measure accurately the component of thrust parallel to its own axis, it is essential that extraneous contributions to the signal be avoided. Among the possible sources of error must be included:

(a) friction

(b) hysteresis

(c) mechanical, electrical, and magnetic cross-coupling between components

(d) torque

These will be considered in turn.

(a) Friction should not be a problem since there are no sliding or rolling contacts in the system. The only contacts between the moving and fixed members are through the springs and flexible ties, and through the fluid in the dashpots. The one exception is the possible slipping between the great circles and the sytrofoam hemispheres if the instrument is struck or vigorously shaken. This can cause a shift of the order of one or two per cent of full range on minimum sensitivity, but has not been found to be a problem under normal operating conditions with a reasonably secure mounting.

(b) Hysteresis will be discussed under the heading of Springs. It is negligible under normal operating conditions.

(c) Mechanical cross-coupling between the three components under static loads is not expected to be a problem,

and this is confirmed with certain reservations by the results of calibration and verification tests. Since the springs are wide (.250 in., or .635 cm.) relative to their thickness (.002 in., or .005 cm.), each pair can flex only in the direction of the axis of its transducer, and can therefore only respond to a component of thrust in this direction. Since the flexible ties are symmetrically disposed, any component of thrust transverse to this axis will be transmitted equally in opposite directions to both ends of the parallelogram and will thus be cancelled. In order for this to hold in practice it is essential that both the flexible ties of a given pair be of the same rigidity and that the three pairs be colinear with orthogonal diameters of the spheres.

Electrical and magnetic cross-coupling between the transducers could conceivably arise due to the fact that the primaries of the three differential transformers are connected in series, and because of the close proximity of the three units. Evidently, however, the changes in apparent load in the excitation circuit due to movement of the cores is entirely negligible, so that the displacement of one transducer does not alter the response of the other two. Evidently, also, the magnetic shielding is sufficient to prevent significant distortions of each magnetic field by the other two.

Adequate proof that cross-coupling due to any factors, mechanical or electrical, is not a significant source of error is seen in the accuracy with which the instrument resolves thrusts into their three components. This is discussed under the heading MECHANICAL AND ELECTRICAL VERIFICATION.

(d) Torsional effects will not be a problem if all the previous design criteria have been satisfied and provided that the spring action of the flexible ties be a linear function of displacement. This last consideration is a reasonable expectation since each tie is rigidly attached at one end to a clamp and at the other end to the PVC great circles, and therefore will flex in the same manner as the springs except that there will be no constraint on the direction of flexing. For this purpose the PVC great circles can be considered rigid since their dimensions are large (0.40 in. thick by .188 in. wide) compared to those of the flexible ties (.008 in. diameter). Their rigidity is increased by their combination as orthogonal great circles.

Under these conditions it can be shown that the addition of a torque will not influence the output of any transducer. For simplicity of illustration a two-dimensional case will be developed first, then the result extended to three dimensions. In Figure 8 the four springs of the x and y components are designated x_1, x_2, y_1, y_2. Fx and Fy are the components of thrust, and τ is the applied torque. Let δx and δy represent the displacements of the x and y transducers, αx_1, αx_2, αy_1, αy_2 be the respective linear displacements measured counterclockwise of the points of attachment of the flexible ties to the great circles, and α_τ be the displacement in all the ties produced by a pure torque τ. Then it follows from the geometry of the system that

$$\alpha x_1 = \alpha_\tau - \delta y \qquad \alpha y_1 = \alpha_\tau + \delta x$$

$$\alpha x_2 = \alpha_\tau + \delta y \qquad \alpha y_2 = \alpha_\tau - \delta x$$

and from its mechanical functioning that

$$Fx = Cx\,\delta x + C_\tau\,(\alpha y_1 - \alpha y_2)$$

$$Fy = Cy\,\delta y + C_\tau\,(\alpha x_2 - \alpha x_1)$$

where Cx and Cy are the force constants of the x and y transducers, and C_τ is the force constant of each flexible tie. Combining the above equations, $Fx = Cx\,\delta x + 2C_\tau\,\delta x$

or $$\delta x = \frac{Fx}{Cx + 2C_\tau}$$

and similarly $$\delta y = \frac{Fy}{Cy + 2C_\tau}$$

These results are independent of τ and α_τ, and are precisely the response of a two-component system in the absence of torque where the force constants of the x and y components are respectively $Cx + 2C_\tau$ and $Cy + 2C_\tau$.

In the three-dimensional system the same nomenclature will be followed, with the additional notation that τx will be the component of torque about the x-axis, $\alpha y_{1,z}$ will be the component of αy_1 about the z-axis, and so on for the three axes and six flexible ties.

Then

$$Fx = \delta x\,Cx + C_\tau(\alpha y_{1,z} - \alpha y_2 z + \alpha z_2 y - \alpha z_1 y)$$
$$Fy = \delta y\,Cy + C_\tau(\alpha z_1 x - \alpha z_2 x + \alpha x_2 z - \alpha x_1 z)$$
$$Fz = \delta z\,Cz + C_\tau(\alpha x_1 y - \alpha x_2 y + \alpha y\ x - \alpha y\ x)$$

$$\alpha y_1 z = \alpha_\tau z + \delta x \qquad \alpha y_2 z = \alpha_\tau z - \delta x$$
$$\alpha y_1 x = \alpha_\tau x - \delta z \qquad \alpha y_2 x = \alpha_\tau x + \delta z$$
$$\alpha z_1 x = \alpha_\tau x + \delta y \qquad \alpha z_2 x = \alpha_\tau x - \delta y$$
$$\alpha z_1 y = \alpha_\tau y - \delta x \qquad \alpha z_2 y = \alpha_\tau y + \delta x$$
$$\alpha x_1 y = \alpha_\tau y + \delta z \qquad \alpha x_2 y = \alpha_\tau y - \delta z$$
$$\alpha x_1 z = \alpha_\tau z - \delta y \qquad \alpha x_2 z = \alpha_\tau z + \delta y$$

Combining these equations as in the two-dimensional case yields the immediate result that

$$\delta x = \frac{Fx}{Cx + 4C\tau}$$

$$\delta y = \frac{Fy}{Cy + 4C\tau}$$

$$\delta z = \frac{Fz}{Cz + 4C\tau}$$

The effective spring constant for each component is therefore that of its own transducer plus that of four of the flexible ties, and is independent of torque. Provided that the linear range of none of these is exceeded, the output of each transducer should be a linear function of one component of thrust alone.

It was originally assumed in designing the instrument that the optimum flexible tie would be one that was capable of transmitting axial forces only, with no rigidity offered to transverse deflections. The preceeding discussion shows that this condition is not necessary. On the contrary, some rigidity in the flexible ties is desirable to provide a restoring force when torsional forces cause the sphere to rotate slightly, since otherwise the radial wires would touch the sides of the holes where they pass through the PVC great circles and the styrofoam shell. Because of the high sensitivity and minute forces involved at low wind speeds, the friction arising from such contacts in the absence of an adequate restoring force might be a significant source of error.

Springs

The two main requirements for the springs are: first, that the elasticity be independent of temperature and constant over the range of operation, and, second, that there be minimal shift

of the zero point due to either hysteresis or slipping in the clamps. After considerable experimenting these problems were discussed with engineers of the Associated Spring Corporation who suggested the procedures which were finally adopted. They also very kindly supplied a sufficient quantity of heat-treated NiSpan-C, a constant modulus alloy of very low hysteresis.

The springs were cut to the required dimensions, then the end sections, where they were to be clamped, were coated with a solution of asphalt in benzine, which evaporated leaving a covering of asphalt on the metal. The whole spring was then immersed in a solution of hydrochloric and nitric acid and the center section etched out to the required thickness. Since the stiffness of a spring is proportional to the cube of its thickness, this procedure ensures that the flexing will take place in the center portion away from the vicinity of the clamps where slipping might occur. The springs are 0.25 inches (0.635 cm.) wide and are made from stock 0.012 inches (0.30 cm.) thick. The etched center section is approximately .25 inches (.635 cm.) long by .002 inches (0.005 cm.) thick (Figure 9).

Etching produced a physically roughened surface, but this fact does not seem to have interfered in any way with the efficiency of the springs. Each transducer unit, which comprises a differential transformer and its spring parallelogram, was tested for hysteresis before being assembled into the sensing head. The test consisted of observing the difference in zero point to which the unit returned after displacement on opposite sides of the relaxed position. All measurements were made with a voltmeter on the output

of the amplifier. Hysteresis was found to be approximately 0.1 per cent of the range of deflection, which is essentially the order of precision of the voltmeter used. A similar test applied to the sphere as a whole after assembling yielded a hysteresis of approximately 0.5 per cent. The difference is probably due to minute deformations and possibly slipping in the PVC great circles and the styrofoam hemispheres, as well as to hysteresis in the flexible ties which are of phosphor-bronze wire with soldered connections at both ends. It will be shown that the flexible ties contribute approximately one third of the total spring constant of each component, and they should therefore receive the same careful treatment in preparation and assembly that the springs were given. This will be done in any future models of the instrument.

Spring Constants

The values of the spring constants Cs, Cy, Cz and C_τ can be computed approximately from the dimensions of the parts. For this purpose Cx, Cy and Cz will be assumed to be equal, as they theoretically would be if the springs had all been etched to precisely the same degree.

If a transverse force is applied to the end of a simple cantilevered spring (Figure 10a), the resulting deflection is given by the relation

$$d = \frac{W L^3}{3 q I}$$ where

d = deflection of the free end of the spring

L = length of the spring

I = moment of inertia of the area of cross-section of the spring about an axis on the neutral surface, normal to the plane of flexing

q = Young's modulus

W = the applied force

In the case of a spring of length 2L clamped at both ends in a "parallelogram" arrangement (Figure 10b), symmetry indicates that an inflection will occur at the center, that is, at a distance L from each end. The stress at this point must therefore be the same as at the end of the simple cantilever of length L, and each half will experience a deflection, d, relative to its own original axis. The total deflection of the moving end where W acts will be 2d. Since each transducer unit has two such springs, as in Figure 10c, the force applied to each will be effectively W/2, producing a deflection

$$d = 2\,\frac{(W/2)L^3}{3qI} = \frac{WL^3}{3qI}$$

which is the same as for a single simple cantilever.

The properties and approximate dimensions of the springs are:

2L = length of flexing portion = .22 in. (.55 cm.)

a = width = .250 in. (.635 cm.)

b = thickness = .0020 in. (.00508 cm.)

q = Young's modulus of Nispan-C = 27.5×10^6 pds./sq. in.
= 19×10^{11} dynes/sq.cm.

$I = ab^3/12 = 6.95 \times 10^{-9}$ cm^4.

Therefore the deflection per unit of force should be

$$\frac{L^3}{3qI} = \frac{0.275^3}{3 \times 19 \times 6.95 \times 10^2}$$

$$= 5.26 \times 10^{-7} \text{ cm/dyne},$$

and the force constant of the spring parallelogram will be

$$k = \frac{1}{5.26 \times 10^{-7}} = 1.90 \times 10^{6} \text{ dynes/cm.}$$

When a thrust is applied in the direction of one transducer unit, the flexible ties on the other two units will bend in a manner similar to that just described for the spring parallelograms, except that four ties will resist a given deflection, as opposed to two springs. Considering the ties alone as resisting a force W, the displacement should be

$$\frac{1}{2} \frac{WL^3}{3 I}$$

The properties and approximate dimensions of the ties are:

$2L$ = length = .28 in. = .71 cm.

r = radius = .004 in. = .01016 cm.

q = Young's modulus of phosphor bronze = 9.8×10^{11} dynes/sq.cm.

$$I = \frac{\pi r^4}{4} = 8.4 \times 10^{-9} \text{ cm}^4.$$

The displacements per unit force will be

$$\frac{L^3}{6qI} = \frac{0.355^3}{6 \times 9.8 \times 8.4 \times 10^2} = 9.0 \times 10^{-7} \text{ cm./dyne}$$

and the force constant for the 4 ties acting together will be

$$k_T = \frac{1}{9.0 \times 10^{-7}} = 1.11 \times 10^{6} \text{ dynes/cm.}$$

The combined force constant of springs plus flexible ties for any one component of thrust will therefore be

$$(1.90 + 1.11) \times 10^{6} = 3.01 \times 10^{6} \text{ dynes/cm.}$$

$$= 3.08 \times 10^{3} \text{ gm./cm.}$$

This agrees very well with the displacement deduced from the output of the differential transformers using the manufacturer's calibration data. With an excitation potential of 3.0 volts, the output of the secondary is 0.030 volts at a displacement of

.005 inch (.0127 cm.), indicating a mean output of 2.36 volts per centimeter. The measured response was approximately 0.8 millivolt per gram force, which implies a displacement of

$$\frac{0.8 \times 10^{-3}}{2.36} = 3.39 \times 10^{-6} \text{ cm./gm.}$$

or a force constant of

$$2.95 \times 10^{3} \text{ gm./cm.} = 2.89 \times 10^{6} \text{ dynes/cm.}$$

Frequency of Free Vibration

The mass of moving parts in any one component can be determined by placing the axis of that component vertical and noting the output of the transducer, then inverting the instrument and noting the change of output. It could be also obtained by summing the weights of the individual parts which move with that component. However, the pieces were not accurately weighted prior to assembly, and the value of approximately 12 grams was obtained by the former procedure.

A simple spring system without damping vibrates according to the familiar relation of simple harmonic motion with a frequency

$$n = \frac{1}{2\pi}\sqrt{\frac{k}{m}}$$

where m is the moving mass and k is the force exerted by the spring per unit displacement.

Substituting $k = 3 \times 10^{6}$ dynes/cm. and

$m = 12$ gm.

$$n = \frac{1}{2\pi}\sqrt{\frac{3 \times 10^{6}}{12}} = 80 \text{ cycles per second}$$

in excellent agreement with the frequencies recorded without fluid in the dashpots (see section on DAMPING). This corresponds to a response time of the order of 1/80 x 4 or .003 second.

Frequency of Torsional Vibration

While a pure rotation of the sphere about any of the axes theoretically should not produce any deflection of the transducers, a resonant oscillation, if it should occur, would almost certainly result in some output due to imperfections in the balance of the components. The frequency of such vibrations would be given by the relation

$$n = \frac{1}{2\pi}\sqrt{\frac{C}{I}}$$

where C is the couple per radian about the axis of rotation due to the flexing and twisting of the flexible ties, and I is the moment of inertia about the same axis of the shell and PVC great circles. Considering rotation about one of the co-ordinate axes, say the z axis, I will comprise three terms: mr^2 for the great circle perpendicular to the axis, $2mr^2/2$ for the two circles which intersect on the axis, and $2MR^2/3$ for the shell. Taking m and M, the masses of each great circle and of the shell as 1.0 and 2.5 gm. respectively, and taking r and R as 3.25 cm. and 3.6 cm. respectively

$$I = 10.5 + 10.5 + 21.0 = 42 \text{ gm.cm}^2$$

The restoring couple, C, consists of the couple about the z axis due to the flexing of the four flexible ties in the x-y plane, and the twisting of the two ties which lie on the z axis. The combined force constant of the four ties has been shown to be 1.11×10^6 dynes per centimeter of circumferential displacement,

corresponding to a couple of 1.11 x 3.6 x 10^6 dyne/cm. about the axis. A rotation of one radian would produce a couple of 1.11 x 3.6^2 x 10^6 = 11.7 x 10^6 dyne/cm. The couple due to the twisting of the z ties is $2 \times \frac{h \pi r^4}{2L} = 2 \times 10^4$ dyne cm./radian where h is the modulus of rigidity of phosphor bronze (3.6 x 10^{11}), L is the length of the tie (0.71 cm.), and r is the radius of the tie (.010 cm.). The couple due to the twisting of the two ties is thus negligible compared to the couple due to the flexing of the other four, so that the frequency of torsional vibrations can be written $n = \frac{1}{2\pi}\sqrt{\frac{11.7 \times 10^6}{42}} =$ 82 cycles per second which is very nearly the same as the frequency of free lateral vibrations.

Damping

If no damping is introduced, the sphere with its associated moving parts is free to vibrate on the springs of the transducers. Oscillograph records made under these conditions indicated frequencies of the order of 80 to 100 cycles per second, the variation from one component to another being due to small differences between the springs. If the sphere were lightly tapped, vibrations would continue with decreasing but appreciable amplitude for a hundred cycles or more.

Provided that the output remains linear in terms of transducer displacement the effects of such high frequency vibrations can be eliminated from the data record by the use of a low pass filter whose cut off is sufficiently below the objectionable frequency. The filters in the ADDReSOR function in this way for

all frequencies above 10 cycles per second. In the present case, however, the vibrations easily exceeded the linear range of the amplifiers, so that a distorted wave form was produced in the output. Any device, such as a filter, which averaged such a wave form would yield an apparent mean whose departure from the true mean was a function of vibration amplitude. For this reason an output filter would not have been sufficient to eliminate the effects of the vibrations, and actual reduction of the amplitude of the vibration was necessary.

To accomplish the required damping, a tiny dashpot was fitted to each component on a cut-and-try basis. The cylinders were made by drilling a hole 7/32 inch (0.552 cm.) in diameter and 1/4 inch (.635 cm.) deep in a plexiglas rod 1/4 inch in diameter. The piston was a piece of brass rod 3/16 inch (0.475 cm.) in diameter and 1/8 inch (0.318 cm.) long. A short length of copper wire soldered to the piston served as a connecting rod. The cylinder in each case was fastened to the internal frame and the connecting rod was connected to the clamp at one end of the transducer. Each of these connections was made with epoxy resin which was allowed to harden with the piston carefully centered in the cylinder. Various silicone fluids were tried and one with a visosity of 760 centipoises was found to be satisfactory.

Assuming that the viscous damping force is proportional to the velocity of the moving parts, the differential equation for damped oscillations can be written in the usual manner

$$m\ddot{x} + a\dot{x} + kx = 0$$

with the solution

$$x \quad Ae^{-at/2m} \cos \left[\sqrt{k/m - (a/2m)^2} \right] t$$

From the oscillograph record $A_1/A_o = 0.2$ approximately, and $T = 10^{-2}$ sec. Then, if m = 12 gm.

$$0.2 = e^{-aT/2m} = e^{-a/2400} = e^{-1.6},$$

and a = 3840 gm. sec^{-1}.

Therefore the frequency with damping,

$$\frac{1}{2\pi} \sqrt{\frac{k}{m} - \left(\frac{a}{2m}\right)^2}$$

is less than the frequency without damping,

$$\frac{1}{2\pi} \sqrt{\frac{k}{m}}$$

by the factor

$$\sqrt{1 - \frac{(a/2m)^2}{k/m}} = \sqrt{1 - \frac{a^2}{4km}}$$

$$= \sqrt{1 - \frac{3800^2}{4 \times 3 \times 10^6 \times 12}} = 0.97 \text{ approximately.}$$

That is, the frequency of free vibrations is reduced by some three per cent. Since this is still an order of magnitude greater than the cut-off frequency of the low pass filter in the ADDReSOR, no significant loss of fidelity will be introduced into any of the spectral components which the system can handle.

If at the time t_o, when the static displacemnts is y_o, a step function of force, F_1, is applied, the response of the system will be given by

$$y = y_1 + (y_o - y_1)\, e^{-at/2m} \cos \left[\sqrt{\frac{k}{m} - \left(\frac{a}{2m}\right)^2} \right] t$$

where $y_1 = \frac{F_1}{k}$.

Critical damping could be achieved by the use of a more viscous fluid such that

$$\frac{K}{m} - \left(\frac{a}{2m}\right)^2 = 0$$

or in other words such that a = 12000 approximately. This would be obtained by letting the viscosity be some four times as great, or in the vicinity of 3000 centipoises. However, it is questionable whether this would be an advantage, since the present damping appears adequate to eliminate excursions into the non linear region, and such residual vibration as still exists probably helps to overcome the slight hysteresis of the system.

MECHANICAL AND ELECTRICAL VERIFICATION

Verification of the mechanical and electrical response of the instrument consisted of establishing: a) that the output of each transducer is a linear function of the force applied parallel to its axis, and b) that if a thrust vector is applied to the sphere in an arbitrary direction, the outputs of the three transducers are proportional to the components of the vector resolved parallel to the axes of the transducers.

a) Two procedures were used to test the linearity of the system to applied force. In the first, the instrument was set with its x axis vertical and weights were placed carefully on top of the sphere to obtain the relation between the output and applied weight. This was repeated placing the y axis vertical, first with one end up, then with the other end up. And finally the same was done with the z axis vertical. This method has the advantage of simplicity, but it leaves a blank region in the middle of the full range, equal to twice the weight of the sphere, in which the performance of the springs cannot be checked. Moreover, it cannot be done using the two high gain settings since the full range of response is less than twice the weight of the sphere. The differential transformer was set in each case to several positions by means of the adjusting screws (s, Figure 2) so that all portions of its normal operating range could be tested. Sample results are shown in Figure 11. It was found that maximum deviations from the best straight line fit (by eye) were less than 2 per cent of full range, and that in most cases the results were linear to within the precision of measurement.

The second procedure for testing the linearity of individual transducer units is illustrated in Figures 12 and 13. Tiny scale pans were made from flakes of styrofoam and were attached to the sphere with fine dressmaker's thread as shown in the illustrations. Since the indicated angle in each case was 45 degrees, the force applied to the sphere equalled the weight of the pan and contents. Weights were added to the two pans so as to take the transducer through its full range of operation, using all gain settings of the amplifier. The results, which are illustrated in Figures 14 - 19, indicate that the response is linear to within 2 per cent at highest gain, and practically to within the precision of measurement at the lower gains.

b) Two procedures were used also to test the accuracy with which a thrust vector of arbitrary direction is resolved into its x, y, and z components. In the first, the instrument was set with one axis horizontal and rotated about this axis. The outputs of the other two components then should describe sine and cosine functions as the weight of the sphere, acting in the vertical direction, is resolved into two orthogonal components by the two supporting transducers. The result of such a test on the x and z components is presented in Figure 20. This procedure was varied by placing weights on top of the sphere in successive positions as the instrument was rotated. The additional weight was similarly resolved into components proportional to the sine and cosine of the angle of rotation.

The second procedure was a further modification of the first, consisting of rotation about two axes simultaneously,

comparing the indicated components of the weight of the sphere and of the additional weight placed on top of it, with the values computed using the sines and cosines of the angles of inclination. The results of such a test rotated about the y axis are summarized in Table 2. In this instance the dish was mounted with the second coupling (v, Figure 3) on top of the stem, so that with the universal joint, W, set at zero angle, the x axis was vertical. The universal joint was oriented so that its lower axis was parallel to the y axis and its upper axis was parallel to the z axis. When bent about both axes, a vertical thrust F on the sphere would have components parallel to the three transducers as follows:

$$Fx = x \text{ component} = F \cos \theta_z \cos \theta_y$$

$$Fy = y \text{ component} = F \sin \theta_z \cos \theta_y$$

$$Fz = z \text{ component} = F \sin \theta_y$$

The errors, that is, the difference between the observed and computed values after normalization, are based in each case upon a single measurement. In other words, these are individual measurements, not the averages of several determinations, and are therefore subject to the full errors of the experimental procedure, as well as those of the instrument itself. In the case of Fx and Fz the discrepancies are small, in nearly all cases 0.03 or less, except at the larger angles. The errors of Fy tend to be of comparable size, except in the vicinity of zero angle where they are excessive. This indicates the existence of a mechanical defect, whose exact nature is not

X

θ_y	Comp. Val.	Obs. - Comp. 2.3	6.0	10.5	Comp. Val.	Obs. - Comp. 2.3	6.0	10.5	Comp. Val.	Obs. - Comp. 2.3	6.0	10.5
		$\theta_z = 0$				$\theta_z = -10$				$\theta_z = -20$		
-38	.79	-.06	-.04	-.04	.78	-.05	-.04	-.04	.74	-.05	-.04	-.04
-28	.88	-.06	-.03	-.03	.87	-.05	-.02	-.03	.83	-.05	-.04	-.03
-18	.95	.01	.00	+.01	.94	-.05	-.01	-.02	.89	-.05	-.04	-.03
- 8	.99	.03	.03	.01	.98	-.02	-.01	-.02	.93	.00	-.01	-.01
2	1.00	.02	.03	.02	.98	.00	.01	.00	.94	-.03	-.01	-.02
12	.98	.02	.03	.01	.96	-.05	.00	.00	.92	-.03	-.01	-.01
22	.93	-.02	.02	.01	.91	-.02	.00	.00	.87	.00	-.01	-.01
32	.85	.00	.00	.00	.85	-.05	-.02	-.02	.80	-.02	-.02	-.01
42	.74	-.01	.01	.01	.73	-.02	.00	.00	.70	-.01	-.01	-.02
		$\theta_z = -30^\circ$				$\theta_z = -40$				$\theta_z = 10$		
-38	.68	-.06	-.03	-.05	.60	-.07	-.05	-.05	.78	-.05	-.04	-.04
-28	.76	-.05	-.03	-.03	.68	-.06	-.04	-.05	.87	-.03	-.02	-.02
-18	.82	-.04	-.03	-.03	.73	-.04	-.03	-.03	.94	-.05	-.01	.01
- 8	.86	-.04	-.02	-.03	.76	-.03	-.03	-.02	.98	.00	.00	.01
2	.87	-.03	-.02	-.02	.77	-.04	-.03	-.03	.98	.02	.04	.02
12	.85	-.03	-.01	-.02	.75	-.02	-.02	-.02	.96	.02	.03	.02
22	.80	-.04	-.02	-.01	.71	-.02	-.01	-.01	.91	.00	.03	.01
32	.73	.00	.00	-.01	.65	-.05	-.01	-.02	.85	-.01	.00	-.01
42	.64	-.04	-.01	-.01	.57	-.06	-.02	-.02	.73	.02	.01	.01
		$\theta_z = 20$				$\theta_z = 30$				$\theta_z = 40$		
-38	.74	-.03	-.02	-.02	.68	-.06	-.03	-.03	.60	-.02	-.01	-.01
-28	.83	-.03	-.01	-.01	.76	-.03	-.01	-.01	.68	-.01	.00	.00
-18	.89	.00	.01	.00	.82	-.02	.00	-.01	.73	-.02	.00	.00
- 8	.93	-.02	.00	.00	.86	.01	-.01	.00	.78	.02	.02	.01
2	.94	-.02	.02	.00	.87	.00	-.02	.01	.77	.01	.01	.01
12	.92	.01	.02	.01	.85	-.01	-.02	.01	.75	.03	.03	.02
22	.87	.02	.03	.02	.80	.02	.03	.02	.71	.02	.02	.02
32	.80	.00	.02	.02	.73	.03	.05	.03	.65	.02	.02	.03
42	.70	-.01	.02	.02	.64	.01	.04	.04	.57	.01	.02	.03

Table 2. (Three pages) Differences between observed and computed values of vector components obtained by tilting the sphere at various angles (see text) and placing weights of 2.3, 6.0, and 10.5 gms on top of it. Differences are expressed as decimals of vector magnitude, or, in other words, decimals of the applied weight. Values on this page are for the X component.

Y

θ_y	Comp. Val.	Obs. - Comp. 2.3	6.0	10.5	Comp. Val.	Obs. - Comp. 2.3	6.0	10.5	Comp. Val.	Obs. - Comp. 2.3	6.0	10.5
		θ_z = 0				θ_z = -10				θ_z = -20		
-38	0	-.02	-.01	-.02	-.17	-.02	.02	.02	-.34	-.03	-.01	.00
-28	0	-.02	-.01	.00	-.17	.00	.01	.01	-.34	.04	.01	.02
-18	0	.02	-.02	.01	-.17	.02	.03	.03	-.34	.04	.02	.03
- 8	0	.04	.05	.04	-.17	.04	.04	.04	-.34	.02	.02	.03
2	0	.09	.10	.08	-.17	.04	.05	.05	-.34	.02	.03	.03
12	0	.04	.03	.02	-.17	.06	.05	.04	-.34	.02	.02	.03
22	0	.00	.00	.00	-.17	.00	.01	.01	-.34	-.01	.01	.02
32	0	-.02	-.02	-.01	-.17	.02	-.01	.00	-.34	-.01	.01	.01
42	0	-.02	-.02	-.02	-.17	.00	.00	-.01	-.34	-.01	.01	.01
		θ_z = -30				θ_z = -40				θ_z = 10		
-38	-.50	.00	.02	.01	-.64	-.01	.01	.01	.17	-.04	-.05	-.03
-28	-.50	.02	.02	.02	-.64	.03	.01	.01	.17	-.02	-.03	-.02
-18	-.50	.02	.02	.02	-.64	.03	.00	.01	.17	-.00	-.02	-.01
- 8	-.50	.02	.02	.03	-.64	.01	.01	.01	.17	.00	.00	.00
2	-.50	.02	.02	.03	-.64	.01	.01	.02	.17	.02	.02	.03
12	-.50	.04	.03	.03	-.64	.03	.00	.03	.17	.02	.02	.02
22	-.50	.02	.02	.03	-.64	.01	.01	.02	.17	.00	.01	.01
32	-.50	.00	.02	.02	-.64	.03	.02	.03	.17	.00	.01	.01
42	-.50	.02	.02	.02	-.64	.03	.03	.02	.17	.00	.00	.01
		θ_z = 20				θ_z = 30				θ_z = 40		
-38	.34	-.04	-.03	-.02	.50	-.07	-.05	-.04	.64	-.03	-.02	-.03
-28	.34	-.06	-.03	-.02	.50	-.04	-.03	-.03	.64	-.01	-.02	-.02
-18	.34	-.01	-.02	-.01	.50	-.04	-.04	-.03	.64	-.01	-.02	-.03
- 8	.34	.01	-.02	.00	.50	-.02	-.03	-.02	.64	-.01	-.02	-.02
2	.34	.03	-.02	.01	.50	-.02	-.02	-.01	.64	-.01	-.01	-.01
12	.34	.01	.00	.00	.50	-.02	-.01	-.01	.64	-.03	-.01	-.01
22	.34	-.01	-.02	.01	.50	.02	.01	.01	.64	-.01	-.01	-.01
32	.34	-.01	-.02	-.01	.50	-.02	.01	.01	.64	-.03	-.02	-.01
42	.34	-.01	-.02	-.01	.50	-.02	.03	.00	.64	-.03	-.01	-.01

Table 2 (continued) Y component

Z

θ_y	Comp. Val.	Obs. − Comp. 2.3	6.0	10.5	Comp. Val.	Obs. − Comp. 2.3	6.0	10.5	Comp. Val.	Obs. − Comp. 2.3	6.0	10.5
		$\theta_z = 0$				$\theta_z = -10$				$\theta_z = -20$		
-38	-.62	.01	.01	.02	-.61	-.02	.00	.00	-.58	-.01	.00	.01
-28	-.47	.03	.02	.02	-.46	-.02	.00	.00	-.44	-.02	.01	.01
-18	-.31	.01	.00	.00	-.30	.02	.04	.00	-.29	.01	.01	.01
- 8	-.14	.01	.02	..02	-.14	.01	.02	.02	-.13	.00	.01	.02
2	.04	.04	.03	.03	.03	.01	.01	.02	.03	.04	.01	.00
12	.21	.03	.01	-.01	.20	.00	.00	.00	.20	-.03	-.01	-.01
22	.38	-.03	-.03	-.03	.37	-.02	-.01	-.02	.35	.00	-.01	-.01
32	.53	.04	-.02	-.01	.52	.00	-.02	-.02	.50	.02	-.03	-.02
42	.67	-.02	-.01	-.01	.66	-.05	.06	-.03	.63	.00	.00	-.02
		$\theta_z = -30$				$\theta_z = -40$				$\theta_z = 10$		
-38	-.53	.01	.00	.01	-.47	-.01	.03	.02	-.61	-.04	-.01	-.01
-28	-.41	.04	.02	.02	-.36	.08	.03	.04	-.46	-.02	-.01	-.01
-18	-.27	.03	.02	.02	-.24	.02	.05	.04	-.30	-.03	-.02	-.01
- 8	-.12	-.01	-.01	.00	-.11	.02	.03	.03	-.14	.03	.02	.02
2	.03	.01	.01	.00	.03	-.01	.01	.01	.03	-.01	.00	.01
12	.18	-.03	-.01	.00	.16	-.01	.01	.01	.20	-.03	-.02	-.01
22	.33	-.03	-.02	-.01	.29	-.01	.00	.01	.37	-.02	-.03	-.02
32	.46	.00	-.01	-.01	.41	.00	-.01	-.01	.52	-.04	-.02	-.01
42	.58	-.01	-.02	.00	.51	.06	.01	.01	.66	-.03	-.03	-.01
		$\theta_z = 20^\circ$				$\theta_z = 30^\circ$				$\theta_z = 40^\circ$		
-38	-.58	-.05	-.02	.01	-.53	-.04	-.05	-.03	-.47	-.05	-.04	-.03
-28	-.44	-.02	-.01	-.02	-.41	-.02	-.02	-.01	-.36	-.01	.00	.00
-18	-.29	-.01	.00	.00	-.27	-.06	-.03	-.03	-.24	.00	-.01	-.01
- 8	-.13	.02	.01	.00	-.12	-.01	-.01	-.02	-.11	-.02	-.02	-.01
2	.03	.01	-.01	.00	.03	-.03	-.03	-.03	.03	-.03	-.02	-.03
12	.20	.00	-.02	-.01	.18	.02	-.02	-.03	.16	-.03	-.03	-.03
22	.35	-.02	-.03	-.02	.33	.00	-.02	-.02	.29	-.03	-.02	-.02
32	.50	-.04	-.04	-.04	.46	.00	-.02	-.02	.41	-.04	-.04	-.03
42	.63	.00	-.04	-.04	.58	-.04	-.04	-.03	.51	-.05	-.04	-.03

Table 2 (continued) Z component

clear, but which may follow from the slight inaccuracies that are known to exist in some of the pieces of the internal assembly. More precise fabrication and assembly can be expected to eliminate the problem.

The response of the instrument has therefore been shown to be linear to static thrusts parallel to the coordinate axes, and to resolve thrusts within 30 degrees of the x axis into their components with satisfactory precision, except for the y component at small angles of incidence. Since the x and z components are the two which are directly involved in measurements of vertical transports, the instrument can be considered mechanically and electrically verified - under static thrusts - for this purpose. Until the present difficulty is eliminated, the output of the y component is subject to more uncertainty.

SELECTION OF THE SPHERE AND AERODYNAMIC VERIFICATION

The drag coefficient of a sphere depends at least in part on the Reynolds number, the surface roughness of the sphere, and the turbulence of the wind stream. The drag coefficient of a smooth sphere is practically constant over a range of Reynolds numbers from about 10^3 to about $3X10^5$, above which it decreases rapidly in the critical region and increases again at still higher speeds. If the surface of the sphere is roughened, the critical region is reached at lower velocities and the reduction of drag coefficient is less pronounced. In both cases vortex systems occur in the wake and eddies are detached in more or less irregular fashion, producing transverse thrusts as the line of separation on the surface of the sphere moves back and forth (Hoerner).

Rosenbrock and Tagg (1951) and Rosenbrock (1951) have described a series of instruments designed to measure gusts in winds at relatively high speeds by measuring the thrust on a sphere. Following experiments by Simmons at the National Physics Laboratory in England they found that they could overcome the problem of these transverse thrusts by perforating the sphere. They also reported finding a drag coefficient that was constant over the operating range of their instruments, which was 40 to 70 miles per hour using a sphere 1½ inches in diameter. These observations are qualitatively corroborated by the present instrument, which has a diameter of three inches and a constant drag coefficient over the range zero to twenty metres per second

(approximately 44 miles per hour). It has not yet been possible to test it at speeds greater than this because of the limitations imposed by the wind tunnel. The normal operating range of the instrument does not exceed approximately 15 metres per second, but can be extended by the use of stiffer springs in the transducers. This was done in the case of the tests which extended to twenty metres per second.

In the light of these considerations we can enumerate the following desirable characteristics for the sphere:

1. There should be no transverse thrusts or spurious indications of either wind speed or direction due to eddy shedding or turbulence induced by the presence of the sphere and its support.

2. There should be no critical region within the operating range, and, preferably, the drag coefficient should be constant over this range.

3. The drag should be exerted in the same direction as the wind blows, regardless of the angle of incidence. That is, the sphere must be aerodynamially symmetrical about any diameter.

4. The sphere should be rigid and not subject to deformation by the thrust of the wind.

5. It should be as light as possible to permit rapid response.

6. During the developmental stage at least, it was desirable that spheres be readily available, inexpensive, and made of a material that was easily worked and modified.

The last three criteria, coupled with the inspiration of a Christmas tree ornament, led to the choice of styrofoam as the material for the spheres. It was found that by the use of a lathe with suitable jigs and outters, hemispheres could be cut very quickly from a block of the material. With an outside diameter of three inches (7.6 cm.) and a wall thickness of 0.187 inch (0.48 cm.), these hemispheres are remarkably rigid and weigh approximately 1.3 grams each. They can be dimpled or perforated simply by touching them with a suitable hot wire or soldering iron tip.

To find the type of shell which best satisfies criterion (1) a series of tests were tried using spheres modified with various arrangements of knobs, dimples, and perforations as well as a plain unmodified styrofoam shell. In each case the instrument was mounted in the wind tunnel with its x-axis directed towards the oncoming wind, the three components of thrust were recorded simultaneously on a graphic recorder, and a calibration curve was derived for the x component versus the square of the wind speed.

A certain amount of variation or "noise" was superimposed on the mean output of each component, amounting to some 2 per cent of the mean in the x component, but as high as ± 10 per cent of the total thrust in the y and z components in some cases. Since it was considered highly improbable that the flow in the tunnel could be subject to such large deviations from the mean direction, these transverse components were attributed to induced turbulence and the shedding of eddies in the wake. The best

sphere was therefore assumed to be the one which indicated the smallest amplitude for such oscillations, and none was considered satisfactory unless the transverse components were of no larger order than the variations of the axial component.

Since the fluctuations will be a small fraction of the mean speed, and if the x component is parallel to the axis of the tunnel, we may write

$$F = F_x = kV_x^2 \quad \text{very nearly, and}$$

$$\frac{\delta Fx}{\delta Vx} = 2kV_x.$$

Also since the velocity and force vectors must have the same direction,

$$Fy = \frac{Vy}{Vx} Fx = kVxVy,$$

and $$\frac{\delta Fy}{\delta Vy} = kVx.$$

Similarly, $$\frac{\delta Fz}{\delta Vz} = kVx.$$

Now if the turbulence is isotropic, $\Delta Vx, \Delta Vy, \Delta Vz$ will be statistically equal, so that the average deviations of the components of force will be twice as great in the axial direction as in the transverse directions. That is, the amplitude of the flutter about the mean, $\overline{Fx}$, of the x component should be twice as great as the amplitudes of flutter about the means $\overline{Fy}$ and $\overline{Fz}$ of the two transverse components. (In this case $\overline{Fy}$ and $\overline{Fz}$ are both zero.)

Since in general we would not expect isotropic turbulence of this scale in a wind tunnel, but rather that $|\Delta Vx|$ should be greater on the average than $|\Delta Vy|$ or $|\Delta Vz|$, the transverse components of force should in general be much less than

the deviations from the mean of the axial component. For this reason, the residual transverse variations which are of the same order as those of the axial component, are regarded as instrumental "noise." With the perforated sphere which was finally selected as optimum, the noise level of all three components for wind speeds of some 4 metres per second or greater was of the order of ± 2 per cent of mean thrust, with maximum excursions of about 3 per cent. This corresponds in the case of the axial component to 1 per cent of mean total speed, and in the case of the transverse components, to 2 per cent of mean total speed. This noise level in the y and z components means that there is an uncertainty of approximately $\pm$ one degree in the instantaneous direction of the wind vector.

The reason for the difference in performance between the various types of sphere has not been directly investigated but the "best" spheres were perforated, and it is assumed that the passage of air through them alters the distribution of pressure in such a way that large eddies do not form and detach in the wake stream. It is also assumed that the residual noise level is associated with non-uniformities of flow around and through the shell. The introduction of an additional screen in the intake region of the tunnel reduced the amplitude of the flutter somewhat in some cases, suggesting that the noise is influenced in part at least by the scale of turbulence of the air stream. This also leads to the hope that further improvement may be possible when another wind tunnel is available for additional testing.

It was found in general that the amplitude of flutter was greatest with a plain unperforated shell, decreasing as the amount

of perforation was increased. The smoothest output was obtained when the number of holes was the maximum that could be made without overlapping. Because of the cellular structure of the styrofoam, the hole density could not exceed a certain critical value without destroying some of the partitions. With a stylus of 3/32 inch diameter (.238 cm.), approximately 500 holes could be made in each hemisphere, representing a total area of approximately 30 per cent of the surface of the shell when allowance is made for the fact that the heated stylus melts a hole whose area of cross section is usually slightly larger than that of the stylus itself. With a 1/16 inch stylus, the number of holes could be increased to about 800 per hemisphere, covering approximately 20 per cent of the surface. Owing to the thickness of the shell, however, the effective exposure presented by these holes to an advancing front of wind is probably much less than that implied by these percentage figures. Thus if one looks at one of the hemispheres with 3/32 inch holes from a sufficient distance to make parallax negligible, one can see through only some 60 holes clustered around the axial diameter. All the remaining holes will be at too great an angle of inclination to the line of sight. Possibly for this reason, the drag coefficient did not seem to vary greatly with the density of holes once the density had reached a point sufficient to reduce the flutter appreciably.

In view of the uncertainty of many factors, including the turbulence of the tunnel and its influence on the response, no attempt was made to correlate quantitatively the number or area of perforations with the amplitude of flutter. Qualitatively, the sphere with the maximum number of 3/32 inch holes was slightly

better than the sphere with the maximum number of 1/16 inch holes, and both were better than any sphere which had much fewer perforations. Knobs and dimples - that is larger roughness features either extending beyond the mean surface or indented into it - did not greatly improve upon the plain styrofoam, and in some cases seemed to worsen it. Presumably the roughness of the plain styrofoam is sufficient to ensure turbulent flow in the boundary layer, and no significant improvement was effected by increasing the size of the individual elements.

Fortunately, the sphere that best satisfied the first criterion also had the most nearly constant drag coefficient (criterion 2). For a smooth sphere in the free atmosphere the critical region corresponds to a Reynolds number of approximately 3.85×10^5 (Bairstow, 1939), implying a speed of some 84 metres per second where the diameter is three inches (7.6 cm.). Corresponding values obtained in wind tunnel tests are in the neighborhood of $R_d = 2 \times 10^5$ or V=65 metres per second (Bairstow, Prandtl and Tietjens, etc.). The critical Reynolds number may be reduced by roughening the surface or by introducing turbulence of a suitable scale into the wind stream. Bairstow, for example, shows a reduction from 2.1×10^5 to 1.15×10^5 by the introduction of a network of cords upstream from the sphere.

The unperforated styrofoam has a grain size of the same order as coarse sand, and the wind tunnel undoubtedly had a high level of turbulence due to its open ended construction and the arrangement of smoothing screens and tubes in the intake. Some reduction of the critical Reynolds number below 2×10^5 could

therefore be expected on account of both of these factors. It was surprising, nevertheless, to find that the critical speed for the unperforated styrofoam sphere was about six or eight metres per second, corresponding to a Reynolds number of $3X10^4$ (Figure 21). In contrast with this, the fully perforated sphere had a drag coefficient that was practically constant throughout the range of the tests ($\doteq$ .49), indicating that thrust was proportional to the square of wind speed to within the precision of the measurements (Figures 22 and 23).

The other types of sphere were all intermediate between these two cases. Dimpling (like a golf ball) reduced somewhat both the critical speed and the magnitude of the change in C_d (Figure 21). Perforating the golf ball with a 1/16 inch hole in each dimple reduced the transition still further, yielding a result that was significantly less linear, however, than the fully perforated sphere.

A number of combinations were tried, such as a perforated front and unperforated rear half, unperforated front and perforated rear, golf ball front and perforated rear, etc. Qualitatively, the results were comparable to those of the golf ball and perforated golf ball, above, with the amplitude of fluctuations decreasing as the area of perforations increased. There was some evidence that perforations in the rear half had more effect than those in the front half, but the tests were not carried far enough to draw definite conclusions from this.

The third criterion, aerodynamic symmetry of the sphere about any diameter, is a requirement if the instrument is to

faithfully resolve the thrust into its three components regardless of the angle of approach of the wind. Since the fidelity of the mechanical system had been established by the procedures described under the heading MECHANICAL AND ELECTRICAL VERIFICATION, the aerodynamic symmetry or asymmetry could be tested by placing the instrument at various angles to the wind stream and comparing the outputs of the three transducers with the computed components of the velocity resolved along the three axes of the instrument.

Since the direction of the air stream in the tunnel was fixed and horizontal, the tests consisted of

a) Turning the instrument about its z axis and measuring the x and y components;

b) Tilting the instrument about an axis parallel to the y axis and measuring the x and z components; and

c) Tilting and turning about both these axes simultaneously, measuring all three components.

In general, any of the symmetrical unperforated spheres, that is, same front and back, satisfactorily resolved the components of thrust within the limits of precision of the measurments. In some cases the amount of flutter made precise values difficult to obtain, but there appeared to be no consistent irregularities in the components. In the case of the perforated spheres, however, a persistent non-linearity is observed in the y component which has not yet been adequately explained. This is illustrated in Figure 24 which shows the x and y components obtained by turning the instrument about its z axis in the wind stream. Fx and Fy

should be equal to F cos θ and F sin θ respectively, but the curves of both are markedly flattened in the vicinity of θ = 0. Since sin θ is very nearly a linear function of θ between -30 degrees and +30 degrees, straight line segments have been used in the graph of Fy to simplify the presentation and accentuate the problem of flattening near zero.

This flattening is apparently not due to a defect in the mechanical linkages of the transducer system to the sphere, since it is not observed either in the static tests described under the heading MECHANICAL AND ELECTRICAL VERIFICATION or when using an unperforated sphere. It seems that the perforated spheres have had a preferred axis of symmetry such that for small θ the thrust is deviated towards the direction of the x axis. It is apparently not due to any obstruction or channelling by the transducer assembly inside the sphere, since the same effect is observed when the internal assembly is fully enclosed by an unperforated shell inside the perforated shell and separated from it by a space of 3/16 inch to allow for the passage of air. This arrangement is called the double sphere in Figure 24. Since the perforation of the double sphere was not strictly random but had some radial symmetry about the x axis, however, it seems possible that this may in some way have created a preferred direction of flow through the shell.

The nonlinearity of the z component is less pronounced than that of the y component at wind speeds above about 4 metres per second. The curves for 10 metres per second in Figure 25, illustrating the results obtained by tilting the instrument about its

y axis in the wind tunnel, show only a slight flattening of Fx and departures from the predicted values of Fz of less than 2 per cent at angles up to 30 degrees. At 3 metres per second, however, the discrepancies are greater, yielding a curve for Fx that is essentially flat to 25 degrees on either side, and errors in Fz up to approximately 5 per cent of vector magnitude.

Results obtained with unperforated spheres composed of dissimilar hemispheres add force to the suggestion that the effect is aerodynamic rather than mechanical. Figure 26 shows the y components obtained by rotating a sphere (a) with the front half plain styrofoam and the rear half dimpled, and (b) with the front half dimpled, the rear half plain styrofoam. The former shows a distortion qualitatively similar to that obtained with the perforated spheres, although the level of flutter was so high as to make a precise determination very uncertain. The latter, on the other hand, with the larger roughness elements in front, shows exactly the opposite distortion, with the slope greatly increased rather than flattened in the vicinity of zero.

The explanation for these effects is conjectured to be due to a greater frictional effect on the flow around the sphere from the larger roughness elements on the dimpled half than on the undimpled half. (It is important to remember that the sphere is nowhere smooth, so that laminar flow is not likely to exist in any portion of the boundary layer.) The effect of this would be to retard the flow slightly over the dimpled half relative to the undimpled half, causing a shift of the separation zone towards the x axis when the rougher half is behind (Figure 27), and

away from the x axis when the rougher half is in front.

This shows that aerodynamic uniformity of the sphere is important, but does not of itself explain why the perforated spheres do not seem to meet this requirement. At the time of writing this question remains unanswered and the performance of the instrument is correspondingly deficient. In practice, corrections for the distortions of both curves can be made by the computer when the data are processed, so that significant error need not be introduced into the computed values of velocity.

The other major limitation of the instrument is the apparent existence of a critical region in the vicinity of 3 metres per second. This does not appear as a change in the drag coefficient but rather in the amount of transverse flutter, which was approximately double that observed at higher speeds, when measured as per cent of total thrust. The velocity at which such a critical region occurs and the magnitude of the flutter are almost certainly functions of the type of spherical shell used, the size and number of perforations and probably also the turbulence level of the wind tunnel. No systematic attempts have been made as yet to isolate these variables or to eliminate the effect. For the present, the instrument should be considered fully proven only for speeds significantly greater than 3 metres per second.

FIELD TEST AND COMPUTED RESULTS

A field test was made on Racing Beach, Cape Cod, December 11, 1962, between 9:30 and 10:30 a.m. The instrument was mounted on a stand on the beach, approximately 25 metres from the water's edge, with the sphere at a height of 2 metres above the beach and about $2\frac{1}{2}$ - 3 metres above water level. The x axis was pointed towards the mean wind, which was blowing directly off the water towards the land, approximately from the southwest, with an unobstructed fetch over water of some 50 kilometres. A surf zone extended an estimated 60 - 100 metres from the edge of the beach with waves of the order of 60 - 100 centimetres high. The water temperature was 4.6°C, and the air temperature at anemometer level was -2.0°, indicating strong instability. The mean wind during the five minutes of record that has been analyzed was 9.25 metres per second, obtained by averaging the x component of velocity computed from the record.

Snow started to fall heavily almost immediately after the run commenced, and continued intermittently during the period of observations. The flakes were large and sticky, and accumulated on the windward side of the support ring and stand, but there was no evidence that either the sphere or the record was adversely affected. The most serious source of error in the measurements was probably the fact that the tie-back rod was left off, allowing the sphere and its internal assembly to vibrate - at times visibly - on the radial wires. This had not been found to be a source of significant error in the wind tunnel, but apparently under the

conditions of this field test the tie-back was necessary. Effects attributed to this cause will be pointed out in the following discussion.

Power was supplied by means of an extension cord from a house which was some 100 metres down wind, and the associated electronic and recording equipment was all in a station wagon some 30 metres down wind from the sensing head. IRIG frequency bands 7, 8 and 9 respectively were used for the x, y and z components, and recorded on $\frac{1}{4}$-inch magnetic tape using a two channel tape recorder. The data were put on one channel, while field notes were simultaneously dictated through a microphone onto the other channel.

Since the ADDReSOR was not working at the time, the data record could not be digitized automatically. It was possible, however, to make a graphic record from the tape by playing it through the discriminators to a multichannel oscillograph. This was done, using a paper speed of 100 millimetres per second to display the high frequency components in maximum detail. The paper was conveniently ruled with lines at a spacing of 5 millimetres, which facilitated reading the data at intervals of 1/20 second. A 5 minute segment of the graphic record was then digitized visually to a precision of one per cent of full scale, and the numbers were punched into IBM cards. This yielded 1200 cards with a total of 6000 sets of x, y, and z readings. Since the discriminator output of the ADDReSOR has a sharp cut-off at 10 cycles per second, higher frequencies, which were undoubtedly present in the original magnetic tape record, were eliminated in

the transcription to graphic form, and digitizing at 20 points per second provided the minimum frequency of sampling necessary to compute all spectral components in the graphic record without aliasing.

Processing the data involved first converting the three components of thrust to their velocity equivalents according to the procedure outlined in Appendix III, then computing the spectra of the three components as well as the cross spectra and coherence of each pair. This was done at the new Analog/Digital Computing Center at the University Heights campus of New York University, using 100 lags to yield the spectra for frequency increments of 0.1 per second from 0.1 to 10 cycles per second. Each spectral estimate has the dimensions metres^2 seconds^{-2} and represents the contribution to total variance by frequencies lying within its particular band. The mean spectral intensity (metres^2 seconds^{-1}) in the band can be obtained by dividing this figure by the width of the band, which in this case is 0.1 cycle second^{-1}. All the spectra presented here were smoothed by the procedure known as hanning (Blackman and Tukey, 1959), according to which

$$S(n) \text{ smoothed} = .25\ s(n - 1) + .50\ S(n) + .25\ S(n + 1)$$

The spectra are introduced here primarily as evidence that the instrument is capable of yielding results of this type. Conclusions should be drawn only with caution from any detail, both because of the omission of the tie-back rod and also because the location and mounting of the instrument were not as carefully controlled as they should be for such measurements. Despite these reservations, however, some general observations are in order.

The output of the z component was such that a positive signal denotes a downwards force. This has negligible bearing upon any of the results except that the cospectrum of u and w is everywhere positive instead of negative. This was an oversight that could have been simply corrected, but was not.

Logarithmic spectra (Panofsky and Deland, 1957) obtained by plotting the product of frequency n times the spectral estimates S(n) against the logarithm of n, are presented in Figures 28-30. Grossly smoothed versions of the u, v, and w graphs are combined for comparison in Figure 31. The peaks which occur at 7 cycles per second in both the u and v spectra are probably spurious effects due to the omission of the tie-back rod. Otherwise, u shows a maximum of energy at the low frequency end, decreasing rapidly towards 0.5 cycles per second, then more gradually to approximately 6 cycles per second. As frequencies above this the graph levels off to the cut-off at 10 cycles per second. The v spectrum drops more rapidly than that for u at the low frequencies, levels out from 0.3 to 2 cycles per second, and the decreases at the u spectrum does until it levels off at the high frequency end, at a level somewhat higher than that of the u spectrum. The spectrum for w is relatively low at frequencies below 0.4 cycles per second, passes through a maximum in the neighborhood of 1 to 2 cycles per second, and then decreases as do the other two at higher frequencies. In the section of the graphs above approximately 5 cycles per second, where the turbulence may be expected to approach isotropy in the inertial

subrange, the energy of both v and w becomes significantly greater than that of u. This is in qualitative agreement with the theoretical prediction of a 4/3 ratio (Hinze, 1959), although the record is probably not adequate to draw conclusions regarding the quantitative relationships.

The logarithmic cospectrum of $u\text{-}\bar{w}$ in Figure 33 shows a decreasing contribution to the stress with increasing frequency to about 5 cycles per second, where the graph levels off at a mean spectral density times frequency of some 0.003 metre^2 seconds^{-2}. The total area under the curve, 0.12 metres^2 seconds^{-2}, is equal to the contributions to covariance by frequencies on the range 0.1 to 10 cycles per second. The contributions of frequencies lower than 0.1 per second was 0.04 metres^2 seconds^{-2}, and the combined total, 0.16, multiplied by ρ, the density of the air, is equal to the indicated stress. Taking ρ as 1.2×10^{-3} and multiplying by 10^4 to convert metres^2 to centimetres^2,

$$\tau_a = 0.16 \times 1.2 \times 10^{-3} \times 10^{-4} = 1.92 \text{ dynes/cm.}^2$$

The ratio 0.12/0.16 indicates that 75 per cent of the indicated stress was due to frequencies on the range 0.1 to 10 cycles per second, and 25 per cent was due to lower frequencies observed in the five minute record. Figure 33 shows that the contribution to the stress becomes negligibly small for frequencies greater than approximately 5 cycles per second, in excellent agreement with the value of 6 cycles per second at 2 metres height and 10 metres per second in Table 1 (Page 11).

Mean values of u, v, and w during the 5 minutes were 9.25, 0.71 and -0.165 metres per second respectively, indicating

that the axis of the instrument was inclined approximately $\tan^{-1}$ 0.71/9.25 (= $\tan^{-1}$ 0.767) or 4½ degrees to the right, and $\tan^{-1}$ 0.165/9.25 (= $\tan^{-1}$ 0.01785), or about 1 degree above the mean wind direction. The latter apparent inclination is of the right order for the upward flow of the air due to the slope of the beach, but may include some error in plumbing the instrument. Regardless of its cause, however, a finite mean value of w indicates that there was a net mass transport of air in the direction of the z axis of the instrument, and it can be shown by the following reasoning that the resulting error in the computed stress was small but not negligible.

Suppose that the z axis is tilted in the x-z plane through a small angle ϕ with the vertical. For small angles, θ, of wind fluctuation in the same plane this will produce negligible error in the u component, which is proportional to V cos $(\theta + \phi)$, but relatively larger errors in w, which is proportional to V sin $(\theta + \phi)$. To a close approximation, the indicated vertical component, w_a, will be given by

$$w_a = w + u \tan \phi$$
$$= \overline{w} + w' + (\overline{u} + u') \tan \phi,$$

consisting of the apparent mean vertical component

$$\overline{w}_a = \overline{w} + \overline{u} \tan \phi,$$

and the apparent turbulent fluctuations of the vertical component

$$w'_a = w' + u' \tan \phi.$$

Now the computer program for the spectra first subtracts $\overline{w_a}$ from w_a, as indicated in the INTRODUCTION, page 5, so that the mass transport term is already eliminated, leaving only the indicated

stress
$$\tau_a = \rho\overline{u'w'} + \rho\overline{u'u'}\tan\phi$$
$$= \tau + \rho\overline{u'^2}\tan\phi$$
$$= \tau + \rho\sigma_u^2\tan\phi$$

where τ is the true stress and σ_u is the standard deviation of u. From the results of the spectral computation, $\sigma_u = 1.148$ metres per second, so that the error term in the expression for the apparent stress is

$$\rho\sigma_u^2\tan\phi = 1.2 \times 10^{-3} \times 1.148^2 \times 10^4 \times -0.01785$$
$$= -0.28 \text{ dynes/cm}^2$$

The true stress, τ, is therefore given by

$$\tau = \tau_a - \rho\sigma_u^2\tan\phi \qquad (2)$$
$$= 1.92 + 0.28 = 2.2 \text{ dynes/cm}^2$$

and the error is approximately 15 per cent of the indicated value.

This calculation serves to show that the results will be subject to error if the instrument is not correctly aligned relative to the mean wind, but also that the error can be computed and eliminated where the angle of deviation is small. The programs for the spectral computations should be so written as to give the means and standard deviations of the three components for this purpose. The same reasoning will apply, of course, to any instrument used for the "direct" measurment of stress in a fixed mounting.

Substituting the value of τ in the relation

$$\tau = \gamma^2 \rho\bar{u}^2$$

indicates the value of γ^2, the coefficient of surface friction, or drag coefficient, to be approximately 0.00224, a value which is slightly lower than the 0.0026 or 0.0028 obtained by others

for this wind speed (Munk 1949, Neumann 1948). Some of the difference may be due to the shortness of the record analyzed and the exclusion, therefore, of still lower frequencies.

Coherence graphs of the three pairs of components are presented in Figures 36-38. Once again, the peaks observed at 7 and 10 cycles per second and the improbably high values found at the high frequency end of the u-w graph are almost certainly due to the omission of the tie-back rod. It is interesting to note the striking similarity between Figure 37 and Figure 33, emphasizing that the coherence of u and w was due much more to the cospectrum than to the quadrature spectrum.

Double logarithmic graphs of the u, v, and w spectra and the uw cospectrum are presented in Figures 39-42. The spectral densities of u and w seem to decrease according to an inverse square relation with frequency, whereas those of v as well as the cospectral densities of u-w seem to fall between this and a -5/3 relation.

DISCUSSION

Merits, Faults, and Modifications

The principal merits of the three-component thrust anemometer that have been demonstrated thus far are:

1. its small size,
2. its speed of response,
3. the linearity of its output (in terms of the square of wind speed),
4. the convenience of three independent outputs corresponding to the three components of velocity,
5. the compactness of the recording technique that is being used, and the flexibility in the selection of recording methods which the instrument allows.

Its principal faults and disadvantages include the following:

1. the nonlinearity in the resolution of small angles, expecially in the y component,
2. the "noise" level, which is excessive at velocities in the vicinity of 3 metre per second, and appreciable but tolerable at higher velocities.

It is not entirely clear from the experimental evidence whether the cause of the nonlinearity in the resolution of small angles is primarily mechanical or primarily aerodynamic in its origin, although the greater weight of evidence seems to favor the latter explanation. In either case, the problem can certainly be solved by more precise fabrication and construction, and by further

experimentation with different types of shell and perforation patterns. Meanwhile, the output can be corrected by a simple modification to the computer program for converting thrust components to velocity components.

The most probable sources of mechanical difficulty are in slight departures from orthogonality of the three transducers, and in defective flexible ties. The ties were made from phosphor-bronze wire that had been coiled and had to be straightened by hand. Their residual curvature, as well as faulty alignments in connecting the ties to both the studs and the clamps are likely sources of error. The use of straight ties and bonded connections to the great circles would probably improve both linearity and consistency of angular resolution. This in turn would be facilitated by using great circles made of thin metal, rather than the thicker PVC circles, and soldering the flexible ties directly to them.

The aerodynamic characteristics of the instrument depend upon the nature of the shell and its perforations. Further experiments are required to determine an optimum design both for linearity of angular resolution and minimum noise level. It may be that a thin shell of molded metal or plastic would be preferable to the relatively thick styrofoam. It is also conceivable that different shell configurations would be optimum at different wind speeds, and that an anemometer should have two or more replaceable shells for use under different conditions. The styrofoam spheres have the evident disadvantage that rain or spray will tend to be absorbed, effectively changing the weight, and hence the zero point of the z component. A metal sphere would be affected much less in this respect.

Provided that the flow of air around the assembly within the sphere does not introduce extraneous thrusts, it is reasonable to expect that the noise level of the instrument, due to eddy shedding and induced turbulence, can be reduced almost to an arbitrarily low level by perforating the shell sufficiently. This follows since if the shell is thin enough and the holes large and close enough, the sphere becomes effectively a cage composed of fine wires, each segment of which should shed eddies at a frequency which will be one or more orders of magnitude higher than those which this instrument is intended to observe.

Another modification which will be tried in the near future, as soon as a wind tunnel is available for testing, is a redesign of the support, replacing the radial wires and support ring by a vertical stem which passes through the sphere, as is used in the instrument designed and built by Flow Corporation, Inc. This arrangement had been considered originally but was rejected in favor of the radial wires in our present design. A more radical departure will be to place the transducers outside the sphere on the support ring and dish, and attached to the sphere by long external flexible ties. This instrument is under construction at the time of writing, and promises the advantages of cheaper construction, easier adjustment and maintenance, and the possible use of a smaller sphere. Furthermore, since there will be nothing inside the shell, there are essentially no restrictions on the pattern of perforations that can be used.

Mounting

One difficulty and potential limitation in the use of the present instrument is the requirement of an essentially

vibration-free mounting. Since the sphere is supported entirely by the transducers, any acceleration of the support appears as a thrust due to the mass of the shell and associated moving parts.

In practice it is not hard to construct a support which meets the requirements on land or on a fixed platform over the water. The problem may prove to be more difficult with a floating support under other than very moderate weather and sea conditions. It is desirable to make measurements in mid ocean under a wide range of weather and sea states, but until the necessary float and mounting have been developed, measurements can be made under essentially equivalent conditions using fixed towers of the type described by Doane (1963). These towers are supported by a submerged buoyant chamber which is held beneath the surface and prevented from moving by a system of anchors with oblique and vertical cables. They have been successfully used in the Great Lakes, and with some modification should be applicable to oceanic work in depths up to 50 fathoms, or perhaps greater.

Additional Applications

In addition to its use for measuring the vertical transport of momentum, the sphere should be readily adaptable for determinations of the transports of heat, and possibly also of water vapor. A tiny bead thermistor or thermocouple could be mounted in one of the holes on the windward side where it would be well ventilated without interfering with the aerodynamic response of the anemometer. Heat and velocity would then be effectively measured by the same instrument, involving no problems of spacial or phase relations other than the matching of the response times

of temperature and velocity elements. As yet there appears to be no device available for the measurement of water vapor which combines the speed of response, smallness of size, and reliability of performance for a similar installation. However, the "humistor" seems to be a major step in this direction, and it is to be expected that such a unit will eventually be produced. When this is the case, it should be possible to combine velocity, heat and humidity sensors in the one spherical head, making an almost ideally compact unit for vertical transport measurements.

Another adaptation which will be attempted shortly is to make the sensing head suitable for use under water as a three-component current meter. Such a device should be useful for the study of orbital motions of waves and various turbulent motions in the sea and could have an especially interesting application in the study of the stress beneath the surface associated with the wind stresses above it.

A Stress Meter

Since thrust is proportional to the square of wind speed, we may write

$$F = kV^2$$

$$\text{or} \quad V = F^{\frac{1}{2}}/k^{\frac{1}{2}}$$

$$\text{and} \quad u = V\frac{F_x}{F} = \frac{F^{\frac{1}{2}}}{k^{\frac{1}{2}}} \qquad \frac{F_x}{F} = \frac{F_x}{k^{\frac{1}{2}}F^{\frac{1}{2}}}, \quad w = \frac{F_z}{k^{\frac{1}{2}}F^{\frac{1}{2}}}$$

as outlined in Appendix III.

It has been shown that the stress is equal to the total vertical transport of horizontal momentum provided that the mean vertical wind speed, $\overline{w}$, is precisely zero. Under these

conditions $$\tau = \frac{1}{T}\int_0^T \rho u w \, dt$$

$$= \frac{\rho}{T}\int_0^T \frac{F^{1/2}}{k^{1/2}}\frac{F_x}{F} \cdot \frac{F^{1/2}}{k^{1/2}}\frac{F_z}{F} \cdot dt$$

$$= \frac{\rho}{kT}\int_0^T \frac{F_x F_z}{F} \cdot dt .$$

But near the surface with a "steady" wind F_x is very nearly equal to F so that to a good approximation

$$\tau = \frac{\rho}{kT}\int_0^T F_z \cdot dt = \frac{\rho}{k}\overline{F_z} \qquad (3)$$

This means that, in theory at least, a direct reading stress meter can be built by simply adding an integrating circuit to the output of the z component of the anemometer.

In practice the feasibility of the method will be limited by the need for very precise erection of the instrument and the maintenance of a highly stable zero point. It is possible to test the hypothesis in principle, however, by use of the 6000 values of Z read from the graphic record which was described in the section FIELD TEST AND COMPUTED RESULTS. These values were read to the nearest 1 per cent - call this one division - of the full range of Z. Since the amplifier was set on gain position 3, the calibration was 5 grams for full range, or 49 dynes per division. The zero reading was taken visually as 55 (that is, the output in still air with the hood on the instrument), and all values were treated by the computer as positive or negative deviations from this. The value of k was 13×10^{-3} grams centimetres^{-1}. The sum of the 6000 readings of Z, added subsequently by computer, was 307,810, giving an average value of 51.302, and a net of 51.302 - 55.000 = -3.698 divisions. This corresponds to a mean component of force, $\overline{F_z}$ = -3.698 x 49 = -181.2 dynes, and hence to an apparent total momentum transport of -181.2 (gm., cm^{-1}.,

sec^{-2}). (Z was positive downwards, negative upwards).

Since the hypothesis is based upon the assumption that the vertical mass transport (or apparent vertical mass transport) is zero, transport of momentum by this term must be subtracted. Making the approximation that $F = ku^2$,

the force on the sphere due to the mean wind will be

$$k\bar{u}^2 = 13 \times 10^{-3} \times 925^2 = 11.1 \times 10^3 \text{ dynes},$$

since $\bar{u}$ was 9.25 metres per second. If we now define ϕ as the angle of inclination of the apparent mean wind relative to the instrument, this mean wind will have a z component of force on the sphere of

$$F_z = F_x \tan \phi = 11.1 \times 10^3 \times -0.01785 = -198.1 \text{ dynes},$$

where 0.01785 is the tangent of ϕ obtained in the section FIELD TEST AND COMPUTED RESULTS. The net mean vertical force on the sphere, $\overline{F_z}$, due to the apparent shearing stress alone is therefore -181.2 + 198.1 = 16.9 dynes (downwards), and the apparent shearing stress, τ_a, is by equation (3)

$$\tau_a = \frac{\rho}{k} \overline{F_z} = \frac{1.2 \times 10^{-3}}{13 \times 10^{-3}} \times 16.9 = 1.56 \text{ dyne/cm}^2$$

This is within 20 per cent of the 1.92 dynes per centimetre^2 obtained for τ_a by means of the cospectrum of u and w, which can be regarded as very satisfactory in view of the additional approximations involved in the large mass transport term. It does not appear worth while at this stage, however, to try to estimate the effect of the angle ϕ on the stress itself, corresponding to the correction term in equation (2) on page 61. Such a correction would be required to convert the value of τ_a derived here to a true stress which could then be compared with the τ obtained from the cospectrum.

Assuming that it were possible to construct such a stress meter, another approximation enables a simple determination of the drag coefficient of the surface beneath. Recognizing that u and v are very nearly equal, and setting $\overline{u^2} = \bar{u}^2$, we can write

$$\tau = \gamma^2 \rho \bar{u}^2 = \gamma^2 \rho \overline{u^2} = \frac{\gamma^2 \rho}{k} \overline{F_x}$$

Combining this with (3),

$$\frac{\gamma^2 \rho}{k} \overline{F_x} = \frac{\rho}{k} \overline{F_z}$$

and γ^2 equals the ratio of the means of F_z and F_x. To test this result we assume that the mean value of F_x is given nearly enough by the thrust corresponding to $\bar{u}$, (since the X values have not been summed), so that

$$\gamma^2 = \frac{16.9}{11.1 \times 10^3} = .00152$$

This is within 20 per cent of the value .00186 which follows from $\tau_a = 1.92$ dynes per centimeter^2 on page 69.

The apparent precision of these results depends, of course, upon the definition of the zero point of Z, and the elimination of the effects of the mass transport term. Such precision is obtainable by the digital computer in summing and averaging 6000 values of w, since it may be assumed that random errors will be effectively cancelled in a sample of this size. To accomplish the same accuracy by aligning the instrument itself would be very much more difficult. The method, however, is intriguing enough, and if successful would be valuable enough, to warrant further investigation.

Conclusion

The instrument in its present form can be used at velocities above about 4 metres per second to yield results which are precise to within 3 per cent of vector magnitude in the x and

z component, and which are readily correctible to the same precision in the y component. Its output is in a form which is convenient for both recording and computing. The instrument itself is functionally simple, and with the anticipated modifications should have wide applications for studies of turbulent transports in the atmosphere, and possibly also in the sea. There is very little doubt that the present deficiencies in its performance can be effectively eliminated by improved fabrication and assembly and by further experiments with different types of shell. Moreover the efficient operating range can almost certainly be extended to lower velocities by modification of the shell and perforation pattern. In the meantime the instrument very usefully extends our capability of observing wind turbulence and vertical transports over both land and sea.

As mentioned in the INTRODUCTION, the present arrangement for recording on magnetic tape was designed to feed data through the ADDReSOR system of the Woods Hole Oceanographic Institution to a digital electronic computer. The derivation of the three components of wind velocity, as well as the computation of stress, vertical transport, the spectra of turbulence, and so forth will be accomplished by suitable programming of the computer. The choice of this method of recording and data processing was purely a matter of convenience, and there is no reason why the output of the three component amplifiers cannot be recorded by any other suitable means such as a multi-channel graphic recorder, a digital paper punch, etc. The primary considerations in choosing any such system, in addition to the fidelity of the record and convenience in the field, will be the ease with which the data can be extracted and supplied to a computer, and the flexibility of the programming which such a record permits.

APPENDIX I: ADJUSTMENTS

When assembling each individual transducer unit, care must be taken to ensure that the core of the transformer passes through the bore without touching the side. A special sleeve was made which threads onto the tie rod and which just passes through the bore. The unit was then assembled with this sleeve replacing the core of the transformer. The springs and clamps were accurately positioned and fastened in place, then the tie rod and sleeve were withdrawn and the sleeve replaced by the core of the differential transformer. These were then mounted in position and the unit was tested for hysteresis. For this purpose a suitable excitation voltage is applied to the primary and the output from the secondary is taken either to a vacuum tube voltmeter or to the input of a differential amplifier. If the core is touching the side of the bore, pronounced and irregular hysteresis effects will be observed when slight displacements are applied to the spring system in either direction.

In general this test will have to be accompanied or preceeded by an adjustment of the position of the differential transformer by means of the two position screws, S (Figure 2), which move the sliding base, E, back and forth. Since the linear range of the differential transformer is only $\pm$.005 inch (.0127 cm.) the transformer must be quite accurately positioned in relation to the core.

When all three transducer units have been individually assembled and tested, the three rings, A, B, and C, are fastened together. The three units should now be accurately orthogonal to one another in combined transducer assembly and the three lines which

would be formed by producing the flexible ties toward the center should all be diameters of the sphere. Ideally, this should follow automatically if all the components have been made with sufficient precision. In practice, however, it has been found necessary to make small adjustments in the following manner.

The collar, S, is slipped over ring C and fastened in place. Four specially made probes are now inserted in the holes in S through which the flexible ties are to pass. Each probe fits just tightly enough that the pointed end accurately designates the position where the inner end of the tie should be joined to the clamp. If the individual transducer unit has been correctly positioned, the small hole which will receive the flexible tie should be at this point. Adjustments consist of moving the mounting beams very slightly on the mounting rings and moving the mounting rings A, B, and C slightly relative to one another. When the correct positions are found all components are firmly secured together.

The three PVC great circles are now loosely assembled around the combined transducer assembly and the whole placed in a special holder and jig. This holder fits over the collar and has slots for two of the PVC rings. The third ring is held accurately positioned in the plane of the equator. The holes which will receive the flexible tie studs are now in line with the holes in the clamps. The other two rings will be positioned automatically by the studs, which have already been soldered to one end of the flexible ties. These are now inserted and the other end of the flexible ties are soldered to the clamps.

The y and z components have thus been aligned and it remains to check the alignment of the x component. Other probes are inserted through the two remaining holes in the PVC rings which will receive the flexible ties of the x component. The pointed ends of these probes are directed to the holes in the clamps. The x component transducer unit is then adjusted in position as necessary to make the two probes colinear and perpendicular to the plane of the y and z components. The flexible ties are then inserted as before and soldered in place.

The eight radial wires are passed through the remaining eight holes in the PVC ring at the equator, then through the collar and the terminal strips. The ends are bent sharply at right angles and soldered to the inner face of the terminal strips. The outer ends of the radial wires are fastened to the insulators at the outer support ring so that the z component will be vertical and the y component horizontal. The x component will then be normal to the plane of the support ring. The machine bolts through the insulators are adjusted so that the sensing head is at the center of the support ring and the tension on the radial wires is approximately equal. The latter can be established by tightening the wires until they emit approximately the same note when plucked. About an octave above middle C seems to be satisfactory, corresponding to a tension of the order of 1.5 kg.

APPENDIX II: PHASE MATCHING

In order to achieve optimum linearity of response it is important that the phases of the excitation voltage, differential transformer output, and the A.C. input bias be matched. It was found that this could be accomplished by placing suitable capacitors across the leads from the differential transformers to the amplifier and across the input from the A. C. biassing transformer. The following procedure was used to determine the size of each capacitor.

(1) The differential transformer was set at its approximate operating position by means of the two position screws (S in Figure 2). This in general is not at the null point and its position can be determined by means of an A. C. vacuum tube voltmeter across the leads from the secondary to the amplifier input. The linear range of the amplifier at minimum gain is about 35 per cent of the linear range of the transducer and it has been found convenient, though not essential, to operate exclusively on one side of the null point. The zero point of the y and z transducers is set approximately at the center of the half range, while that of the x transducer is set near the null point. At zero, therefore, y and z will have an output of approximately 10 to 15 millivolts while x will have an output of approximately 3 millivolts.

(2) The D. C. output bias was set at + 2.5 volts. In order to do this, the input to the amplifier was shorted out by setting the switches to Calibrate and Band Center.

(3) The input short was removed by returning the Cal-Op switch to the operating position. The A. C. input bias was

then set so that the output of the x component amplifier was zero volts, and that of the y and z amplifiers was 2.5 volts. These are the respective zero points of the three components.

(4) A cathode ray oscilloscope was connected to the output of the demodulator circuit, and with the amplifier set to maximum gain the A. C. bias was adjusted to give minimum output as seen on the CRO. Ideally the shape of the trace should be that of a half wave rectifier for finite output (Figure 43, a) reducing to a straight line as the zero point is approached (Figure 43, b). However, if the transducer output and the A. C. bias output are not in phase there will be a residual wave form as the null point is passed (Figure 43, c). Capacitors were now added across the output from the A. C. biassing transformer until the best straight line was obtained at null.

(5) A gentle thrust was applied to the sphere by pressing it with a finger. The pattern on the CRO was again the typical half wave form whose amplitude is proportional to the applied thrust. This was increased until a distortion of the wave form began to appear. Since the demodulator is the first part of the circuit to be overloaded, the first indication of overload should be the appearance of a wave form on the other side of the zero line (Figure 43, d). If the applied voltages are in phase the new wave form will be symmetrical as in part d of the figure. If the voltages are not in phase the wave form will be distorted as in Figure 43, e. Capacitors were added across the leads from the transformer secondary to the amplifier input until the wave forms when overloaded were symmetrical as in Figure 43, d.

(6) In the case of the y and z components, procedure 5 was repeated with a thrust applied in the opposite direction. It was found that the same capacitor was needed at both extremes, indicating reasonable consistency in the phase of the transducers over the range of operation.

(7) Procedures 4, 5, and 6 were repeated to make sure that the corrections applied at each point have not altered the requirements at the other points. The values of capacitance that were used to balance the present instrument are listed in Table 3.

	COMPONENT		
	x	y	z
Signal Input:	.0046	.0045	.0068
A. C. Bias:	.45	.35	.53

Table 3. Values of capacitance (MF) added in phase matching.

Laboratory Adjustments

Preliminary to operation in the field, each component in turn should be adjusted and calibrated in the laboratory by the following procedure.

1. Mount the instrument on the test stand in the normal operating position and make all electrical connections. Adjust the regulated power supplies to exactly + 15 and - 15 volts. Allow 15 minutes warm up.

2. Adjust the excitation voltage to exactly 9.0 RMS by means of the variable dropping resistor.

3. Using a vacuum tube voltmeter, check the zero point output of each transducer. These should be approximately 3 millivolts for the x transducer and 10 to 14 millivolts for each of y and z. If necessary, adjustments are made by moving the differential transformers with the positioning screws, which can be reached by passing a fine screw driver through appropriate holes in the sphere.

4. Connect a high impedance DC voltmeter to the output of the z amplifier; set the Cal-Op switch to Cal (Calibrate) and the Calibration switch to Band Center; set the gain switch to position 1 (maximum gain); adjust the DC output bias of the z amplifier to 2.5 volts.

5. Turn the Cal-Op switch to Op (Operate) and adjust the AC input bias until the z amplifier output is between 1 and 2 volts.

6. Place a 1.0 gram weight top of the sphere and observe the resulting increment of output. This should be exactly 2.0 volts, and the gain of the amplifier should be adjusted until the differ-

ence between the output with the weight on top and without the weight is precisely this amount.

7. Turn the Cal-Op switch to Cal and the Calibration switch to lower Band Edge. The amplifier output should now be 0.0 volts. Turn the Calibration switch to Upper Band Edge where the output should similarly be 5.0 volts. If these values are not obtained, adjust the calibration potentiometer until they are correct. Turning the calibration switch through its three positions should then yield the following outputs from the z amplifier; Lower Band Edge = 0.0 volts, Band Center = 2.5 volts, and Upper Band Edge = 5.0 volts.

8. Using a frequency meter or electronic counter, adjust the VCO of the z component to emit the frequencies corresponding to Lower Band Edge, Band Center and Upper Band Edge respectively as the Calibration switch is turned through its three marked positions.

9. The z component is now correctly adjusted, and procedures 4 to 8 should be repeated for each of the x and y components in turn. For this purpose the instrument is turned so that the axis of the component to be tested is vertical, which can be done by bending the mounting shaft at the universal joint. The x component need only be tested in the "face up" position but the y and components should be tested lying on first one side then the other. If a slight difference is found between the sensitivities on the two sides - due to slight phase shift in the transducer - a compromise setting should be used for the amplifier gain adjustment.

Field Procedure

1. Set up the instrument taking due care to ensure that the mounting stem is vertical and that the x axis is pointed towards the mean wind. Make electric connections.

2. See that the power supplies are giving exactly +15 and -15 volts. Allow 15 minutes warm up. Adjust excitation volts to 9.0.

3. Set all three amplifiers to position 1 (maximum gain), set the Cal-Op switch to Cal and record calibration routine on magnetic tape. This routine consists of a 30 second recording of each lower band edge, band center, and upper band edge in succession, and is used by the ADDReSOR and computer to establish the range on which the data are to be digitized.

4. Place hood over the instrument to exclude all air currents and set the amplifier gain switches to the position which is appropriate for the wind speed to be observed. By means of the AC input bias, adjust the zero point of the x component to 0.0 volts and of the y and z components to 2.5 volts each, at the output of the amplifiers.

5. With the hood still in place make a 30 second recording of the zero points.

6. Remove the hood and make the data run, recording on magnetic tape.

7. Repeat the calibration routine.

8. Replace the hood and record the zero point once more.

Data Processing

Since the outputs of the three components of the system are each proportional to one component of thrust, the magnitude of

the total thrust of the wind, F, can be obtained directly from the relation

$$F = \left[(CxEx)^2 + (CyEy)^2 + (CzEz)^2 \right]^{\frac{1}{2}} \qquad (a)$$

where the C's are the calibration factors and the E's are the electrical outputs of the three amplifiers. And since the drag coefficient is constant over the range of operation,

$$F = kV^2 \quad \text{or} \quad V = k^{-\frac{1}{2}} F^{\frac{1}{2}} \qquad (b)$$

where $k = \frac{1}{2}\rho C_d A$.

The velocity vector and the force vector must act in the same direction, from which it follows that

$$F_x : F_y : F_z : F = V_x : V_y : V_z : V, \text{ and}$$

$$\left.\begin{aligned} V_x &= \frac{F_x V}{F} = \frac{F_x F^{\frac{1}{2}}}{k^{\frac{1}{2}} F} = \frac{F_x}{k^{\frac{1}{2}} F^{\frac{1}{2}}} \\ V_y &= \frac{F_y V}{F} = \frac{F_y}{k^{\frac{1}{2}} F^{\frac{1}{2}}} \\ V_z &= \frac{F_z V}{F} = \frac{F_z}{k^{\frac{1}{2}} F^{\frac{1}{2}}} \end{aligned}\right\} \qquad (c)$$

The determination of vertical transport of any quantity by the turbulent flux method involves correlating V_z with the quantity in question. In the case of the vertical flux of horizontal momentum, V_z is correlated with V_x or the resultant of V_x and V_y. One of the first steps in the computation, therefore, is the derivation of the components of velocity from equations (c). It is important to remember that relation (b) applies to the total vectors of velocity and force, and cannot be applied to individual components except in the limiting case where the other two components are zero. If this mistake is made, one encounters the interesting paradox that the force and velocity vectors are not -

parallel to one another! The disadvantage of having a response which is proportional to the square of wind speed as compared to a linear response, is negligible when the data are to be processed by high speed computer.

ACKNOWLEDGEMENTS

I particularly wish to express my appreciation to:

Adjunct Professor Andrew F. Bunker who served as my thesis advisor during the development of the instrument;

Professor Gerhard Neumann who first interested me in this problem and under whom I did most of my graduate training in Oceanography;

Mr. David D. Ketchum, who designed the electronic circuitry for the instrument (Mr. Ketchum was formerly with the Woods Hole Oceanographic Institution, and is now with Ocean Research Equipment, Inc.)

Professors Richard M. Schotland and Willard J. Pierson, Jr., for many helpful discussions and suggestions;

Mr. Stuart D. Smith and Mr. Vincent Beck of the Bedford Institute of Oceanography, for their valuable assistance in testing the instrument and in preparing this material for presentation;

Mr. James A. Elliott of the Bedford Institute and my son, Edward Doe, for assistance in the tedious job of digitizing the data;

The Woods Hole Oceanographic Institution for providing the facilities and partial financial support for the development of the instrument;

The Ford Foundation for a pre-Doctoral fellowship;

The staff of the Round Hill Field Station of Massachusetts Institute of Technology for the use of their wind tunnel and technical assistance in testing and calibrating the instrument.

REFERENCES

Bairstow, Leonard, 1939: Applied Aerodynamics, 2nd ed., London.

Bunker, Andrew F, 1955: Turbulence and Shearing Stresses Measured Over the North Atlantic Ocean by an Airplane - Acceleration Technique. Jour. Meteorol. 12, 445-455.

Cramer, Harrison E, Frank A. Record, and James E. Tillman, 1962: Studies of the Spectra of the Vertical Fluxes of Momentum, Heat, and Moisture in the Atmospheric Boundary Layer. Mass. Inst. Technol., Meteorol. Dept., Final Rep. under Contract DA-36-SC-80209 for Meteorol. Dept. U. S. Army Electronic Proving Ground.

Deane, Roger E., 1963: Limnological and Meteorological Observation Towers in the Great Lakes. Limnol. and Oceanog. 8, 1, 9-15.

Hinze, J. O., 1959: Turbulence, an Introduction to its Mechanism and Theory. McGraw-Hill, 586 pp.

Hoerner, Sighard F.: Fluid-Dynamic Drag. Publ. by the Author, 148 Busteed Drive, Midland Park, N. J.

Ketchum, David D., and Raymond G. Stevens, 1962: A Data Acquisition and Reduction System for Oceanographic Measurements. Mr. Sci. Instrumentation 1, 55-60.

MacCready, P. S. 1953: Structure of Atmospheric Turbulence. Jour. Meteorol., 10: 434-49.

Mather, John R., ed., 1954: The Measurement of Potential Evapotranspiration. Drexel Institute of Technology, Laboratory of Climatology, Publications in Climatology, VII, 1.

Munk, W. H., 1947: A critical wind speed for air-sea boundary processes. J. Marine Research 6, 203.

Neumann, G., 1948: Über den Tangentialdruck des Windes und die Rauhigkeit der Meeresoberfläche. Z. Meteorol. 2, 193.

Panofsky, Hans A., 1953: Statistical Properties of the Vertical Flux and Kinetic Energy at 100 Meters. Pennsylvania State College, Div. of Meteorol., Sci. Rep. No. 2

_____ and Raymond J. Deland, 1957: Structure of Turbulence at O'Neill, Nebraska, and its Relation to the Structure at Brookhaven National Laboratory, Upton, Long Island. College of Mineral Industries, Pennsylvania State University, Final Rep. under Air Force Contract AF 19(604)-1027.

_____ and R. J. Deland, 1959: One-dimensional Spectra of Atmospheric Turbulence in the Lowest 100 Meters. Advances in Geophysics, 6, 41-64, Academic Press.

Perepelkina, A. V., 1957: Some Results of Investigation of the Turbulent Fluctuations of Temperature and of the Vertical Component of Wind Velocity. Bull. Acad. Sci. U. S. S. R., Geophys. Ser. No. 6, 765-778.

Portman, Donald J., 1957: Soil Temperature Instrumentation. Exploring the Atmosphere's First Mile, Ed. by Lettau and Davidson, 17-20, Pergamon Press.

Prandtl, L. and O. G. Tietjens, 1934: Applied Hydro- and Aero-mechanics. Dover Publications Inc., New York 1957, 270 pp.

Priestley, C. H. B., 1959: Turbulent Transfer in the Lower Atmosphere. University of Chicago Press, 130 pp.

Rosenbrock, H. H.: The design and Development of Three New Types of Gust Anemometer. The British Electrical and Allied Industries Research Association, Tech. Rep. C/T106, 37 pp.

_____ and J. R. Tagg, 1951: Wind- and Gust-measuring instruments developed for a Wind-power Survey. Proc. Inst. Elect. Engineers, Vol 98, Part II, 64, 438-447.

Vehrencamp, J. E., 1952: Development of a Boundary Shear Stress Meter, Univ. of Calif., Dept. of Engineering, Los Angeles. Tech Rep. No. 52-22, prepared under Contract No. N6-onr-275, 1952.

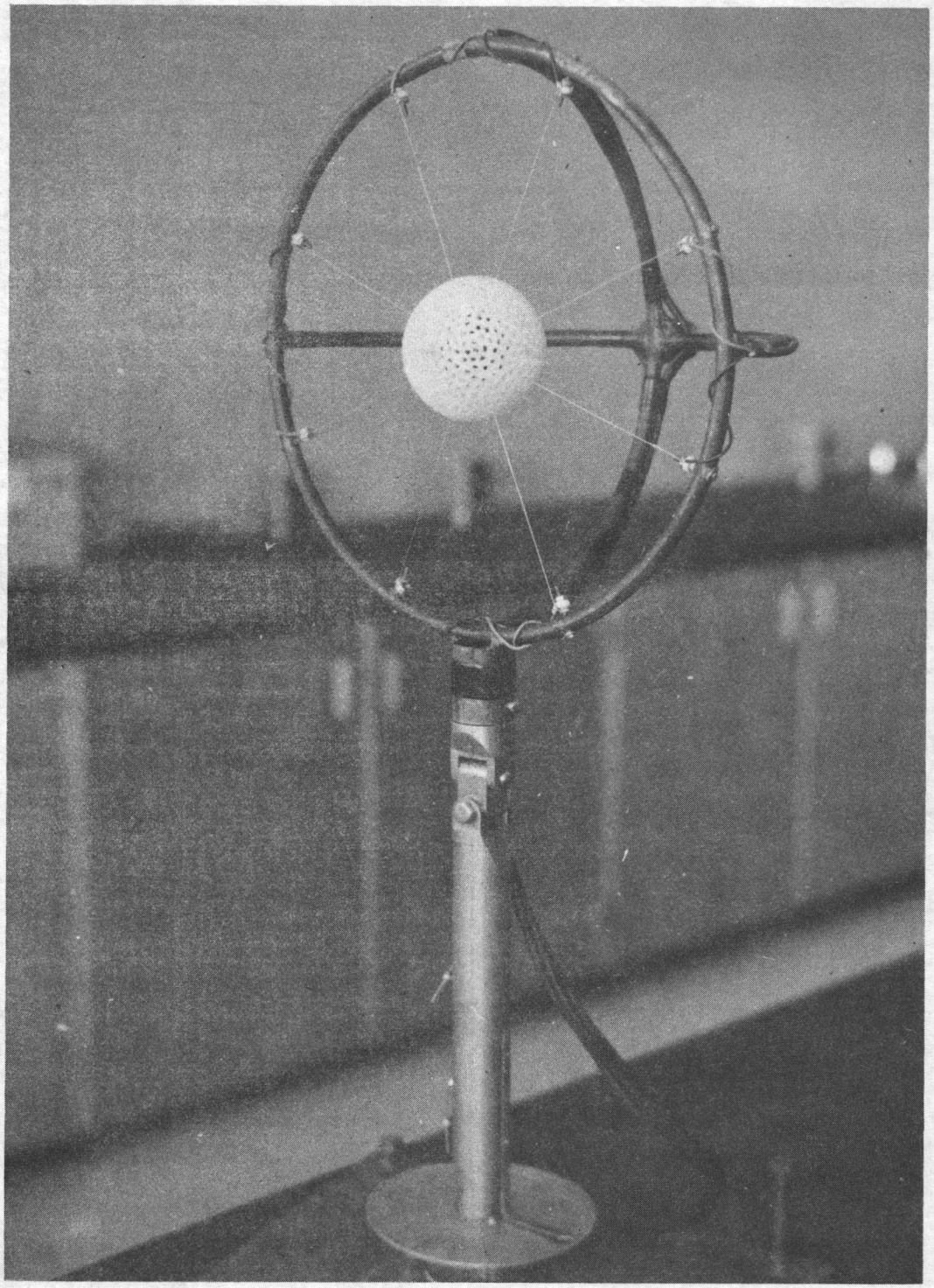

Figure 1. The three-component thrust anemometer.

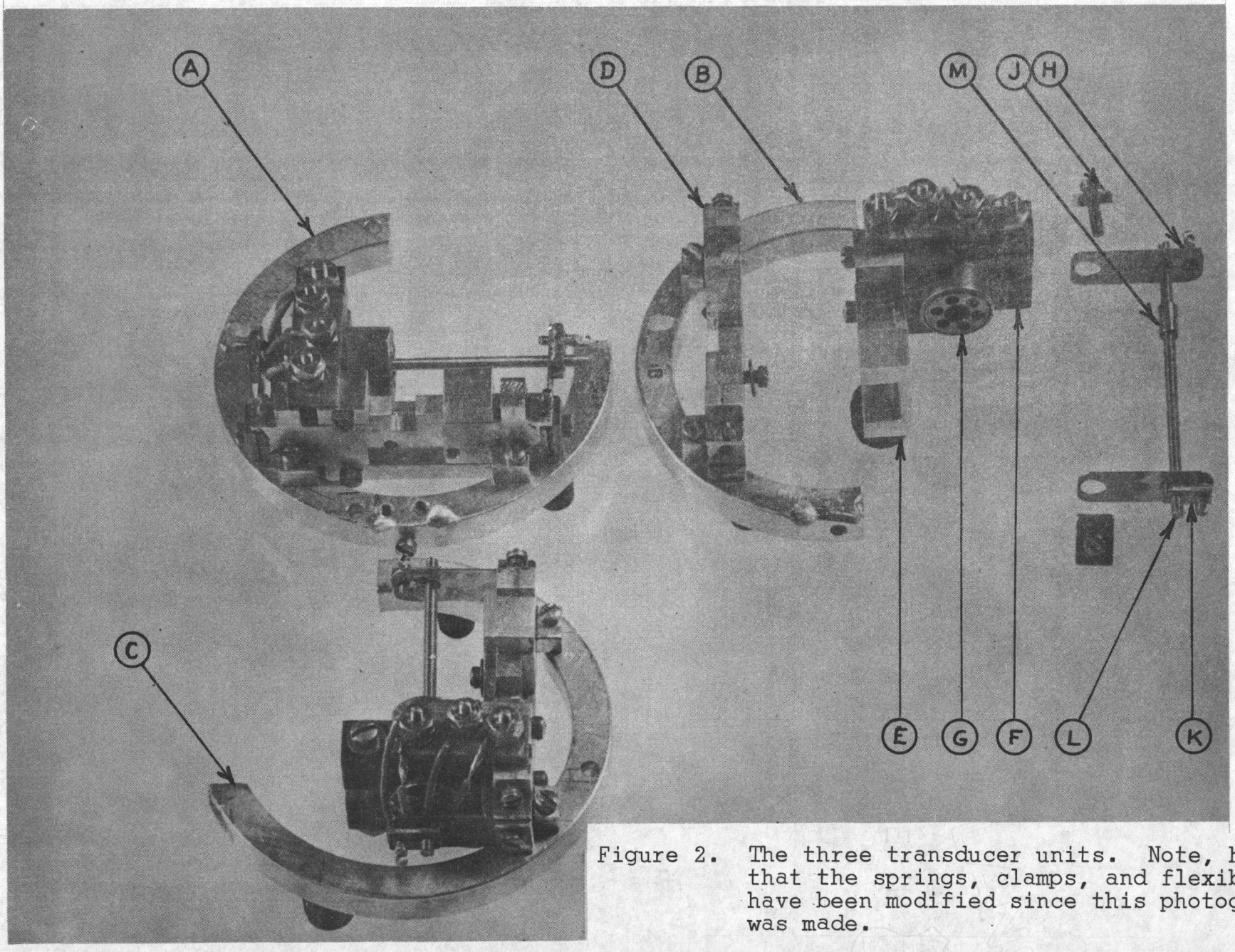

Figure 2. The three transducer units. Note, however, that the springs, clamps, and flexible ties have been modified since this photograph was made.

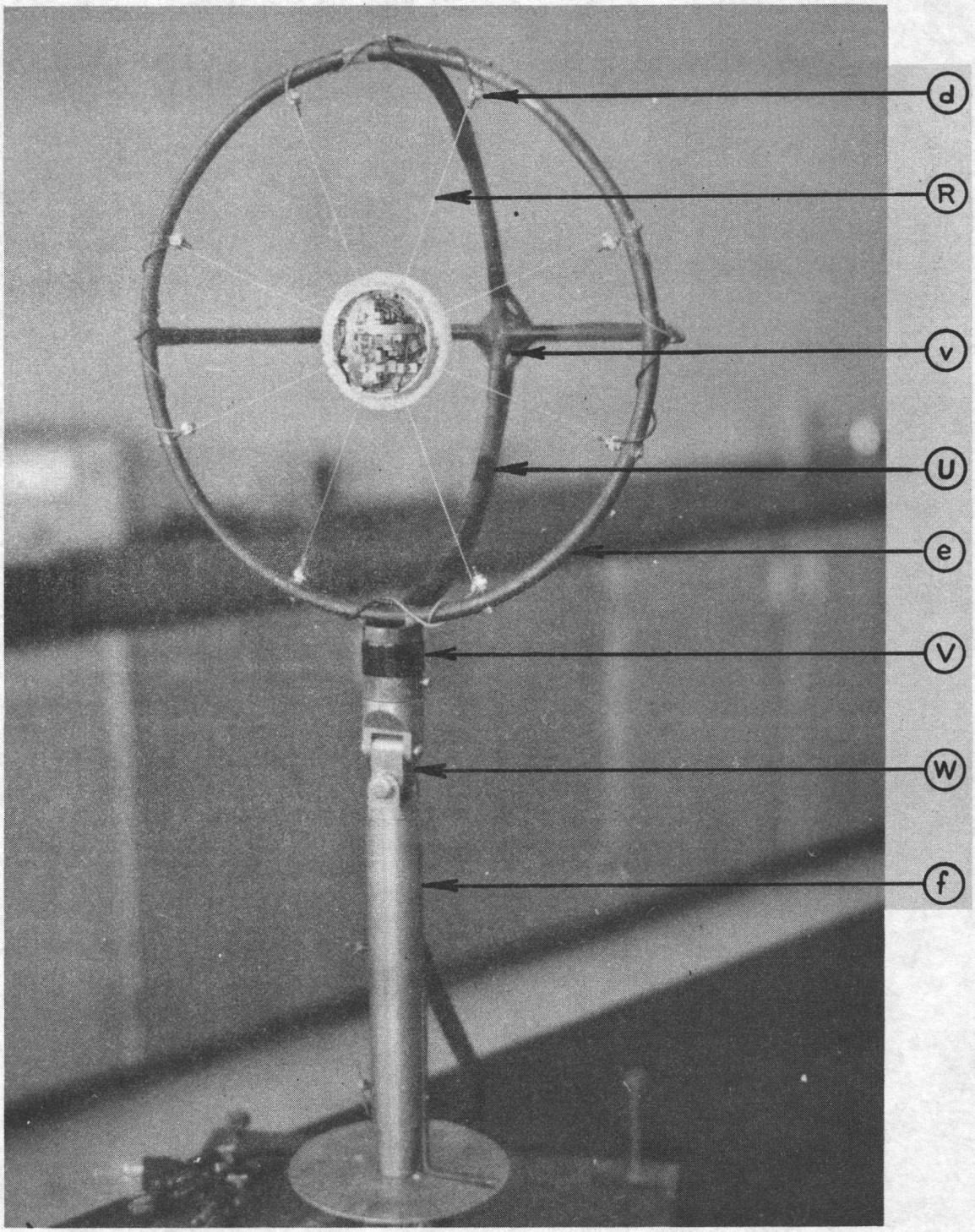

Figure 3. The sensing head with the front hemisphere and PVC great circles removed. This photograph shows the rear hemisphere cemented directly to the flexible ties.

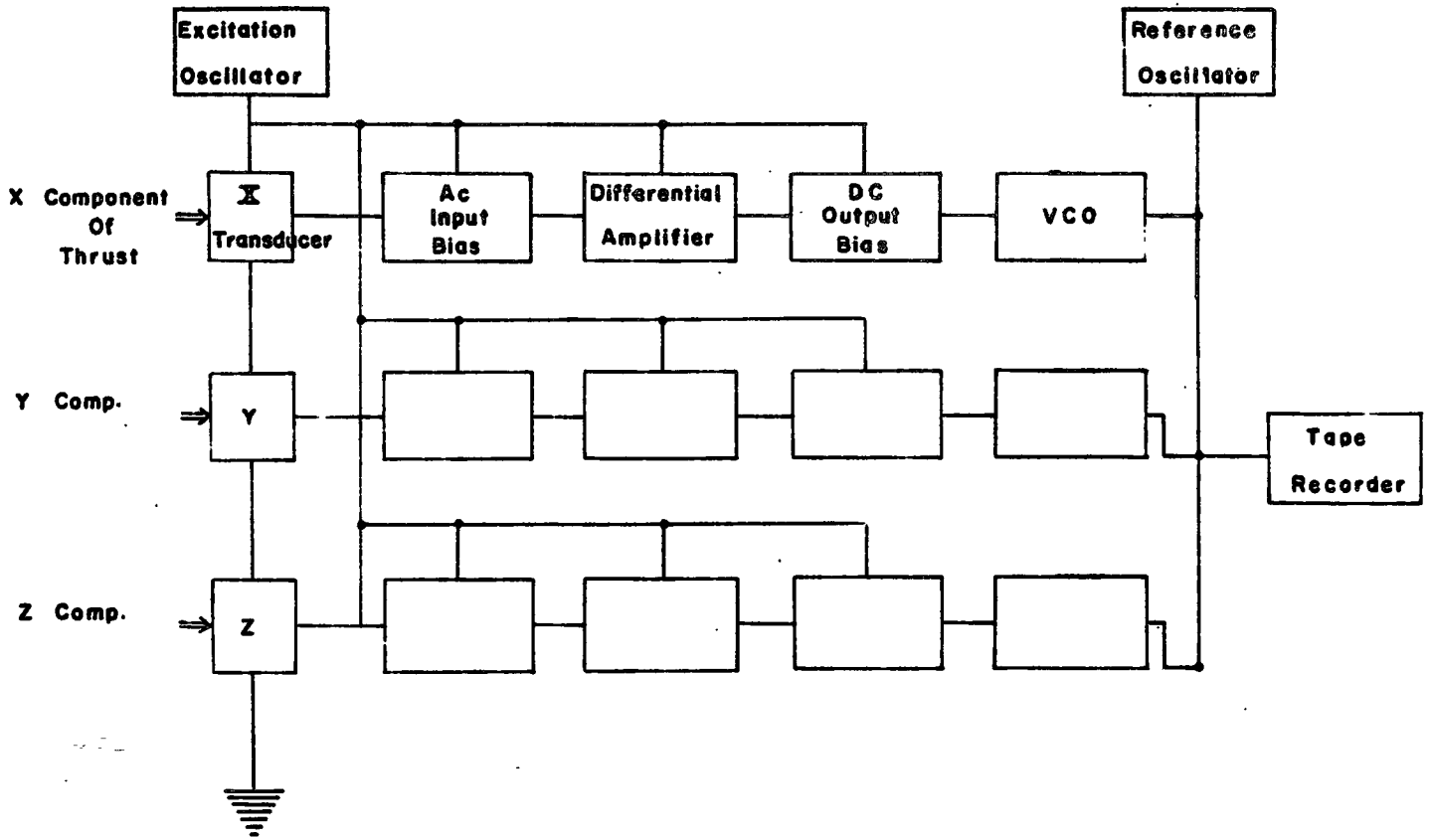

Figure 4. Electric circuit - schematic.

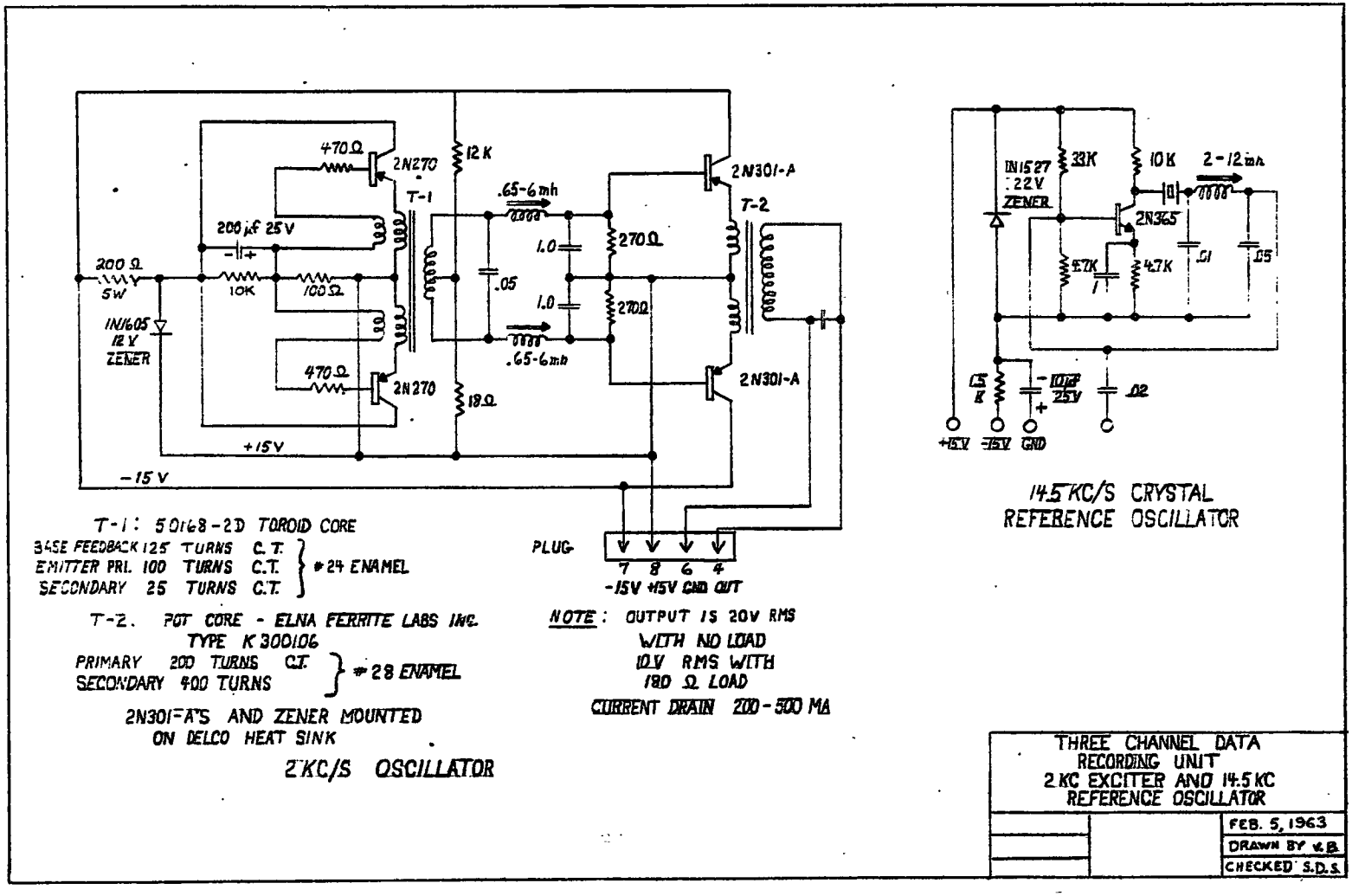

Figure 5. Circuit diagrams of Excitation Oscillator and Reference Oscillator.

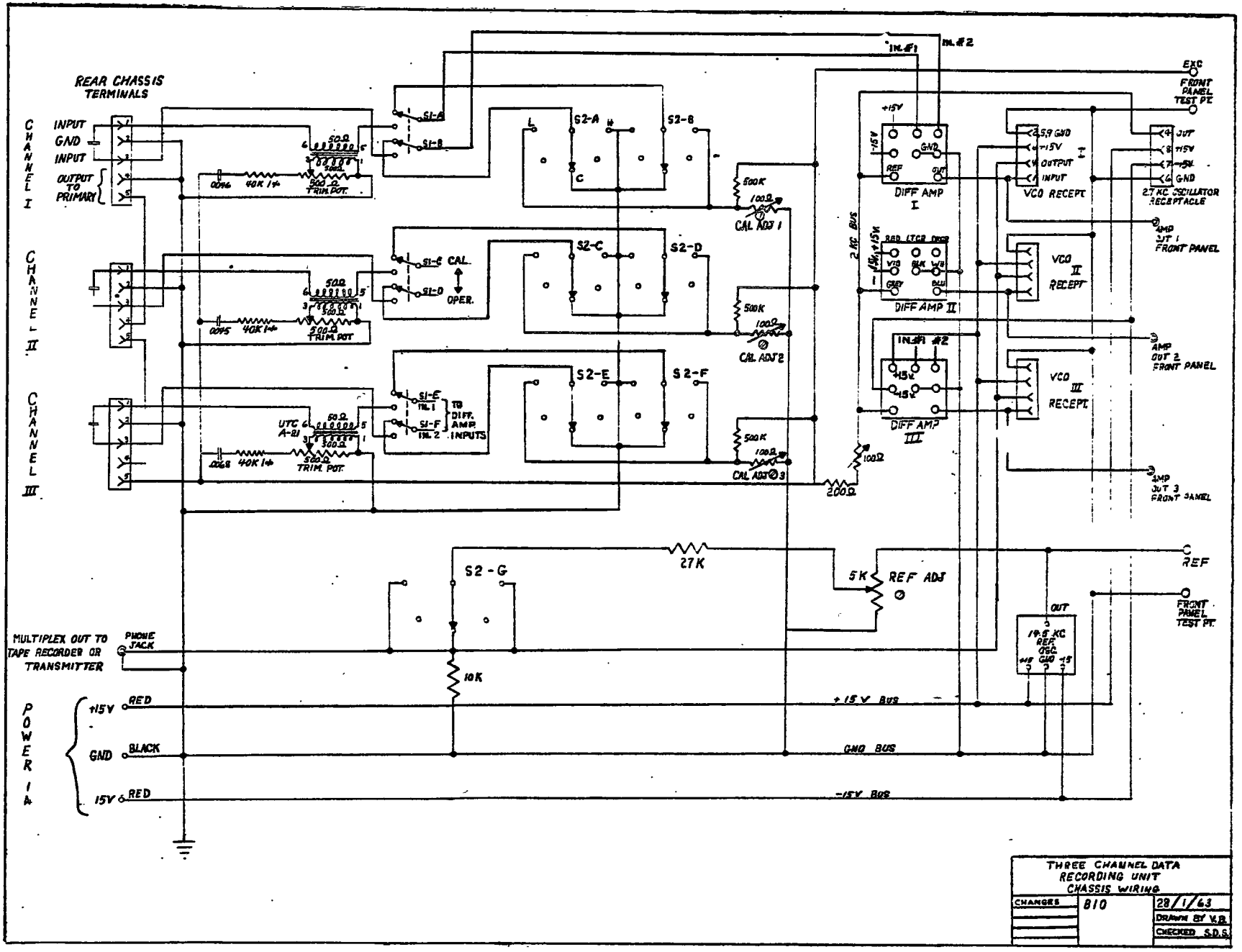

Figure 6. Wiring diagram of amplifier chassis.

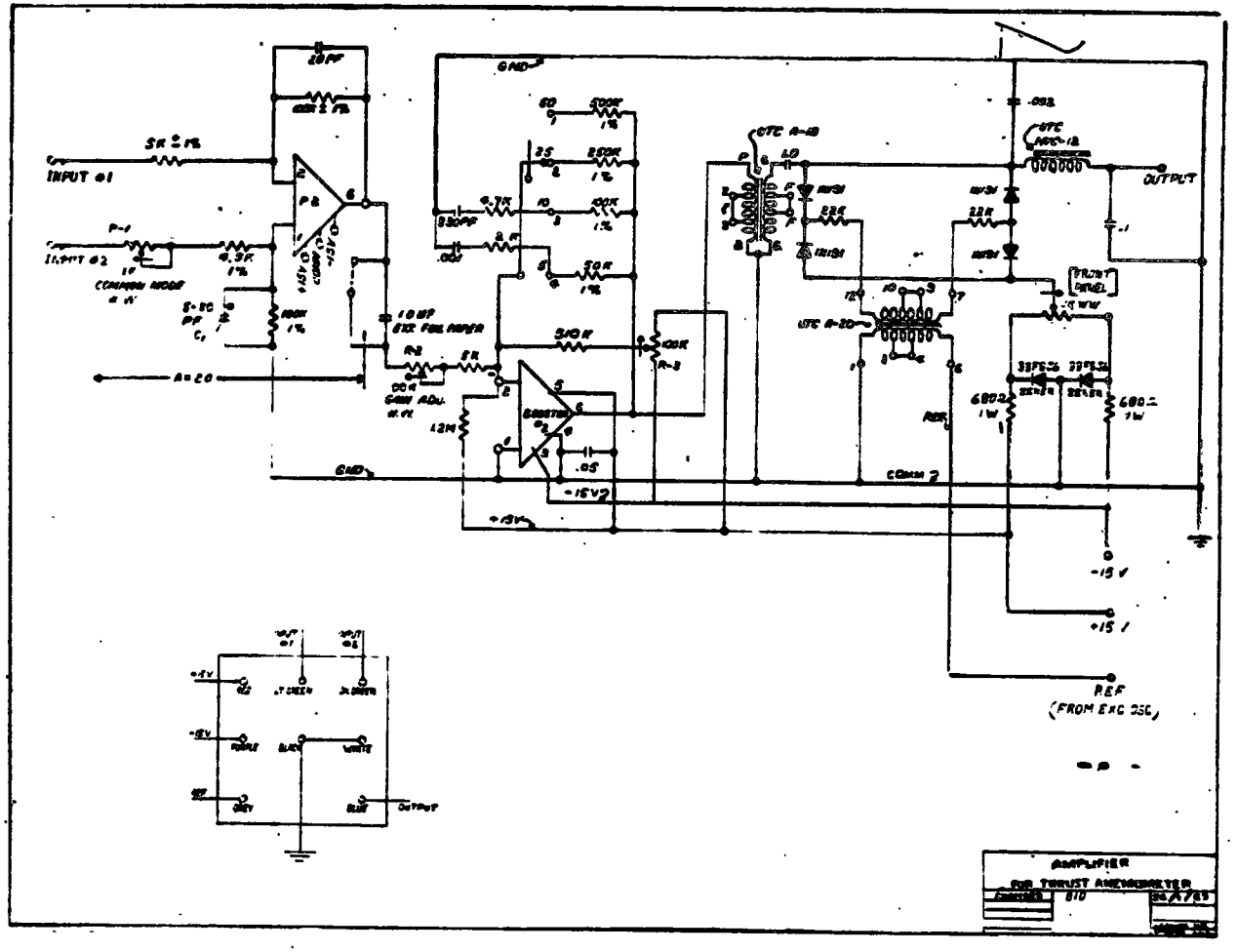

Figure 7. Amplifier circuit diagram.

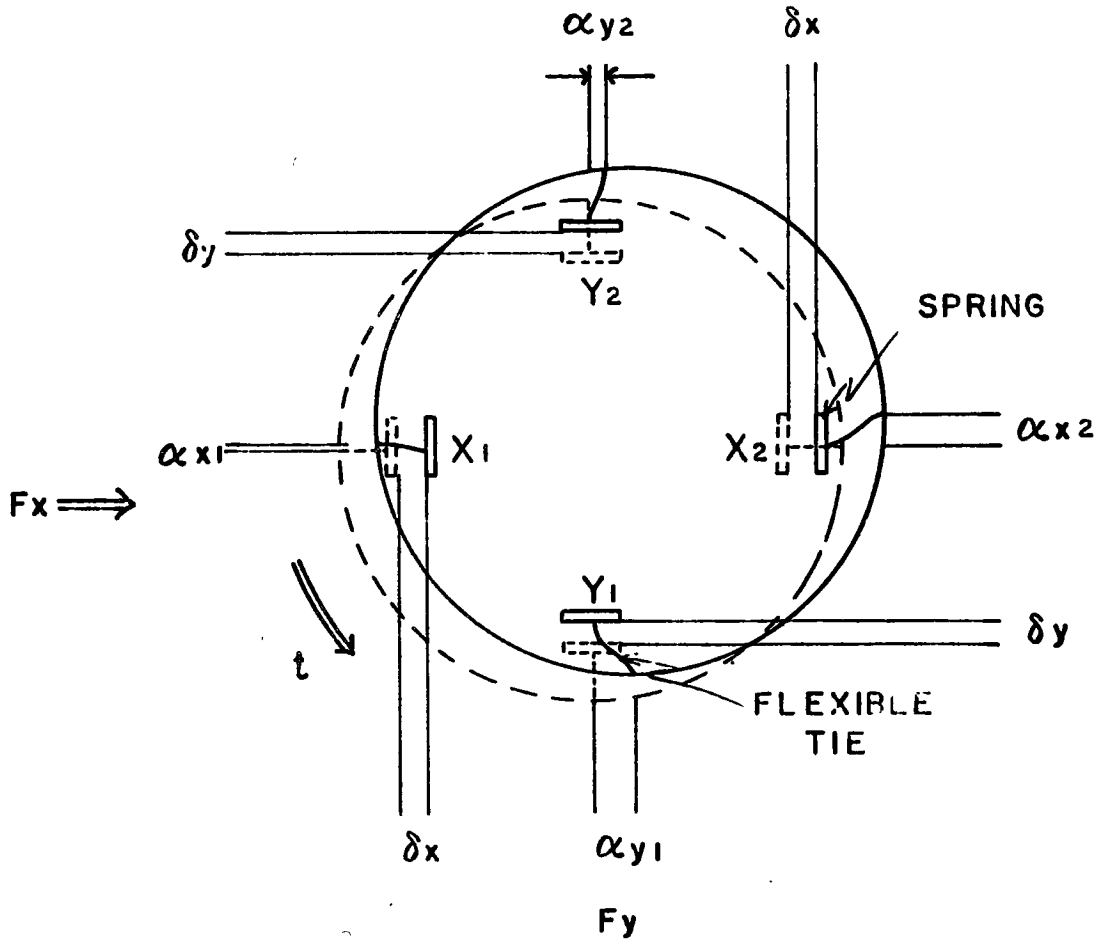

Figure 8. Schematic displacements of springs and flexible ties under combined thrust and torque.

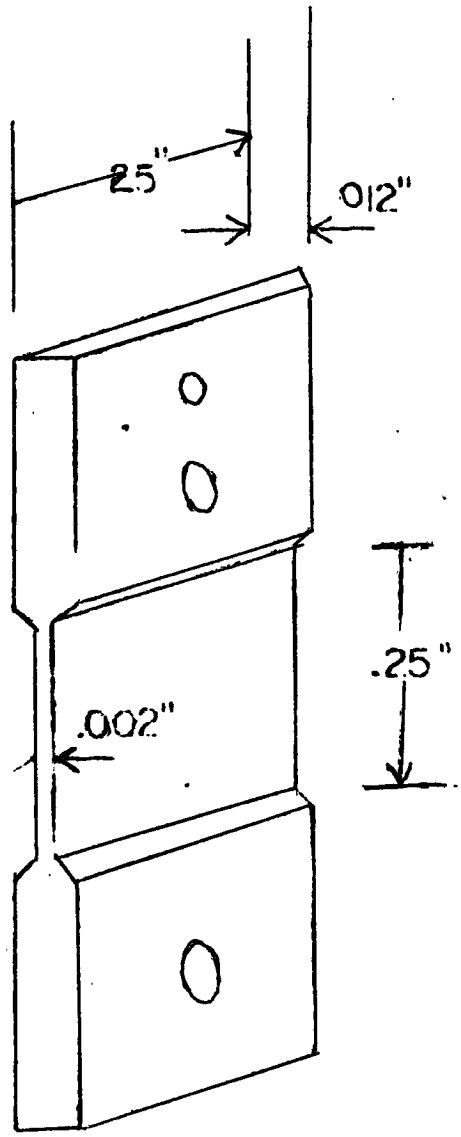

Figure 9. Transducer spring (not to scale).

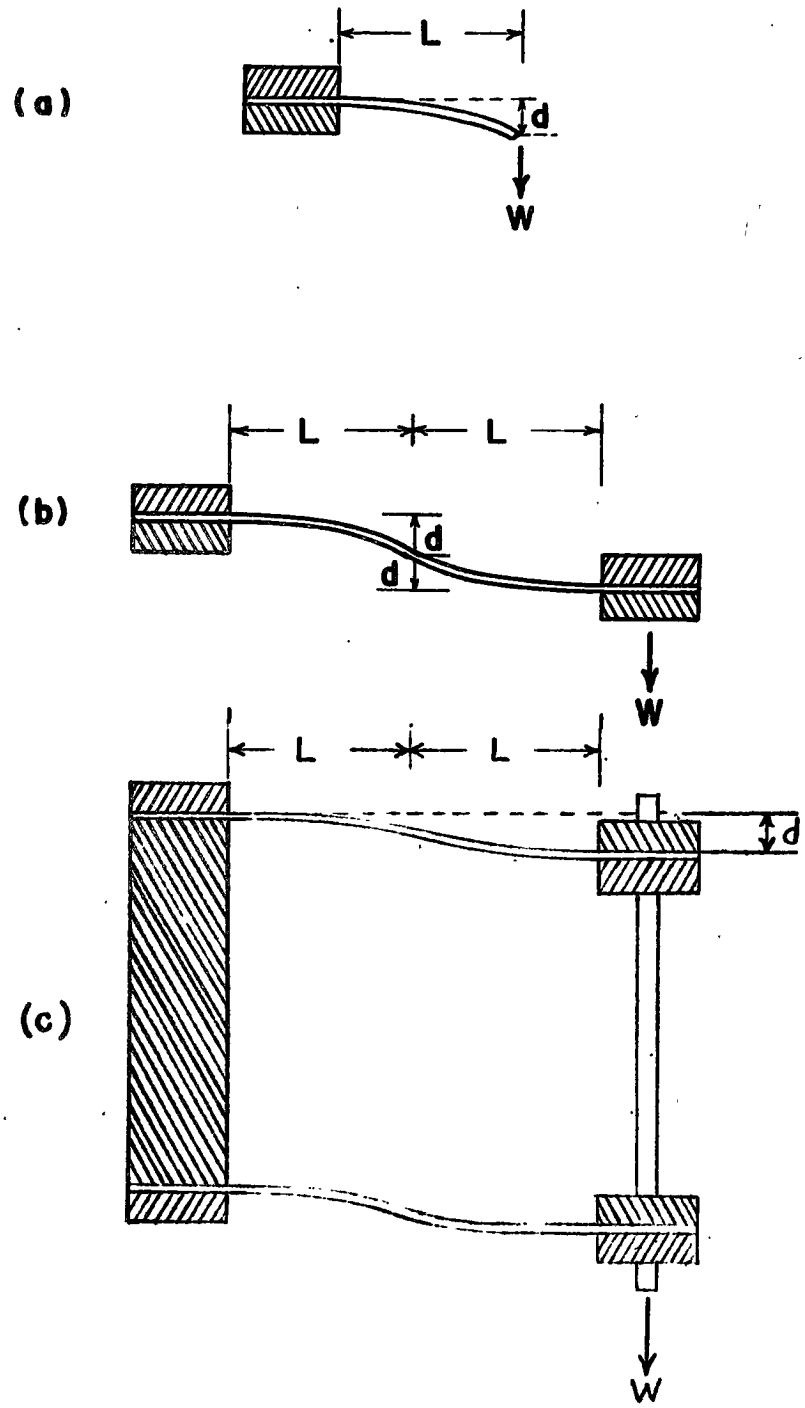

Figure 10. Flexure of springs.

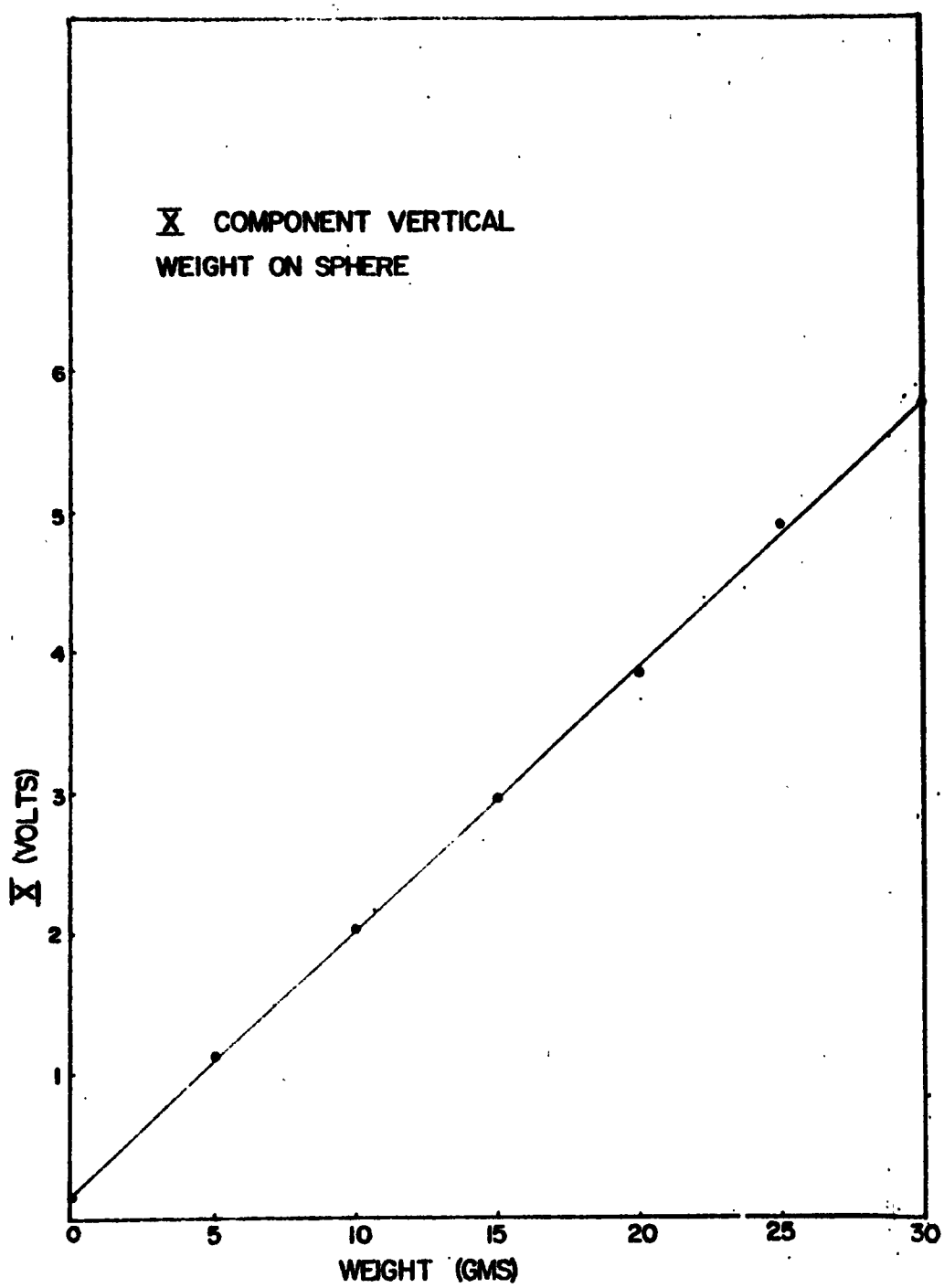

Figure 11. Response of x component to weights placed on sphere.

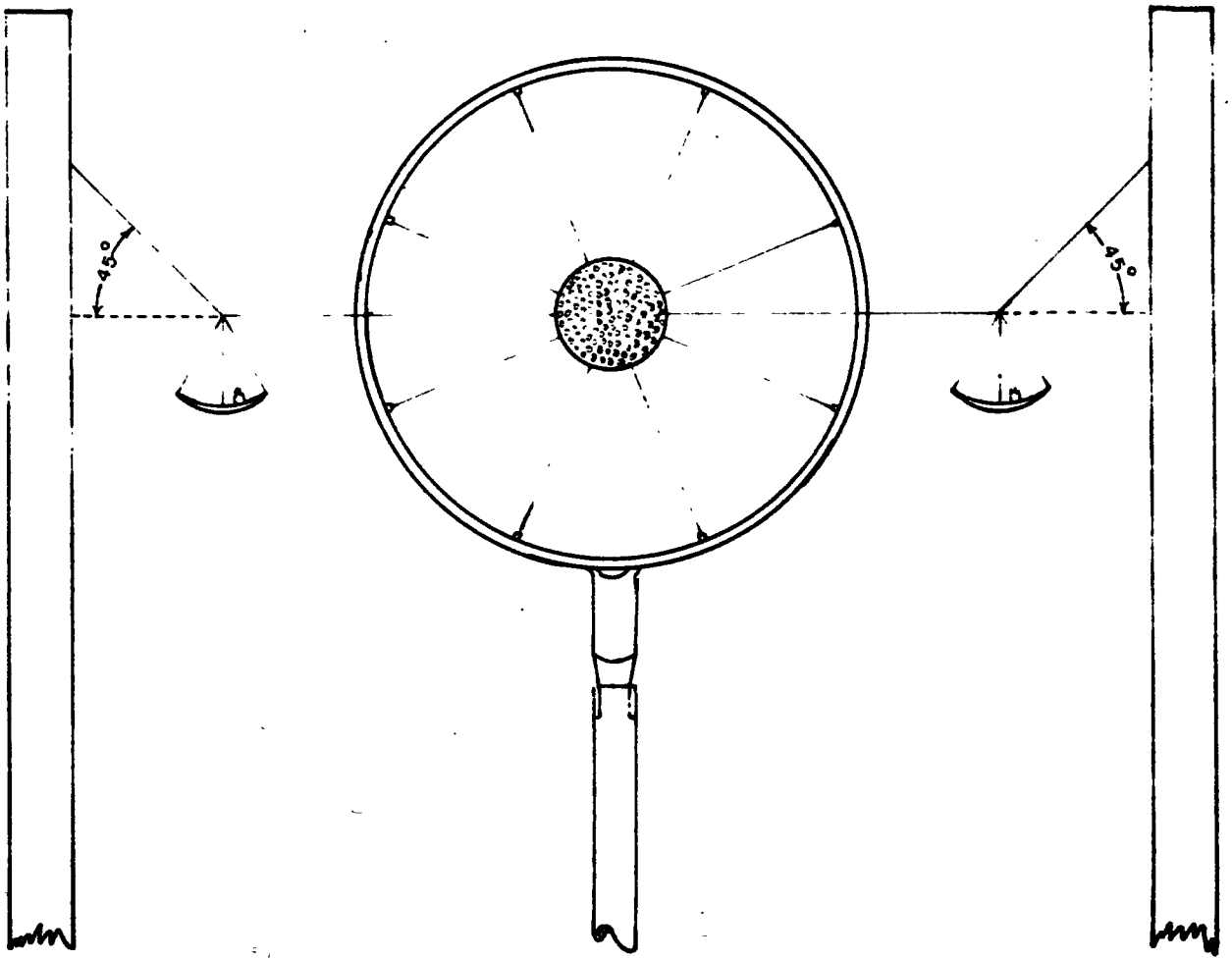

Figure 12. Method of applying static horizontal thrust to sphere without friction.

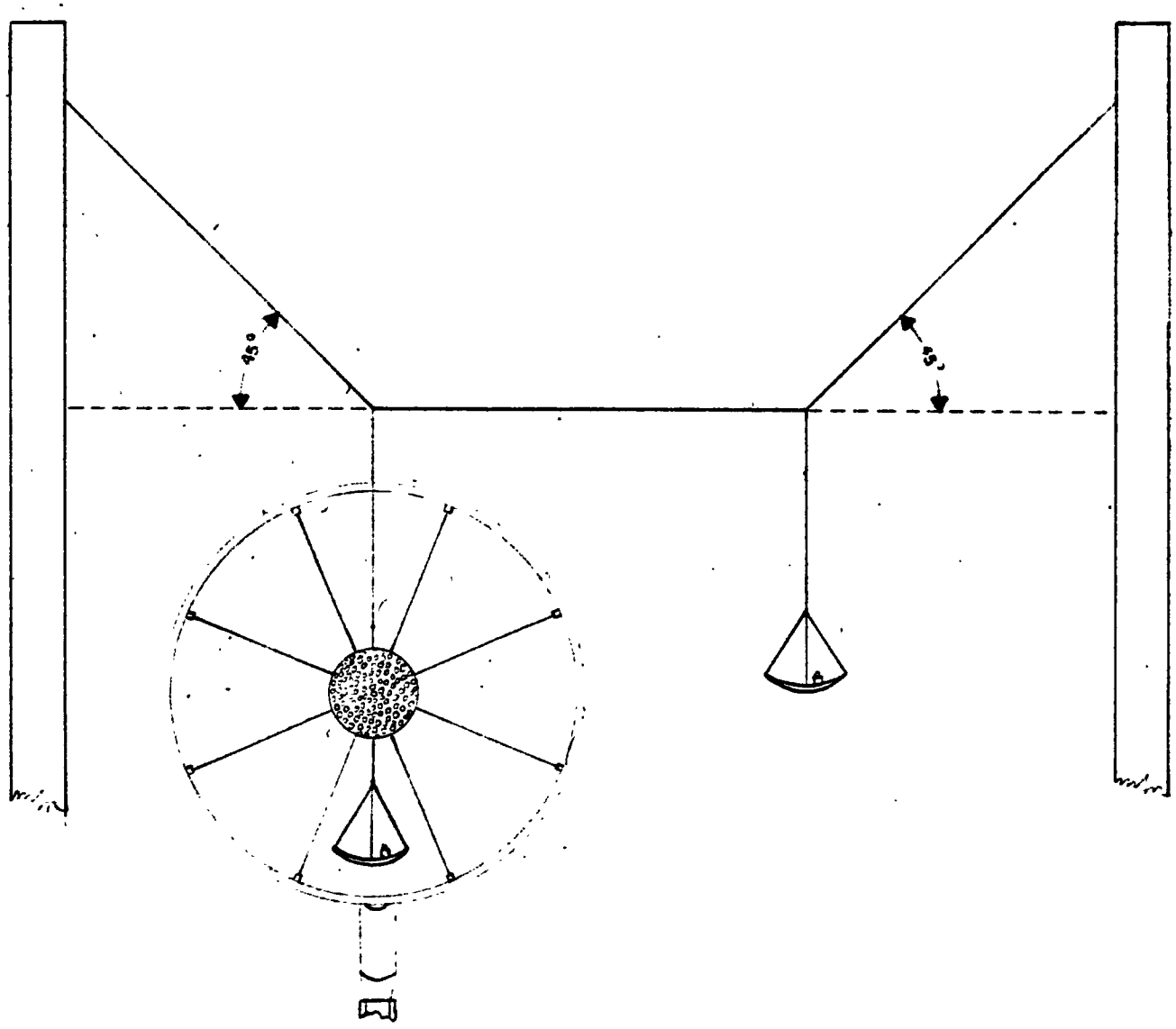

Figure 13. Method of applying static vertical thrusts to sphere.

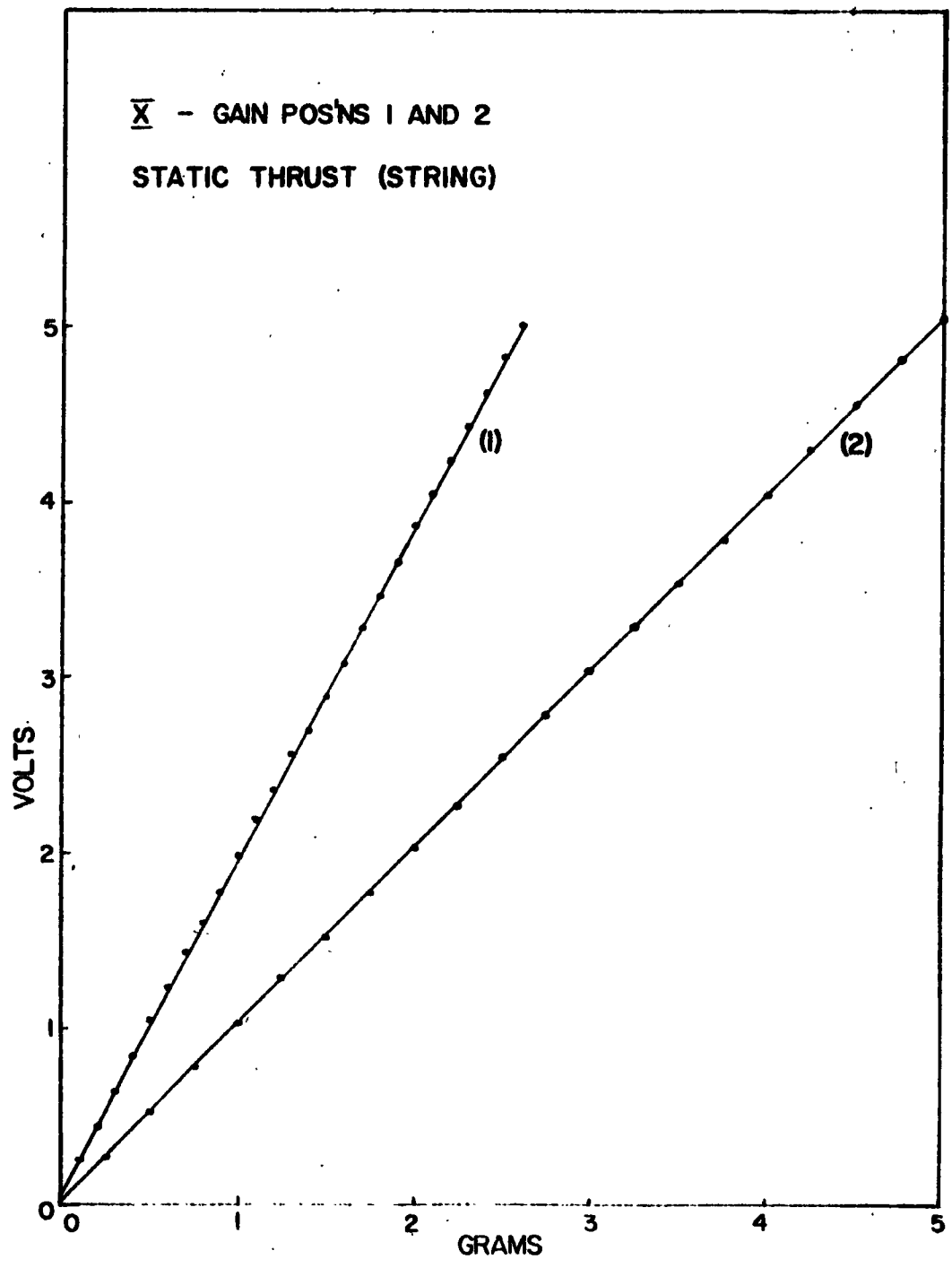

Figure 14. Response of x component to static thrust - high gain positions.

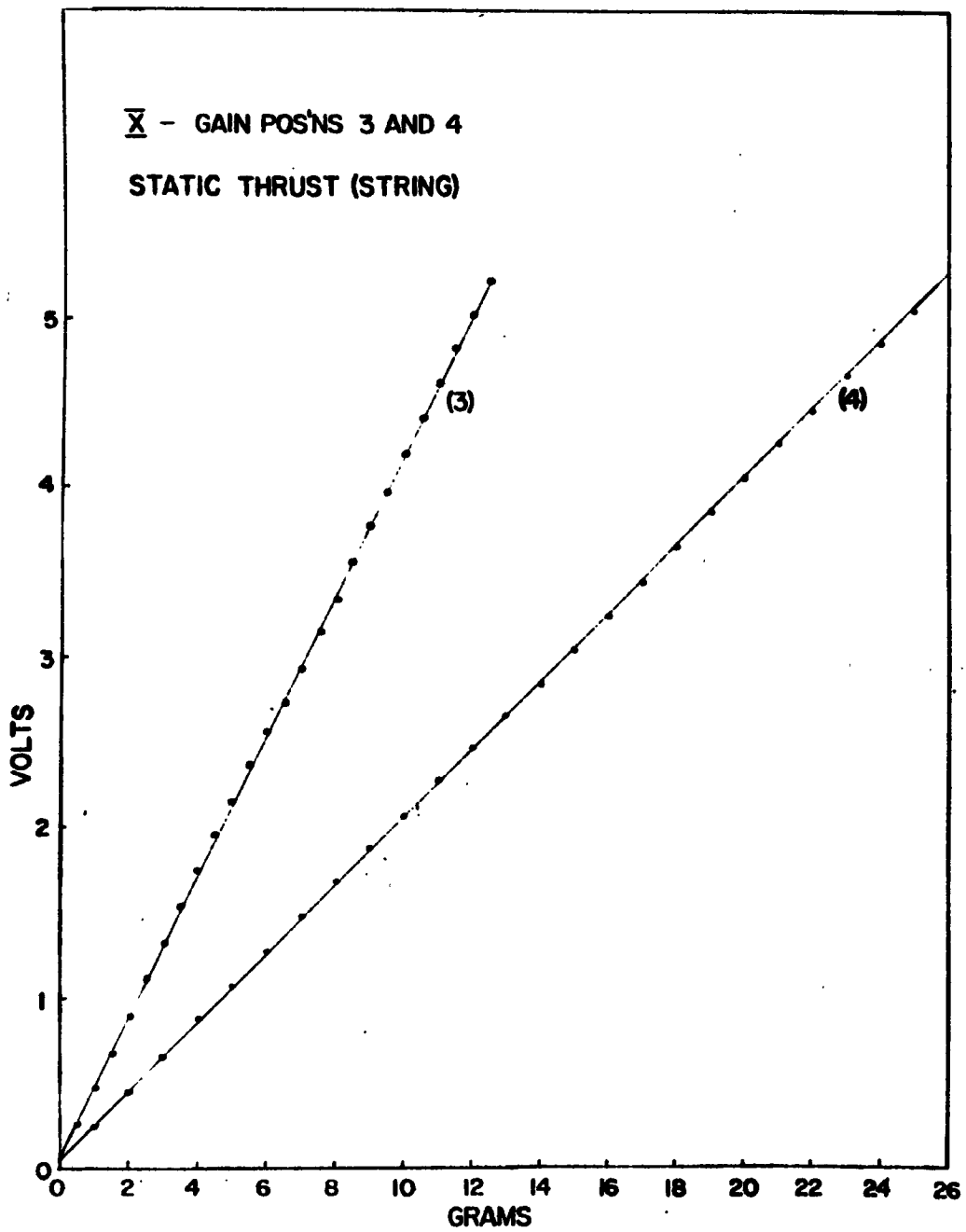

Figure 15. Response of x component to static thrust - low gain positions.

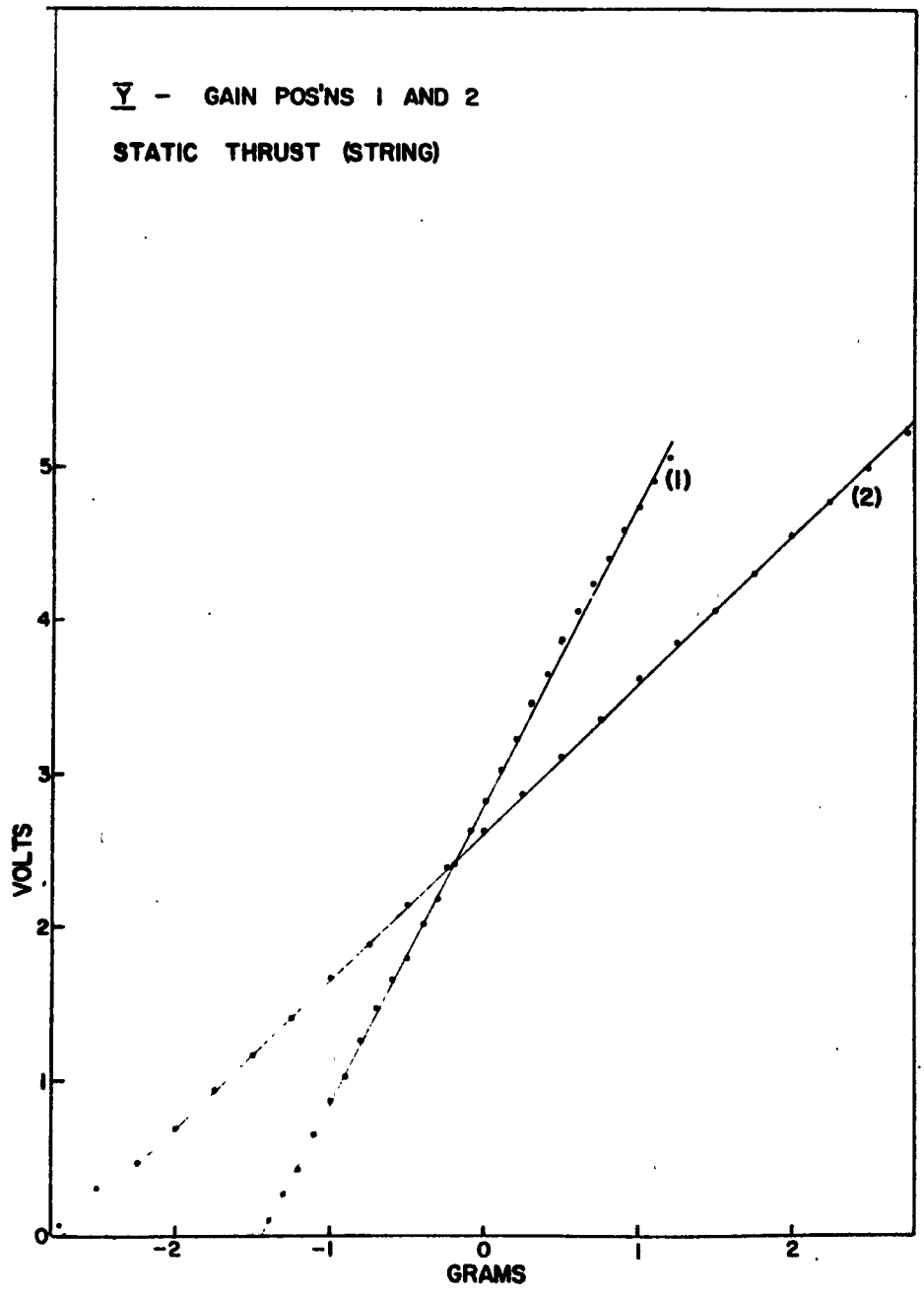

Figure 16. Responses of y component to static thrust - high gain positions.

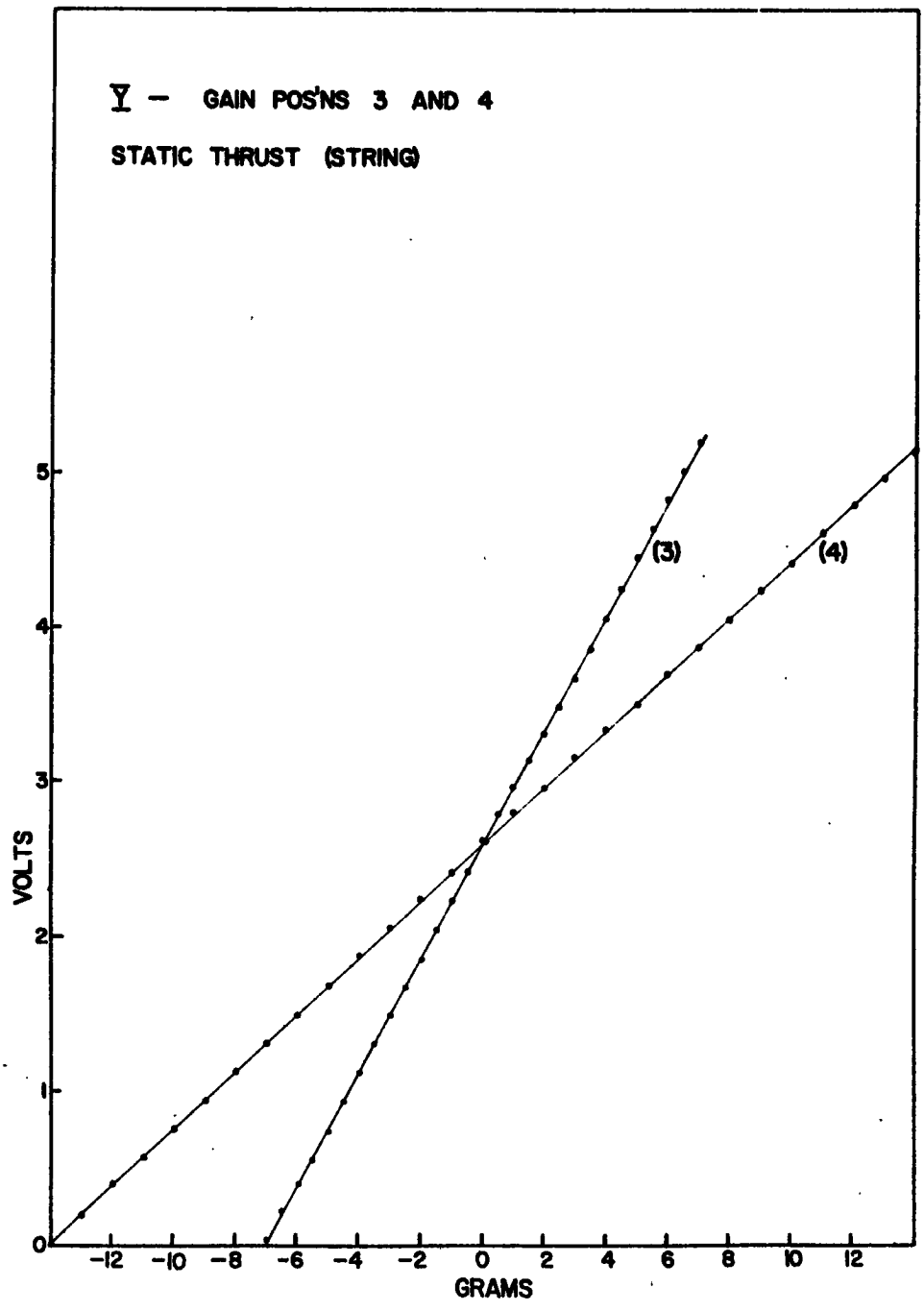

Figure 17. Response of y component to static thrust - low gain positions.

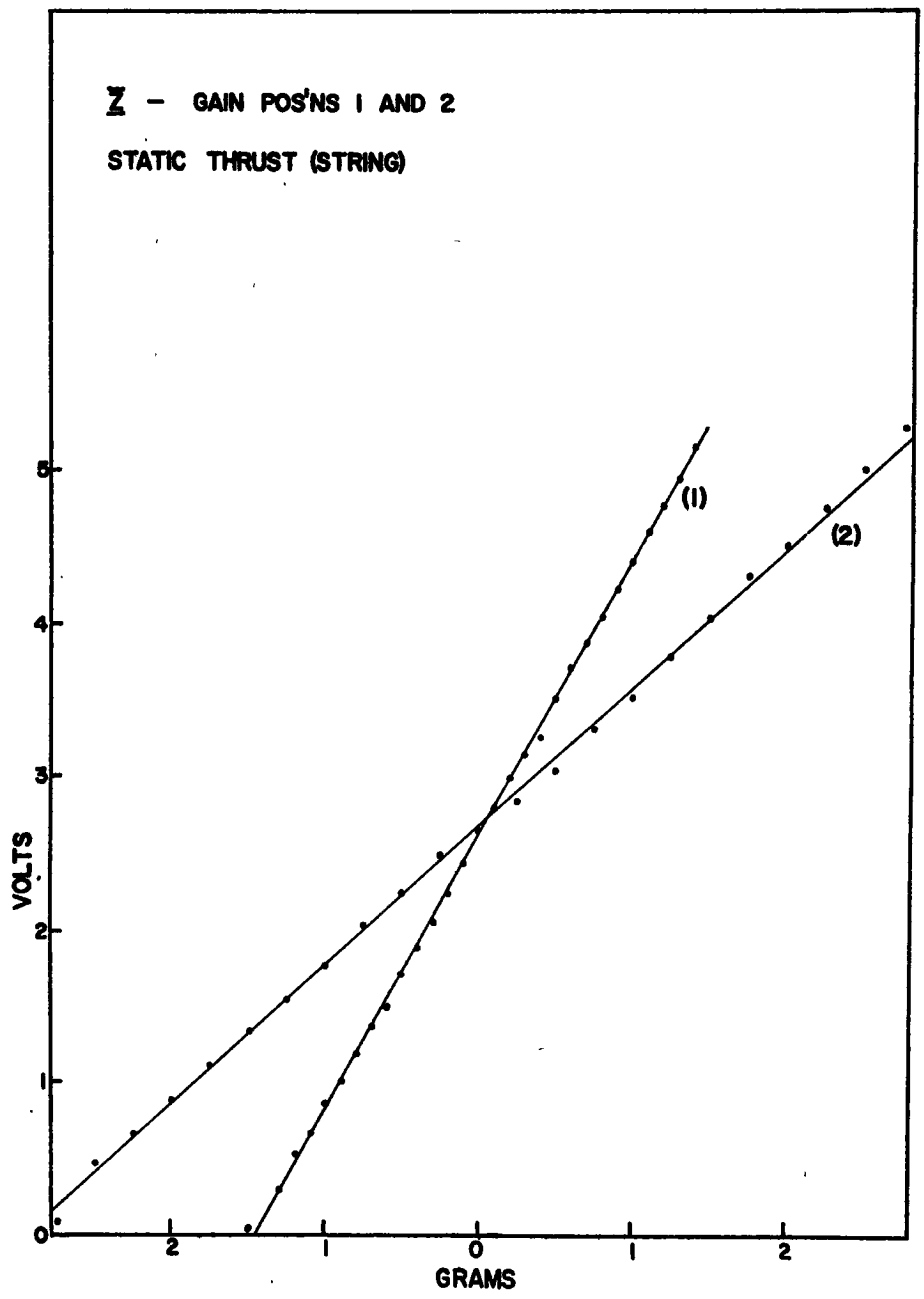

Figure 18. Response of z component to static thrust - high gain positions.

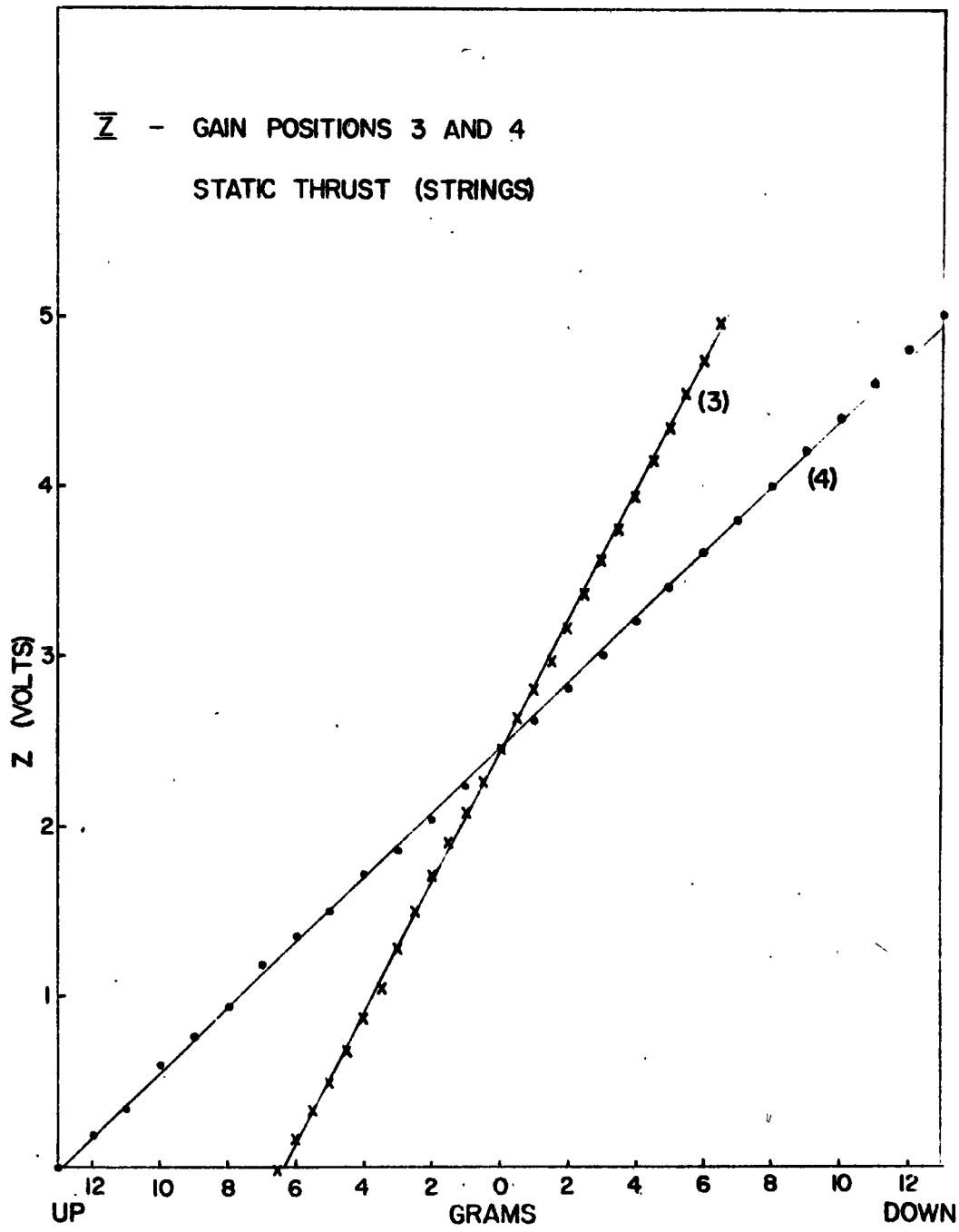

Figure 19. Response of z component to static thrust - low gain positions.

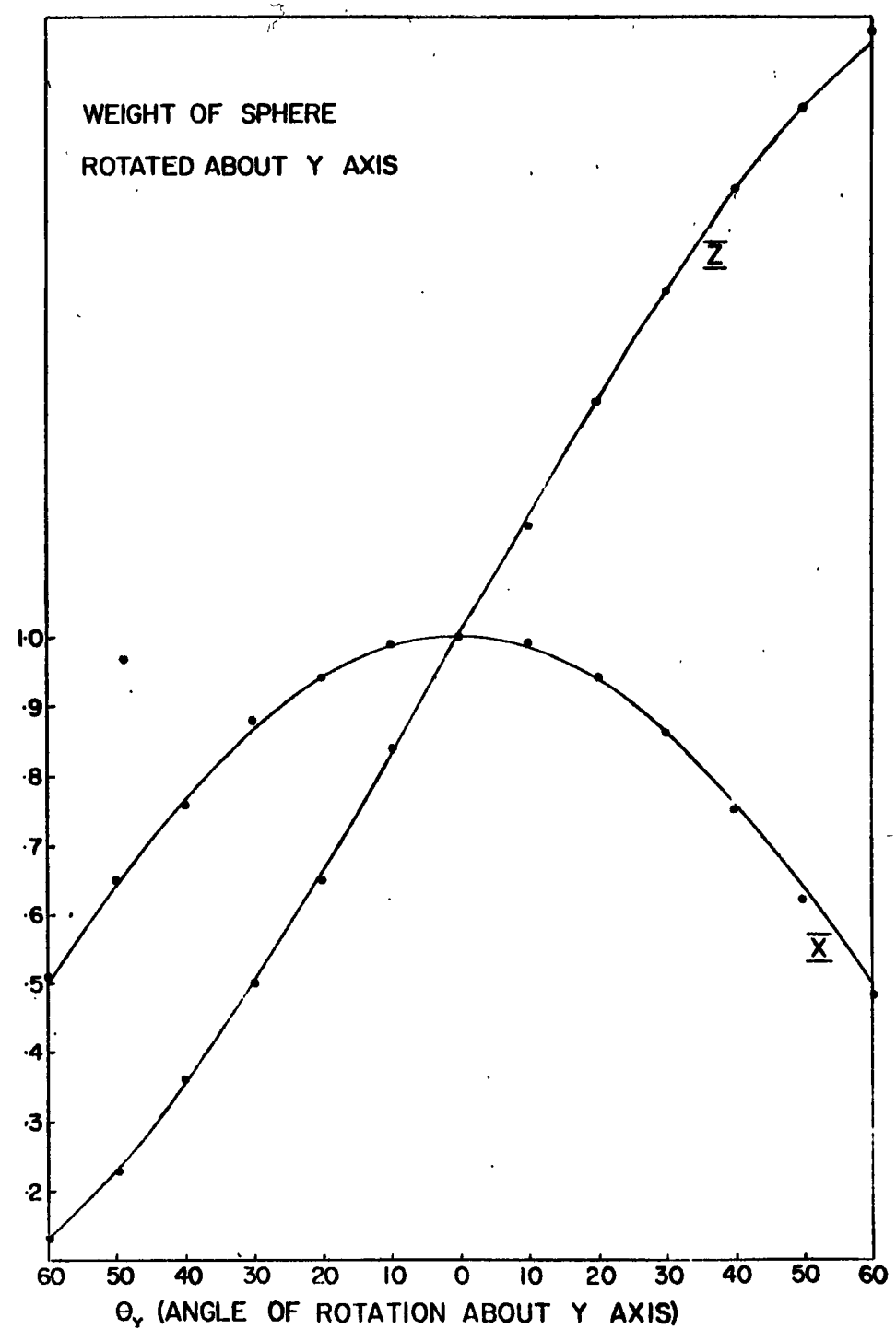

Figure 20. Response of x and z components to weight of moving parts as instrument was rotated about its z axis.

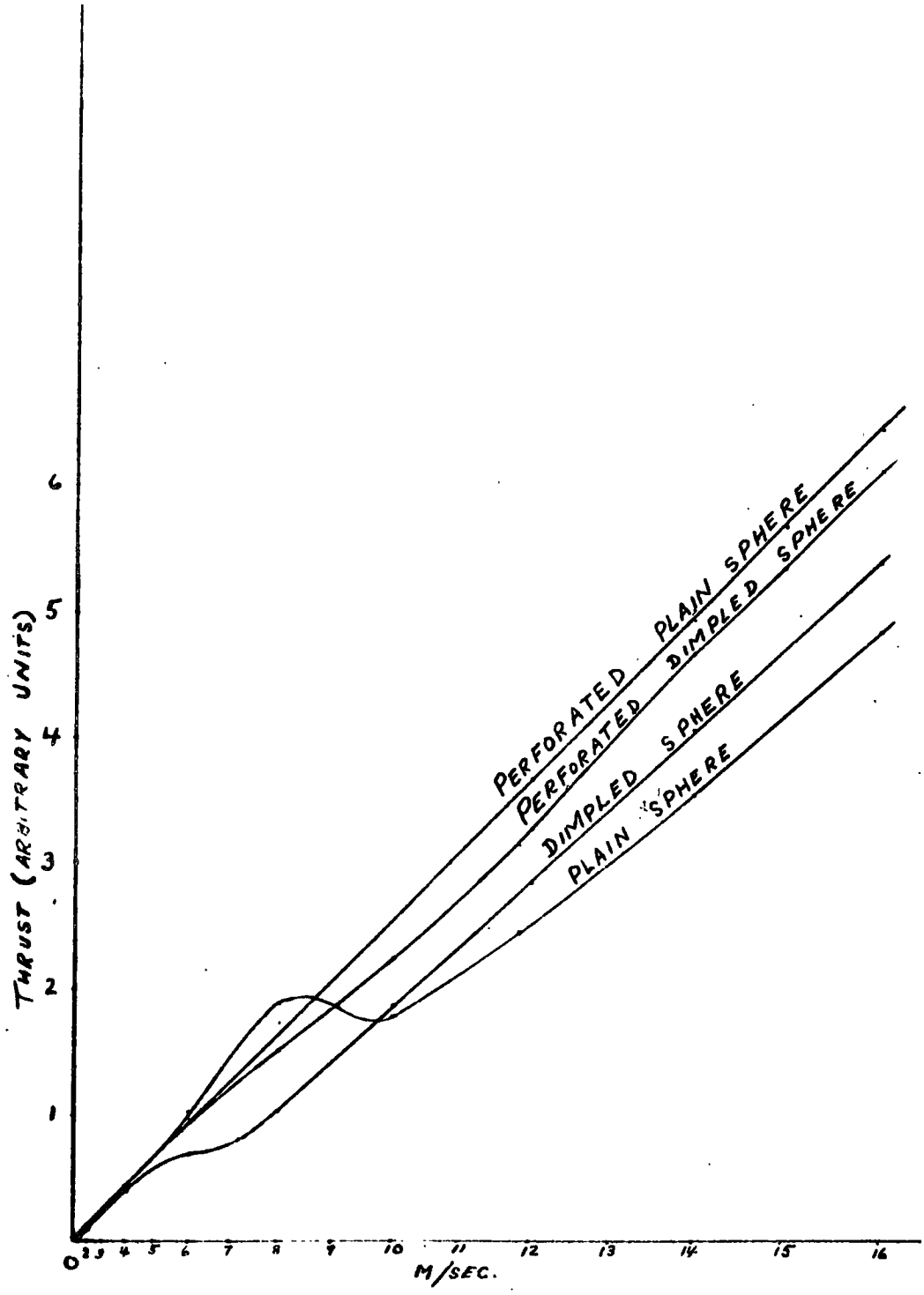

Figure 21. Calibration curves of four different spheres. Output of x component is plotted against square of wind speed.

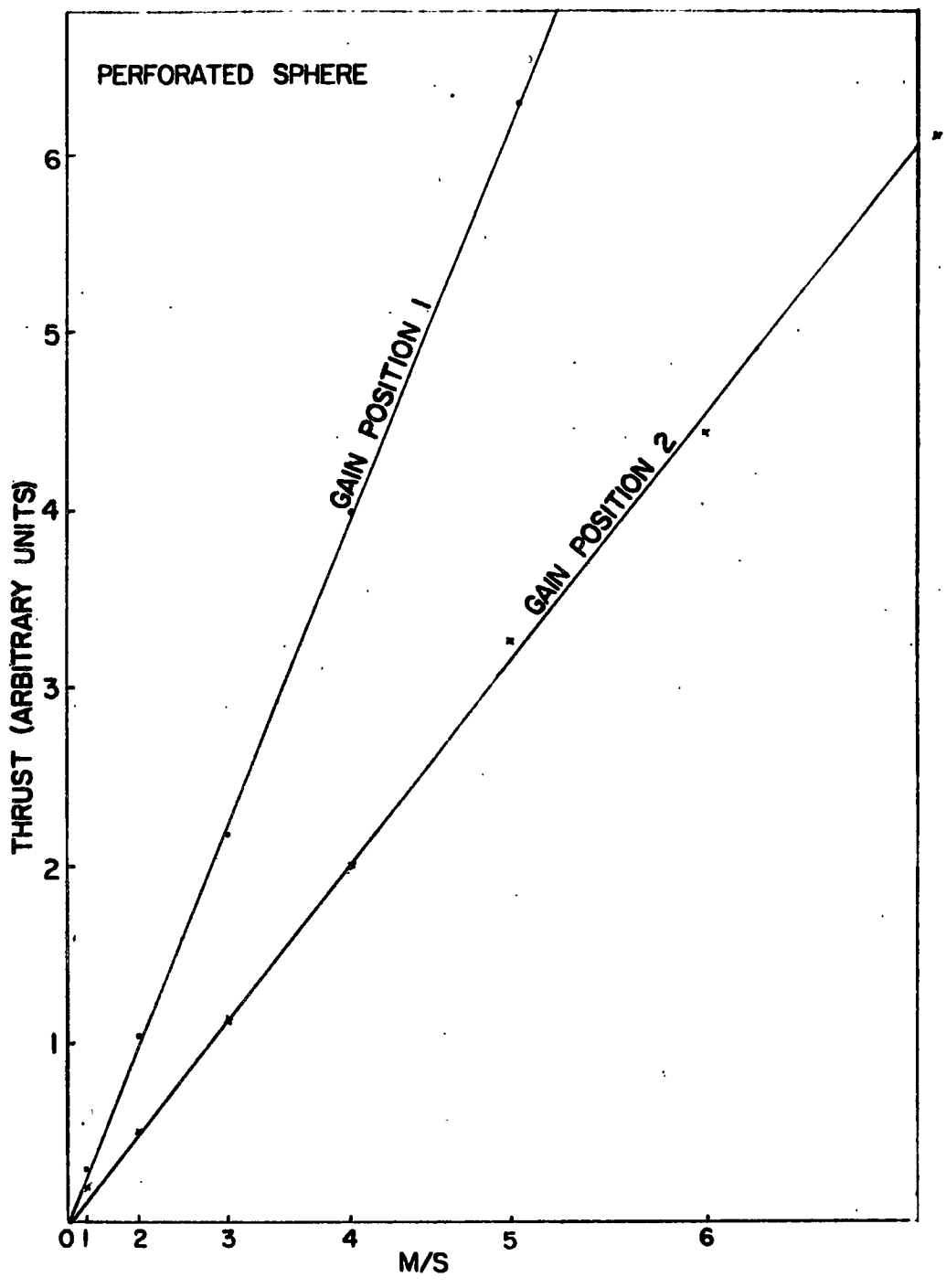

Figure 22. Calibration of x component in wind tunnel - high gain positions. Output is plotted against square of wind speed.

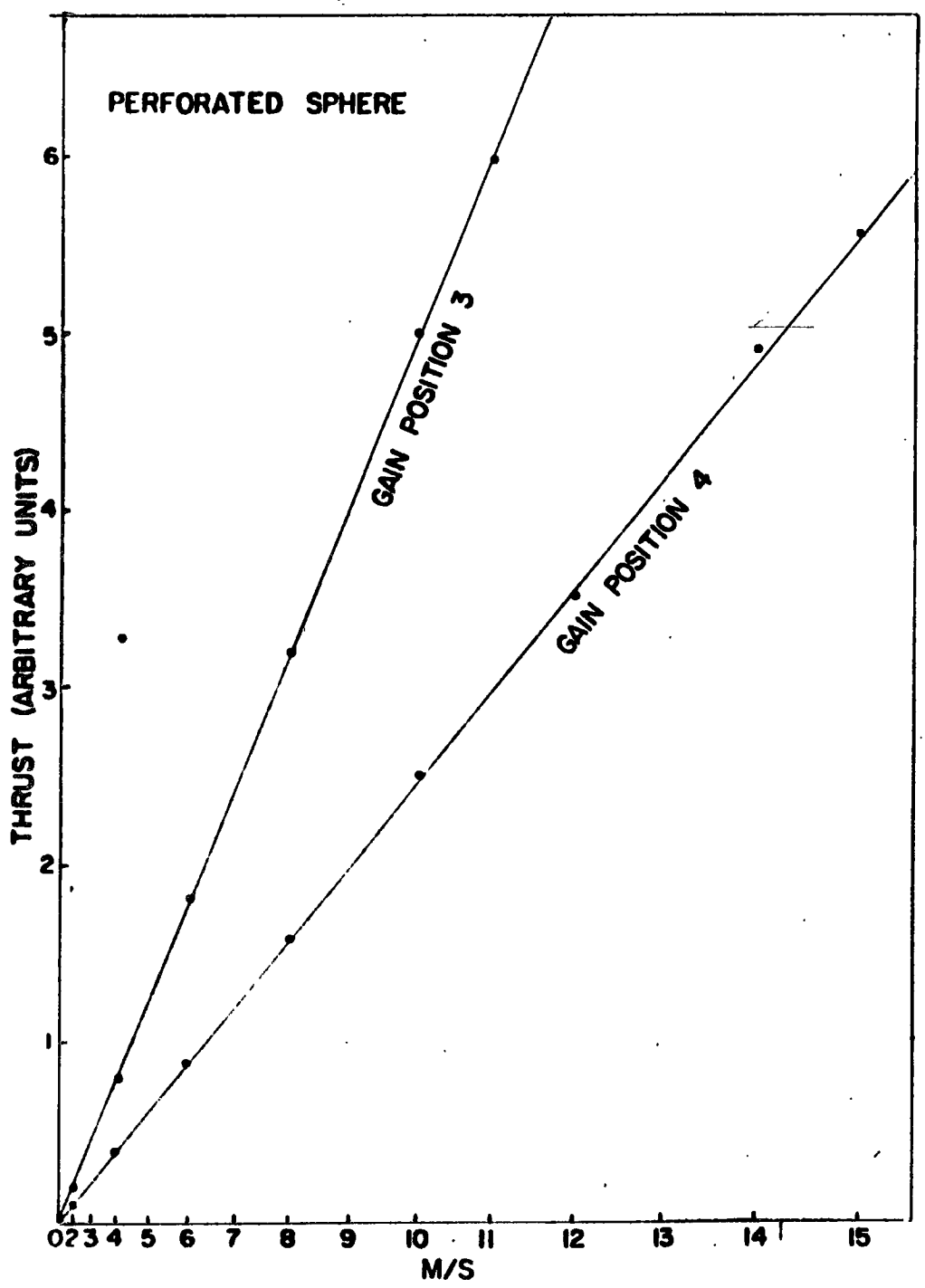

Figure 23. Calibration of x component in wind tunnel -low gain positions. Output is plotted against square of wind speed.

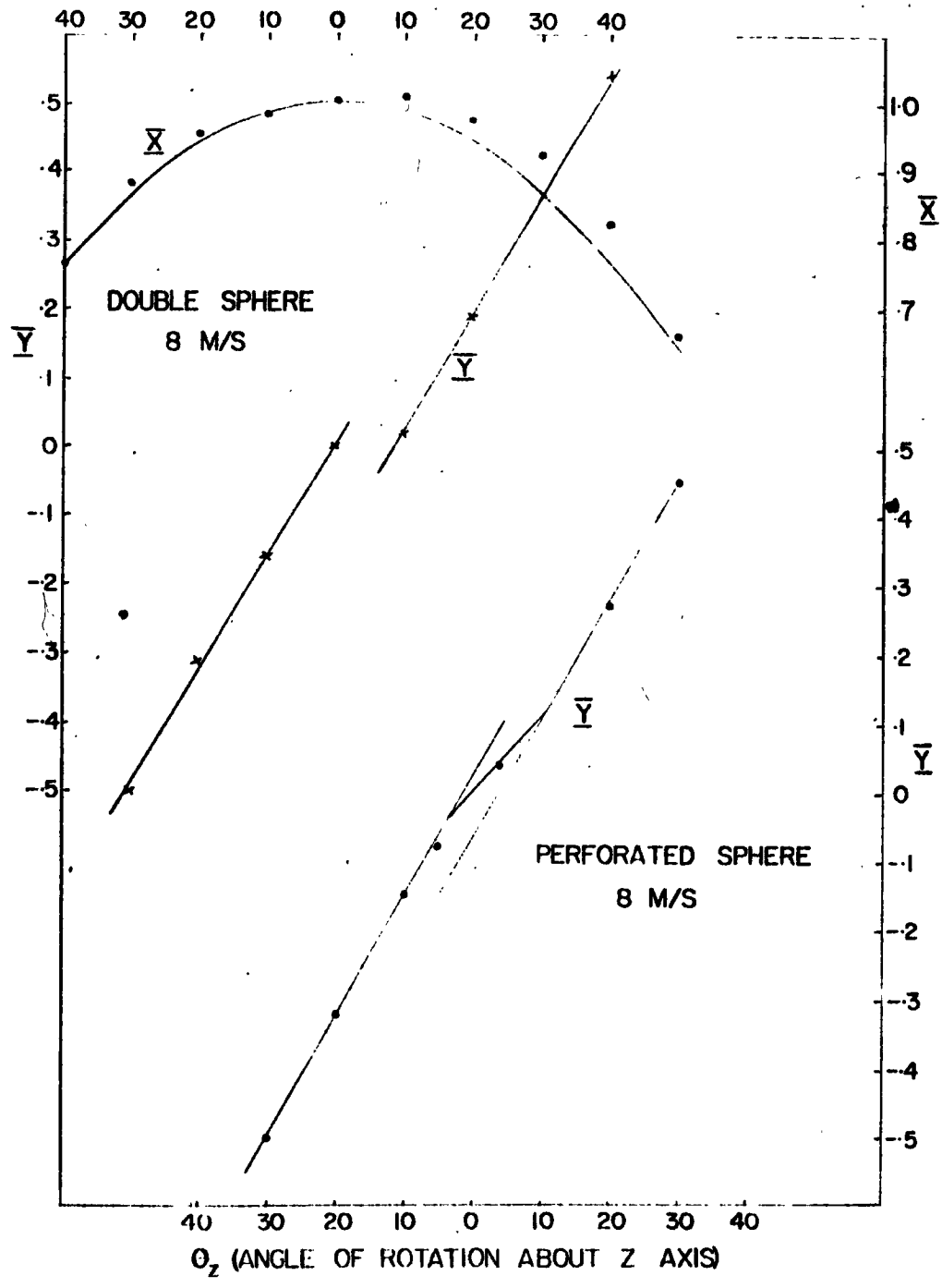

Figure 24. Response of x and y components to wind of constant speed as instrument was rotated relative to wind direction.

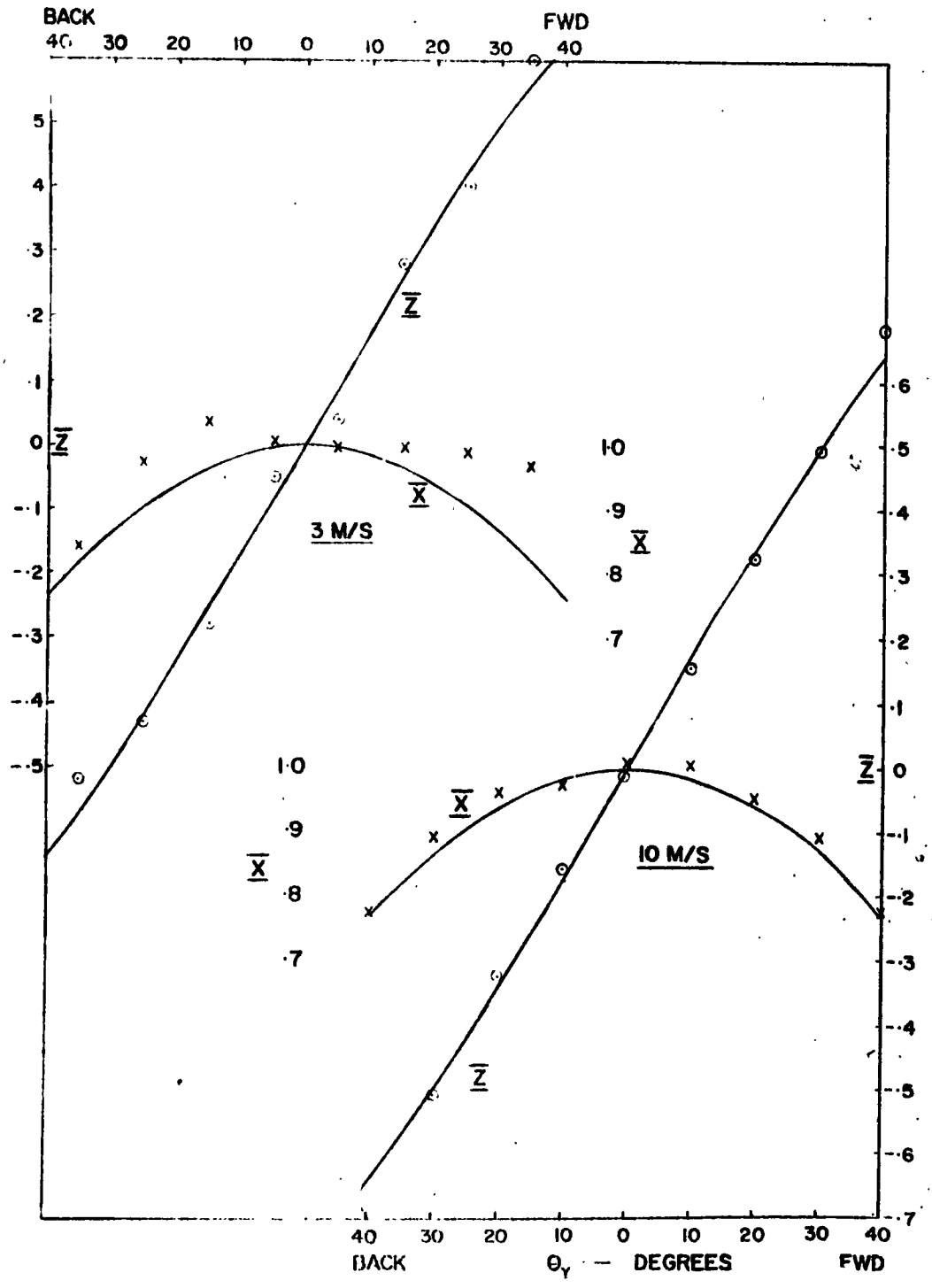

Figure 25. Response of x and z components as instrument was tilted relative to horizontal wind.

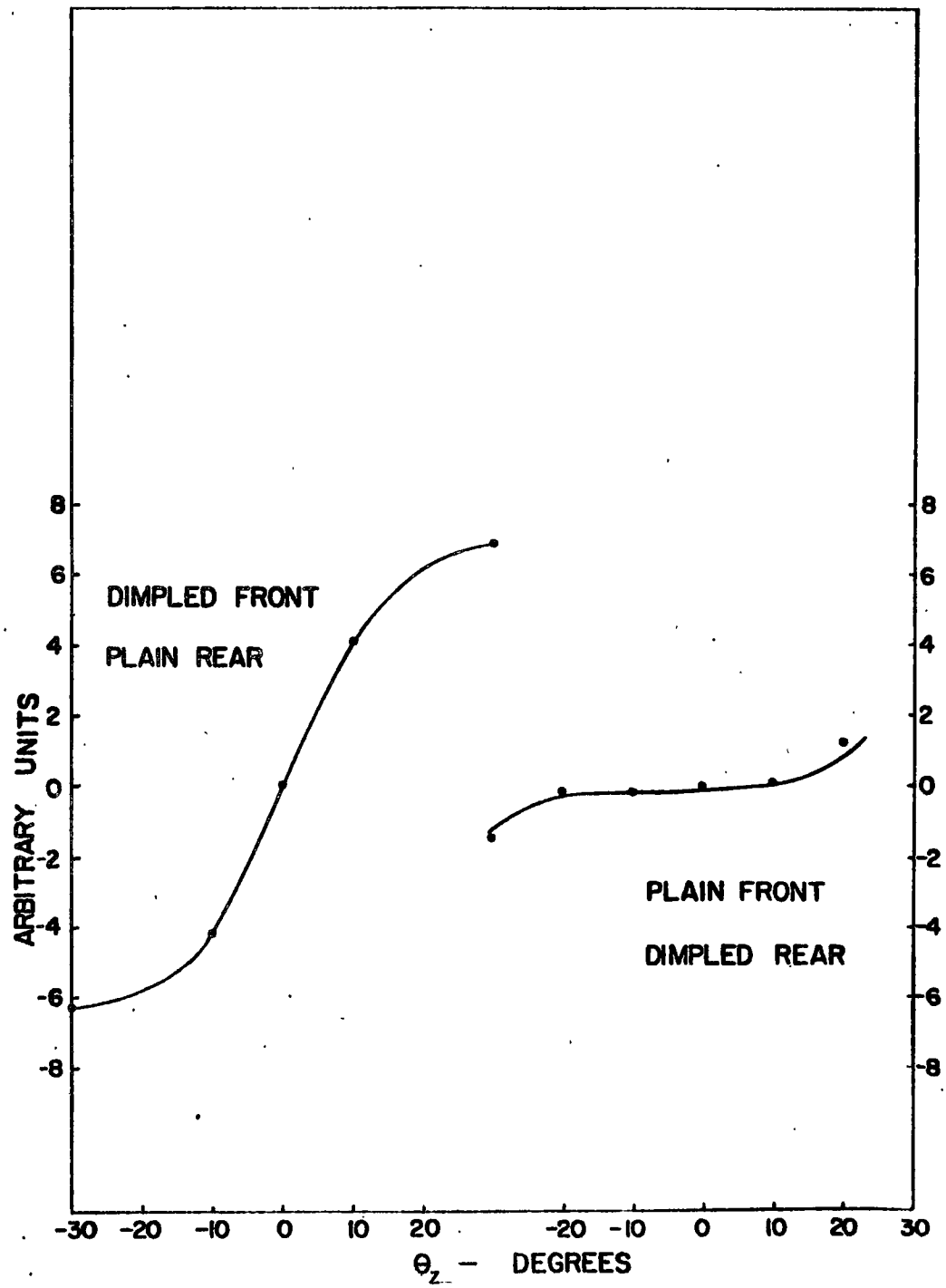

Figure 26. Asymmetric spheres. Response of y component as instrument was rotated with dissimilar unperforated hemispheres installed.

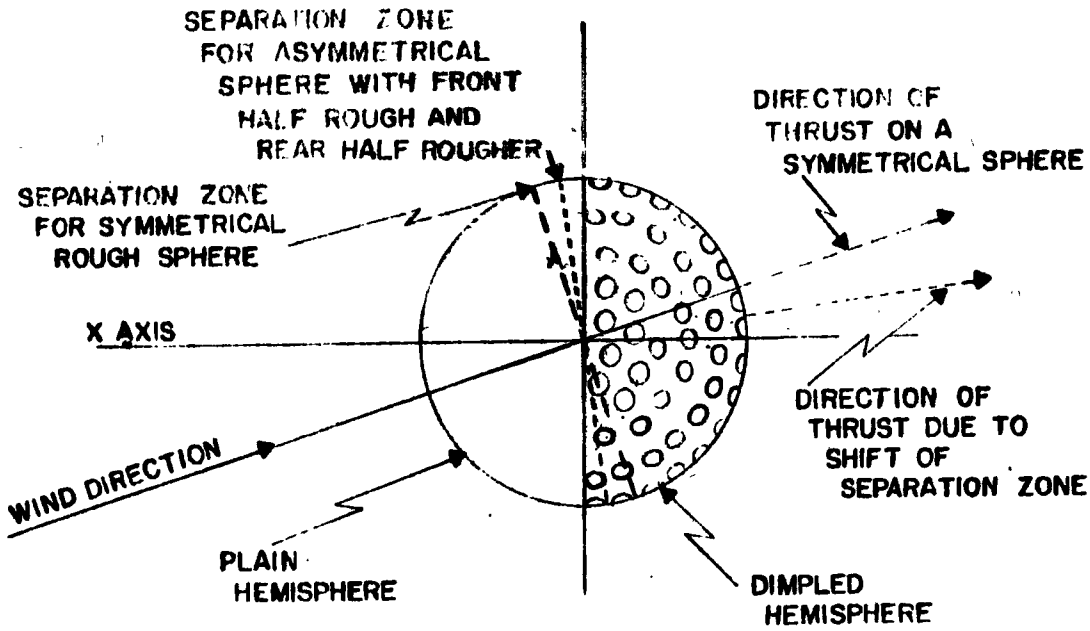

Figure 27. Presumed shift of separation zone and deviation of thrust vector when rear hemisphere has greater surface drag than front hemisphere.

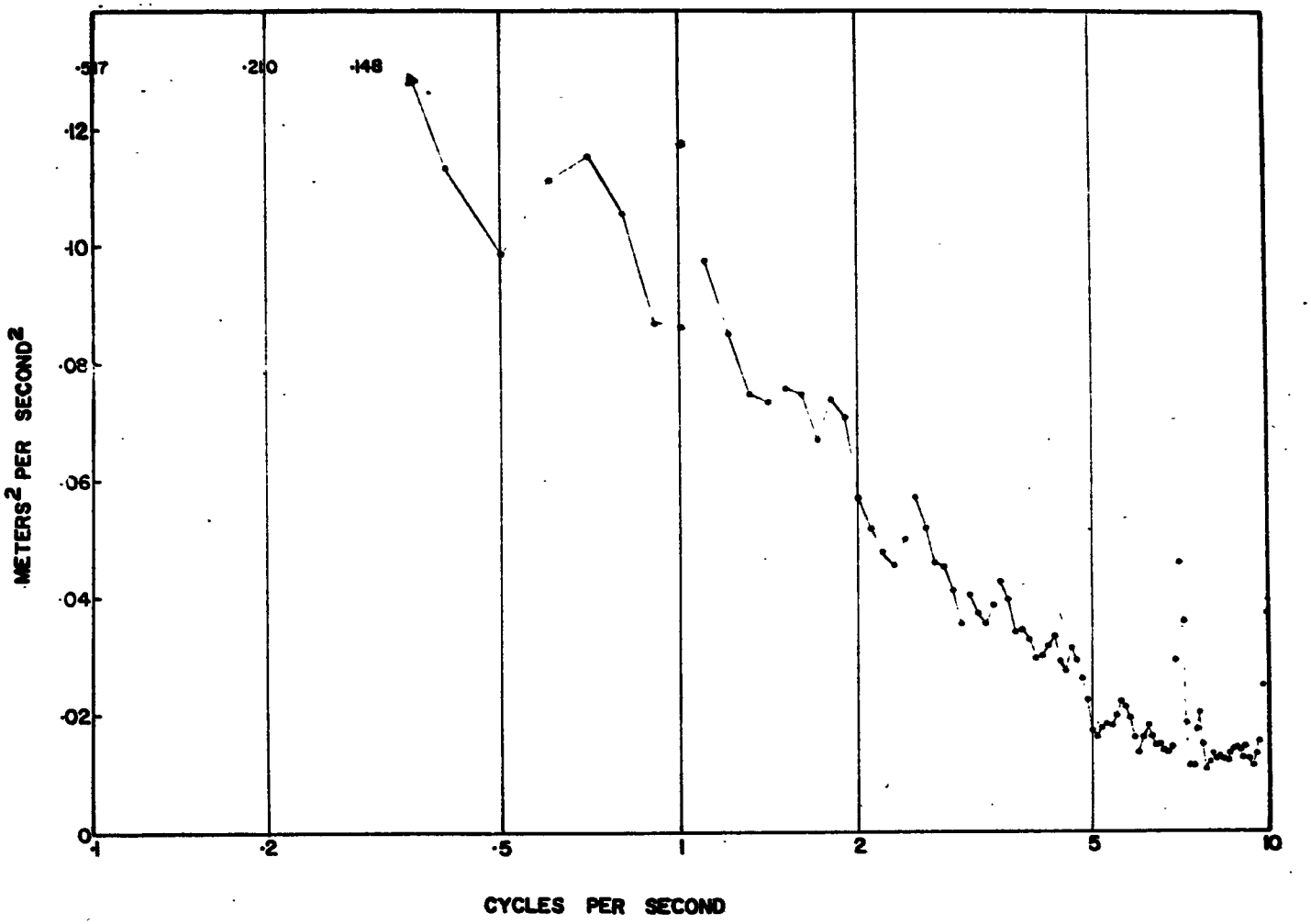

Figure 28. Logarithmic spectrum of u.

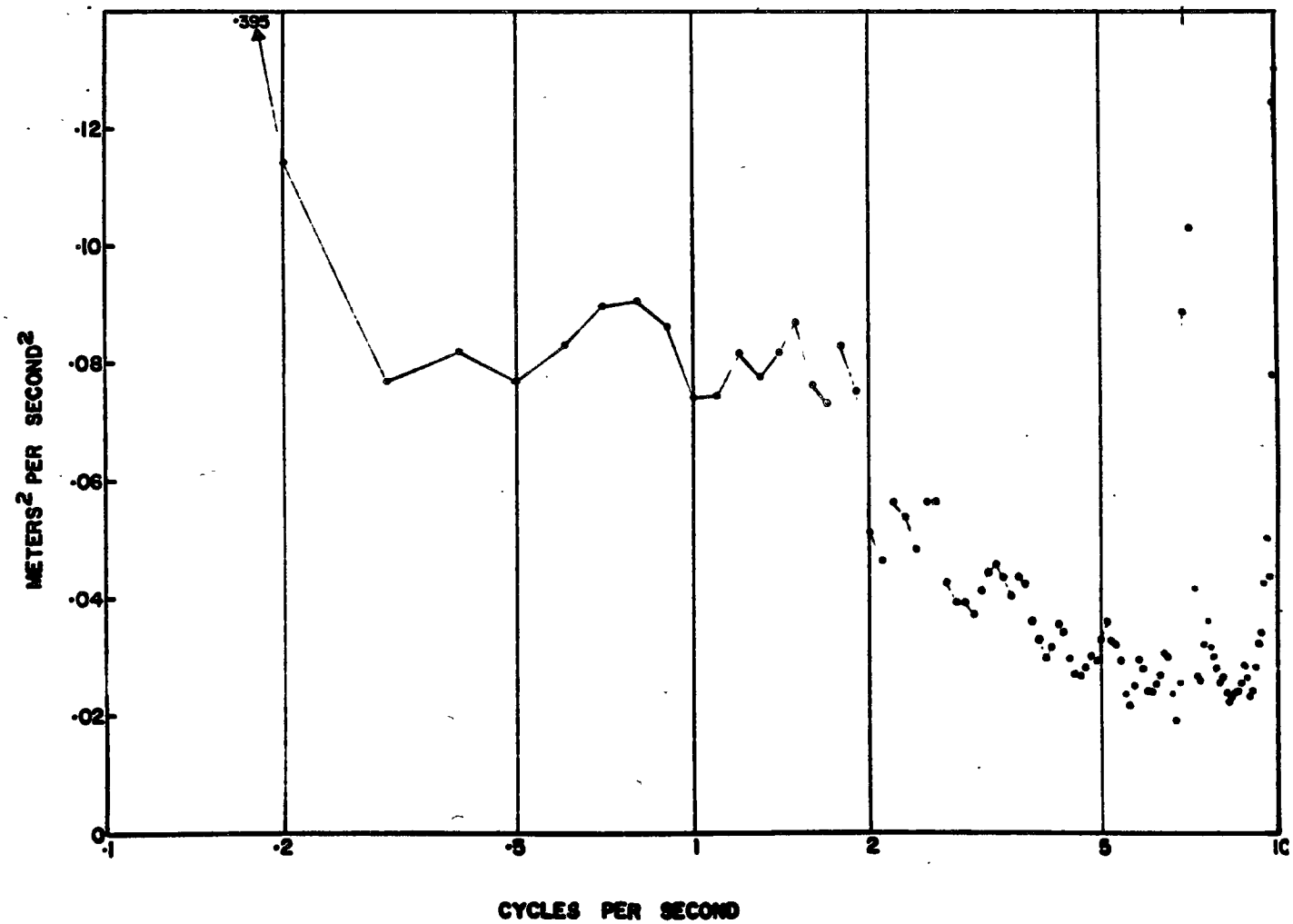

Figure 29. Logarithmic spectrum of v.

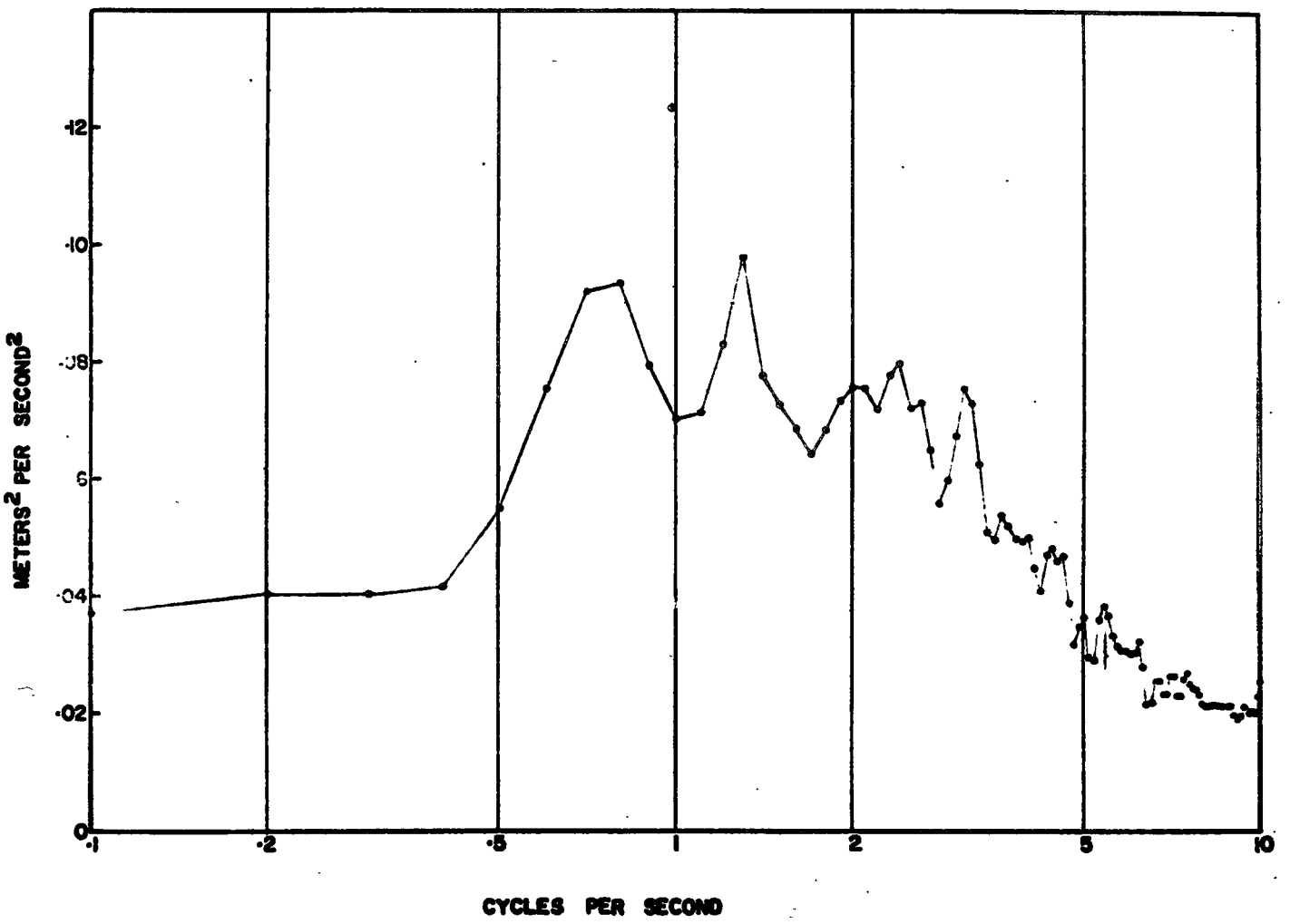

Figure 30. Logarithmic spectrum of w.

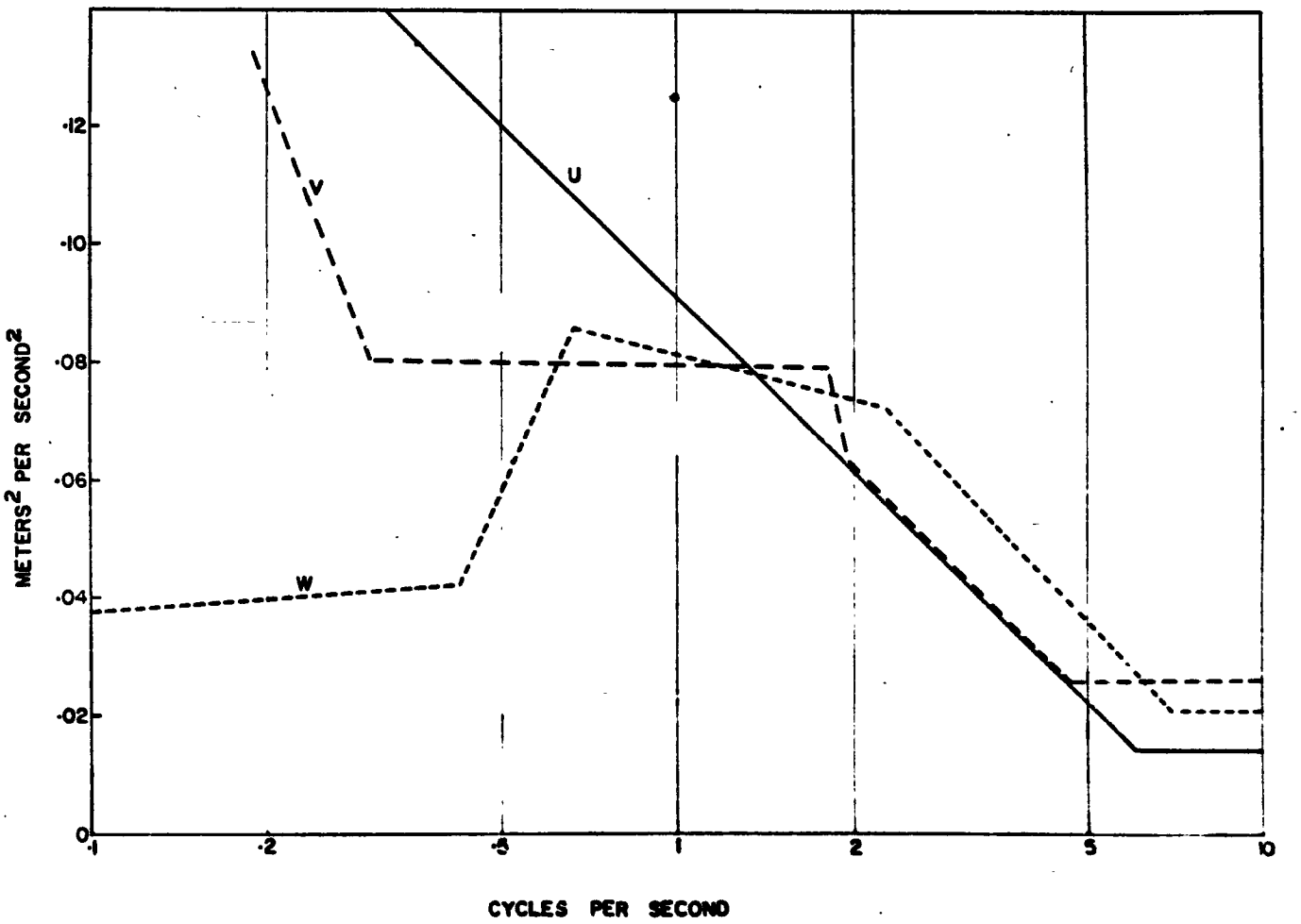

Figure 31. Logarithmic spectra of u, v, and w grossly smoothed.

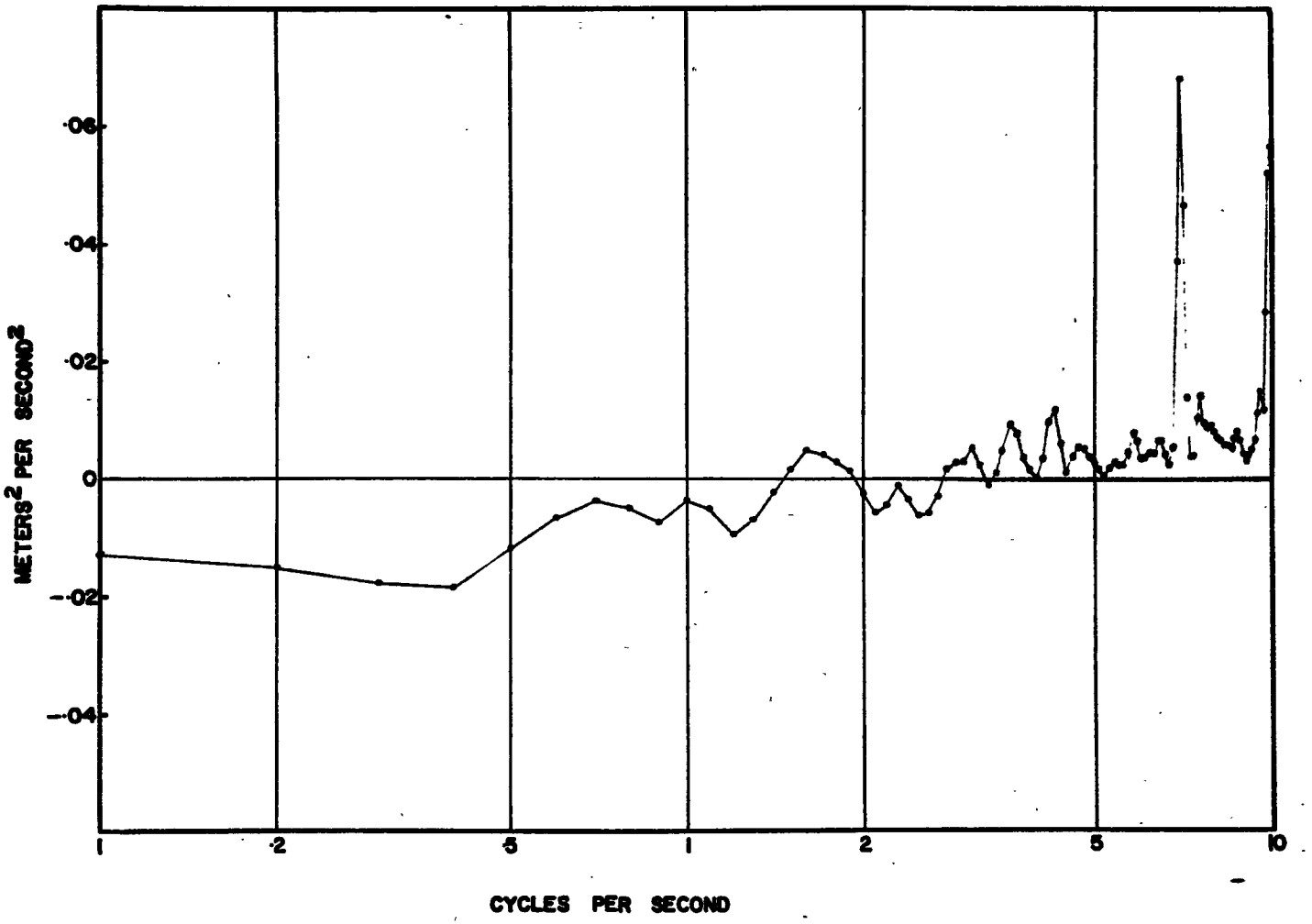

Figure 32. Logarithmic cospectrum of u and v.

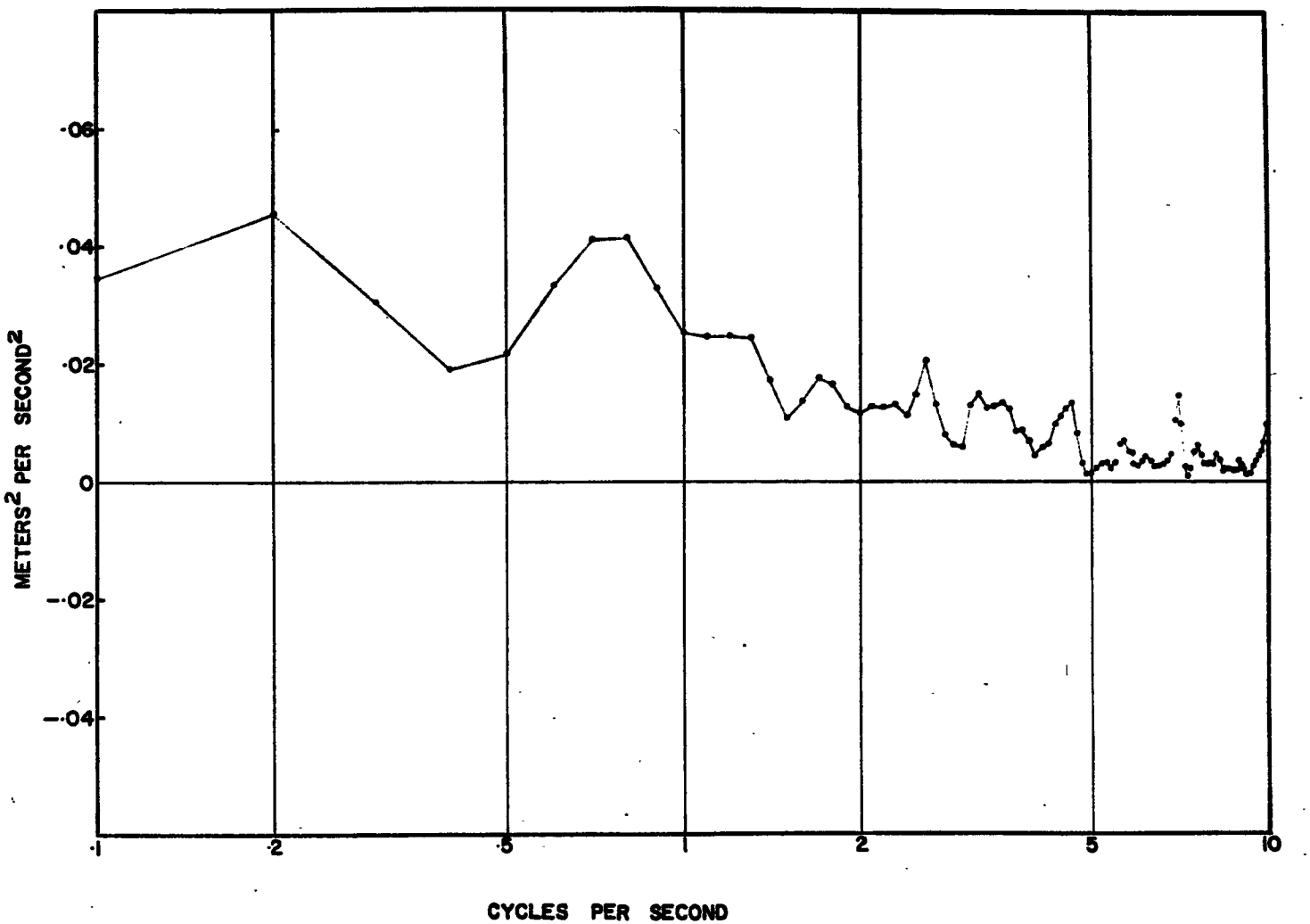

Figure 33. Logarithmic cospectrum of u and w. Note that w was taken positive downwards.

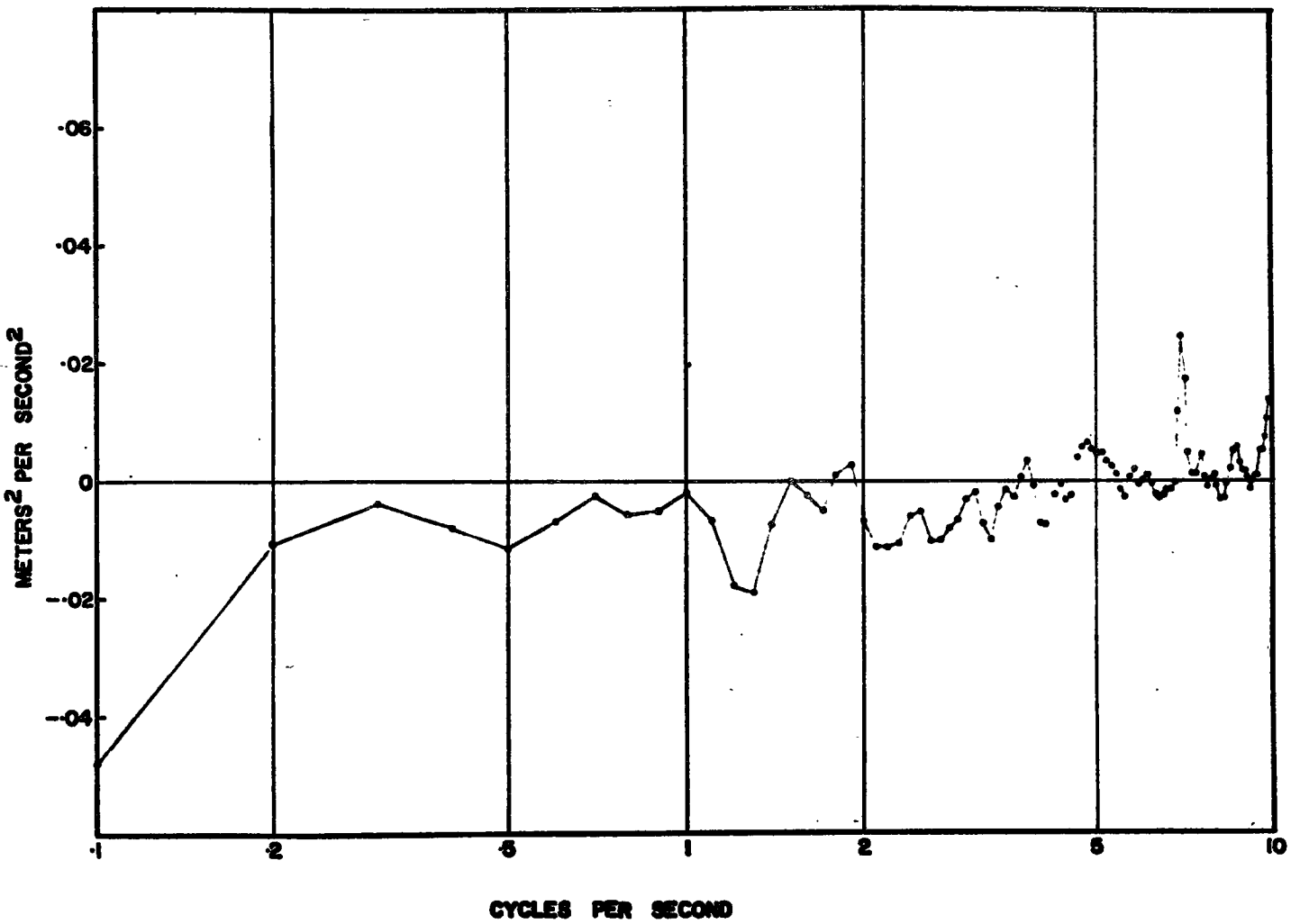

Figure 34. Logarithmic cospectrum of v and w.

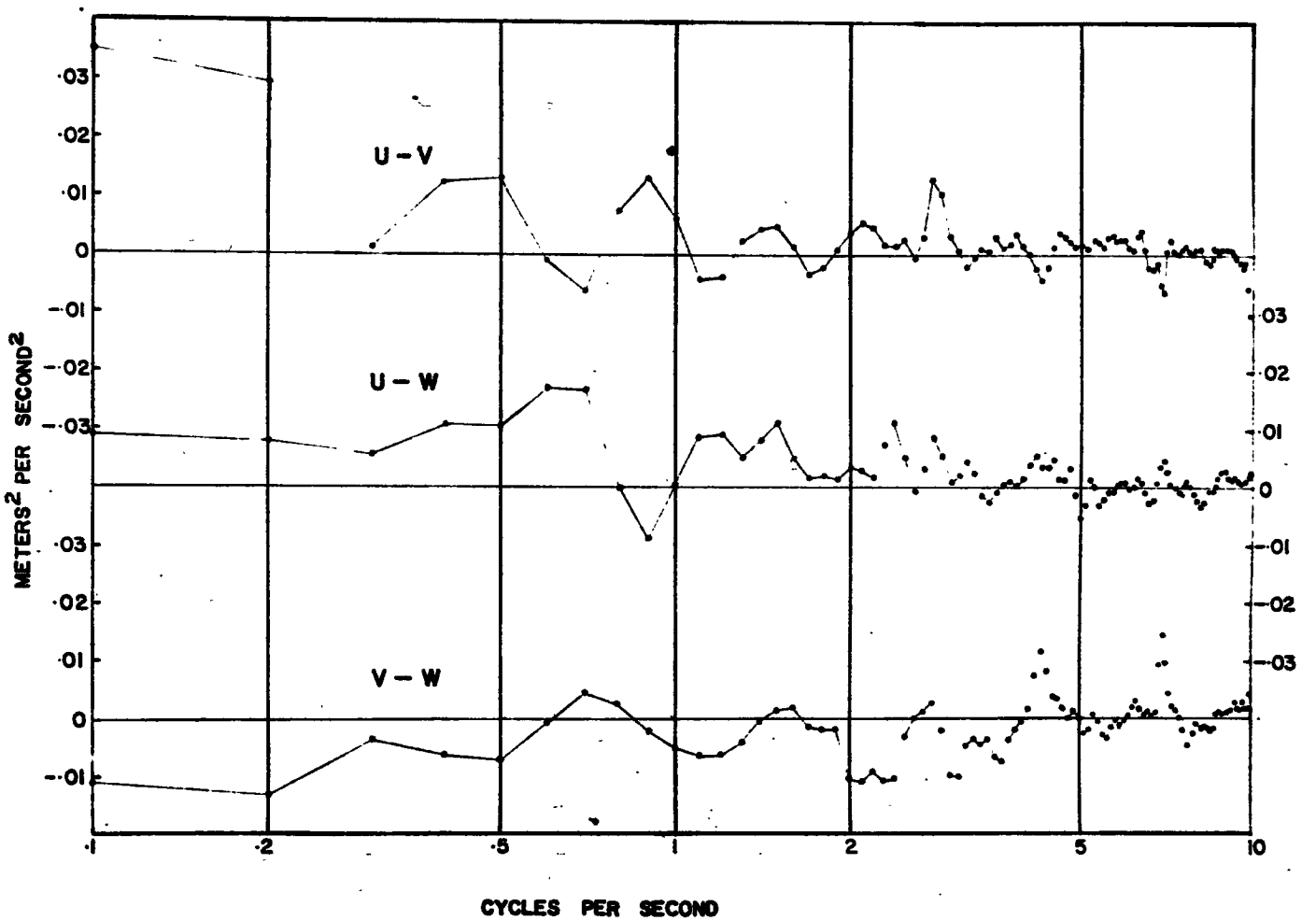

Figure 35. Logarithmic Quadrature spectra of u and v, u and w, v and w.

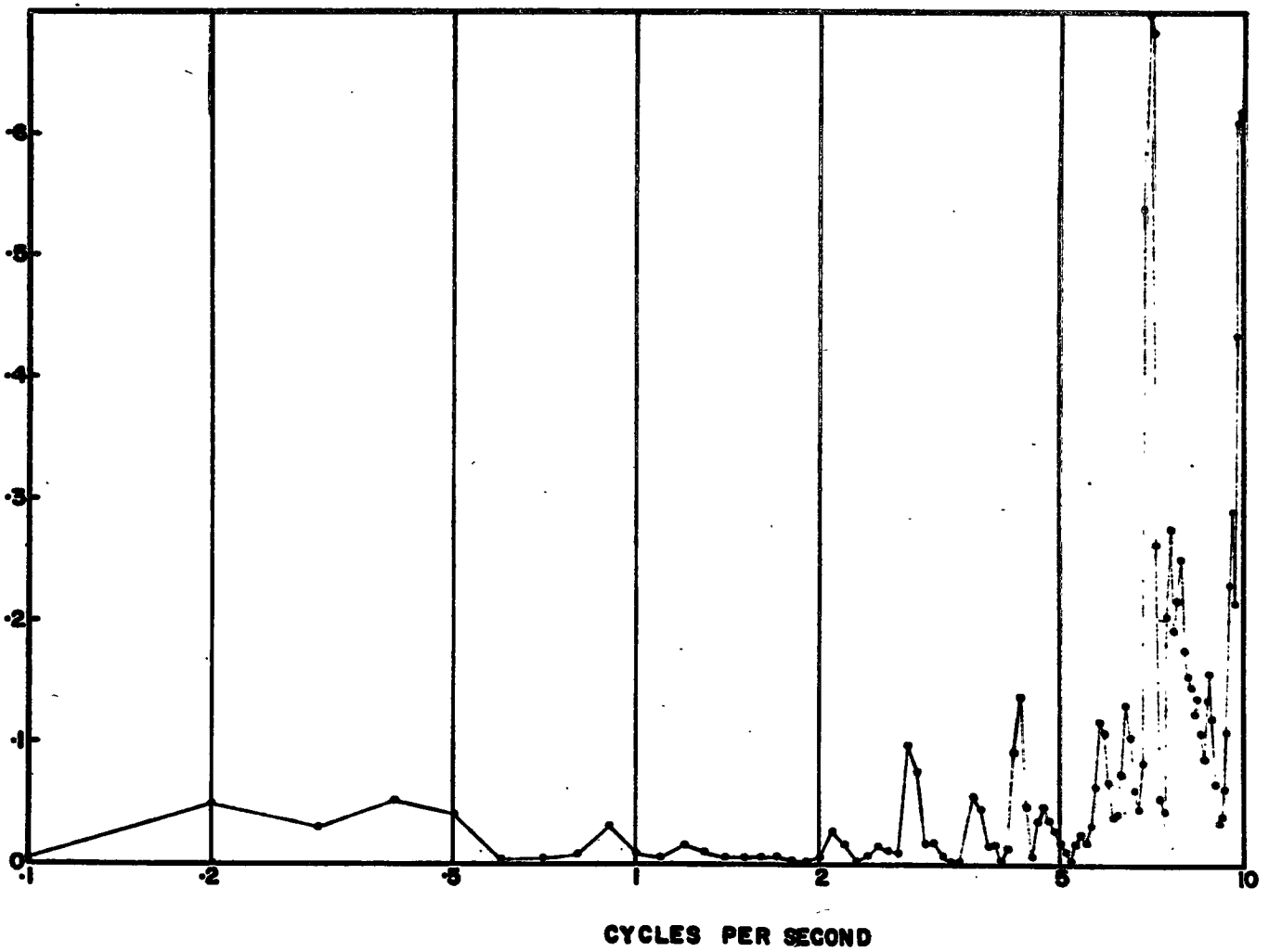

Figure 36. Coherence of u and v.

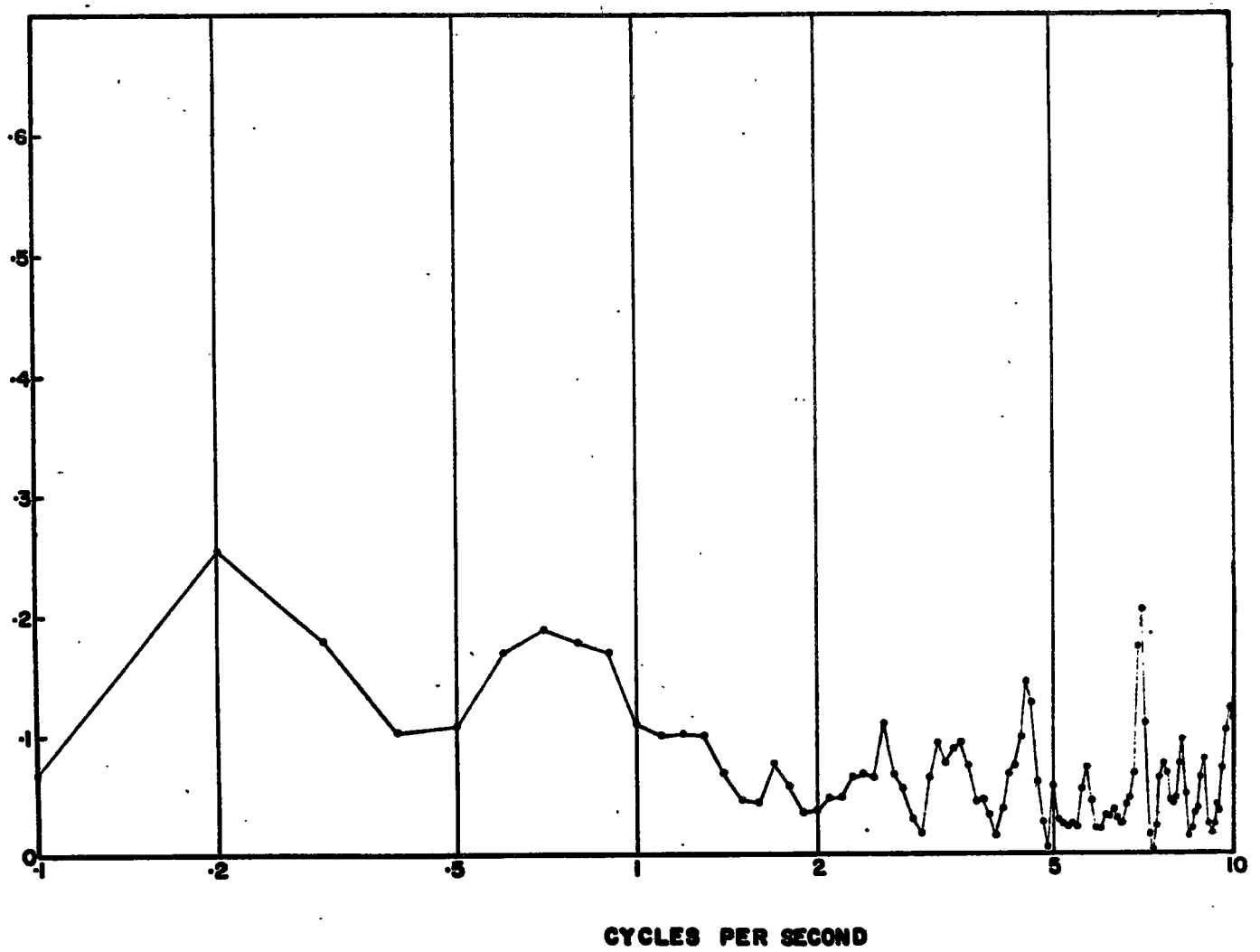

Figure 37. Coherence of u and w.

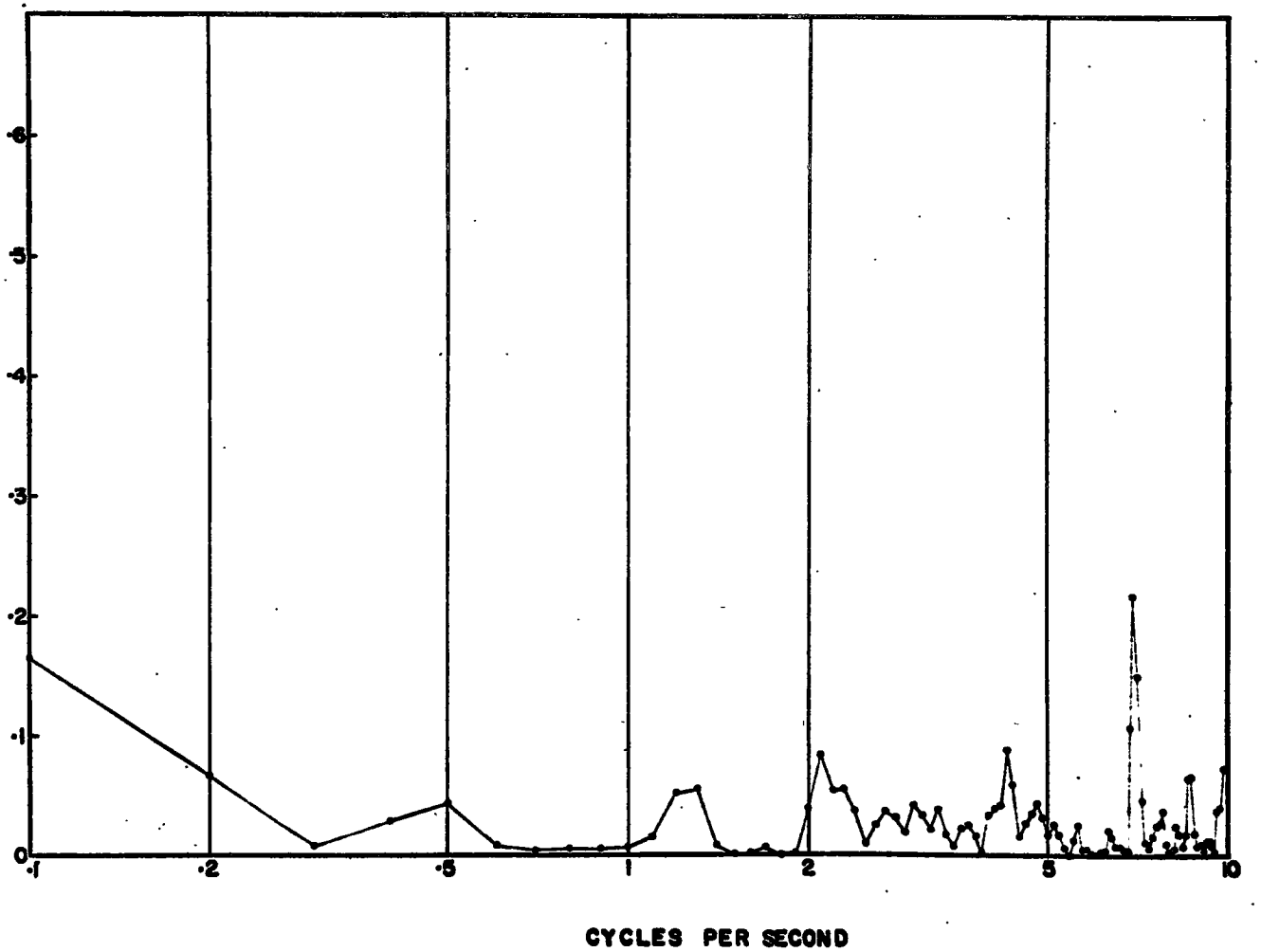

Figure 38. Coherence of v and w.

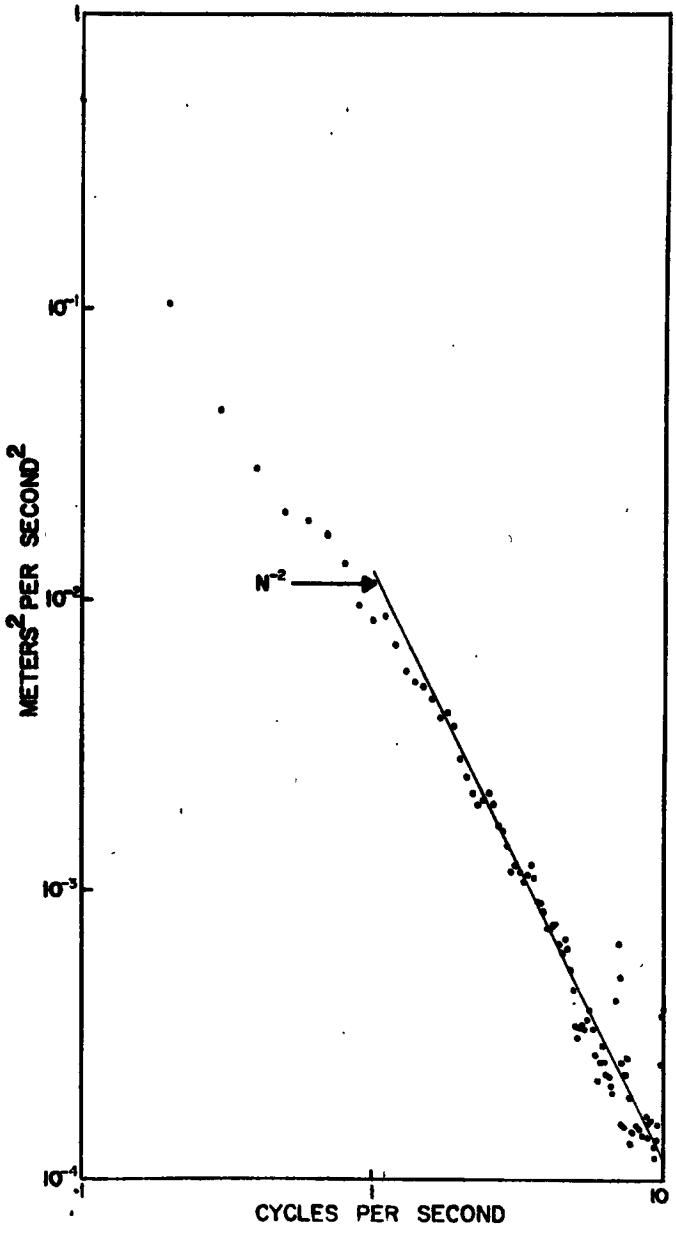

Figure 39. Double logarithmic spectrum of u.

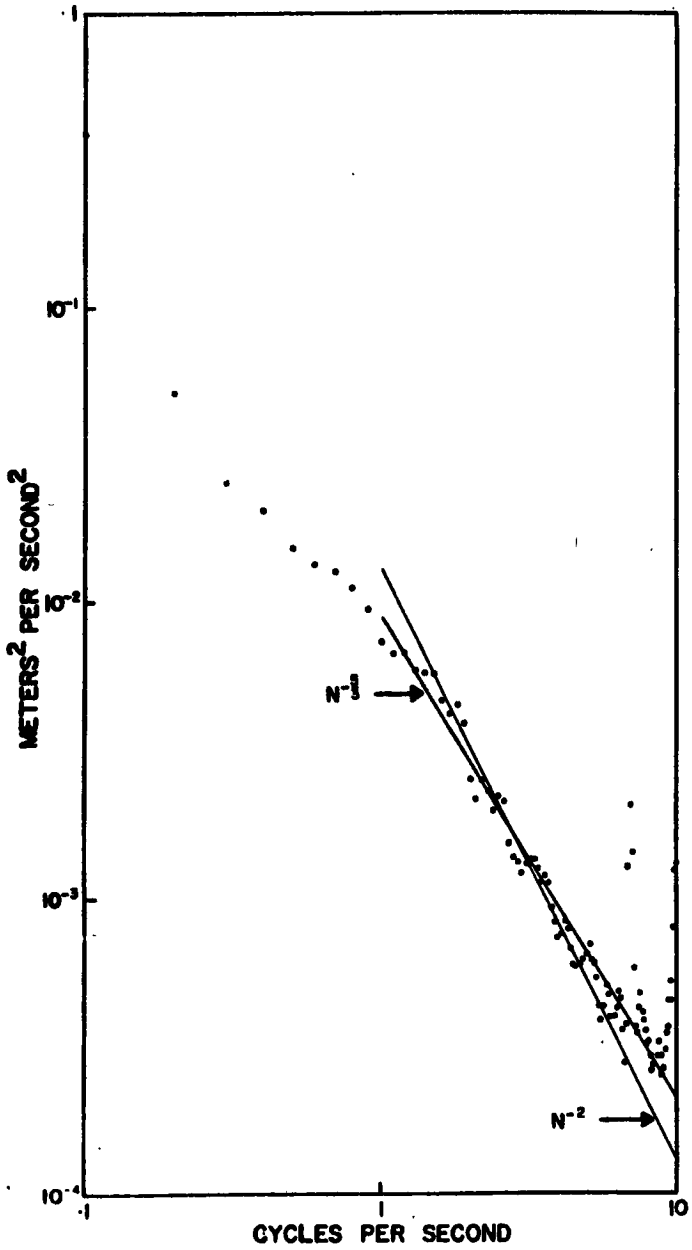

Figure 40. Double logarithmic spectrum of v.

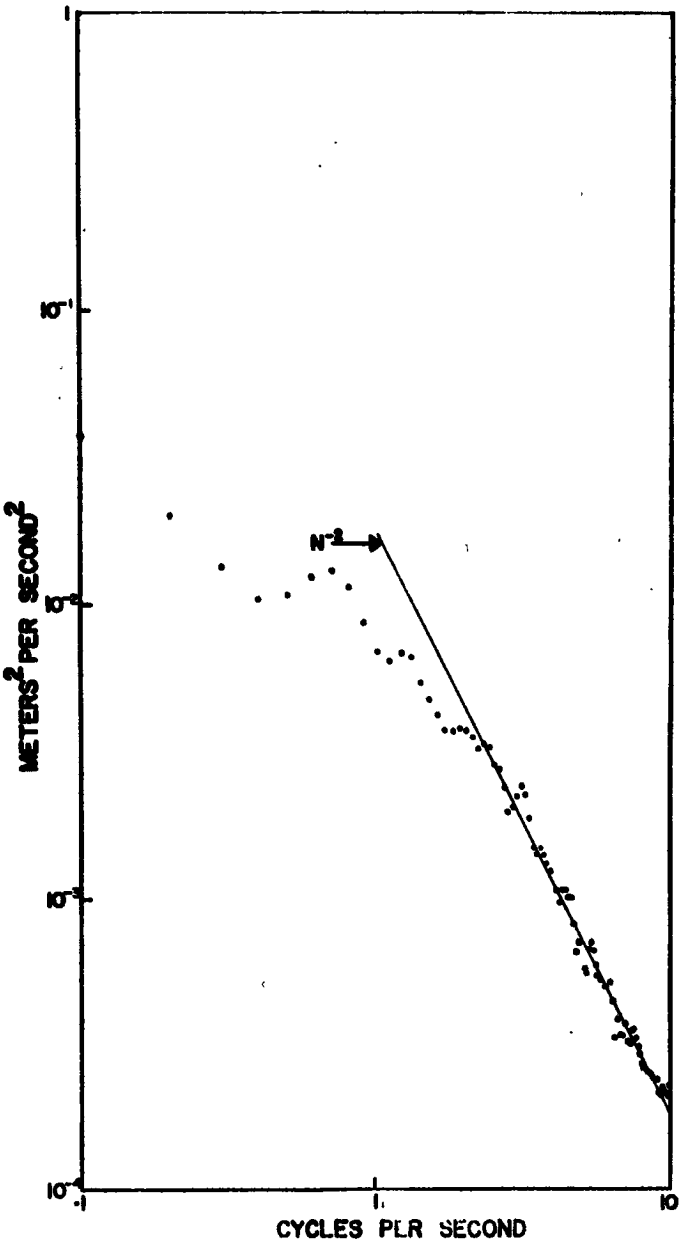

Figure 41. Double logarithmic spectrum of w.

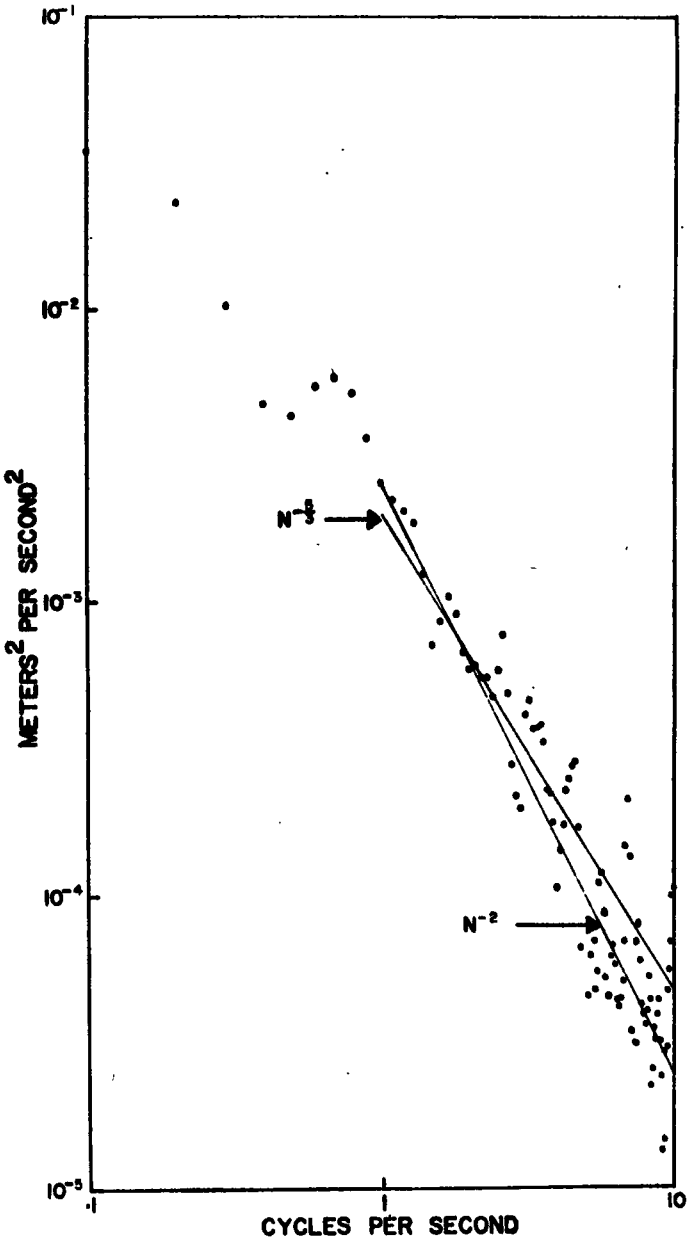

Figure 42. Double logarithmic cospectrum of u and w.

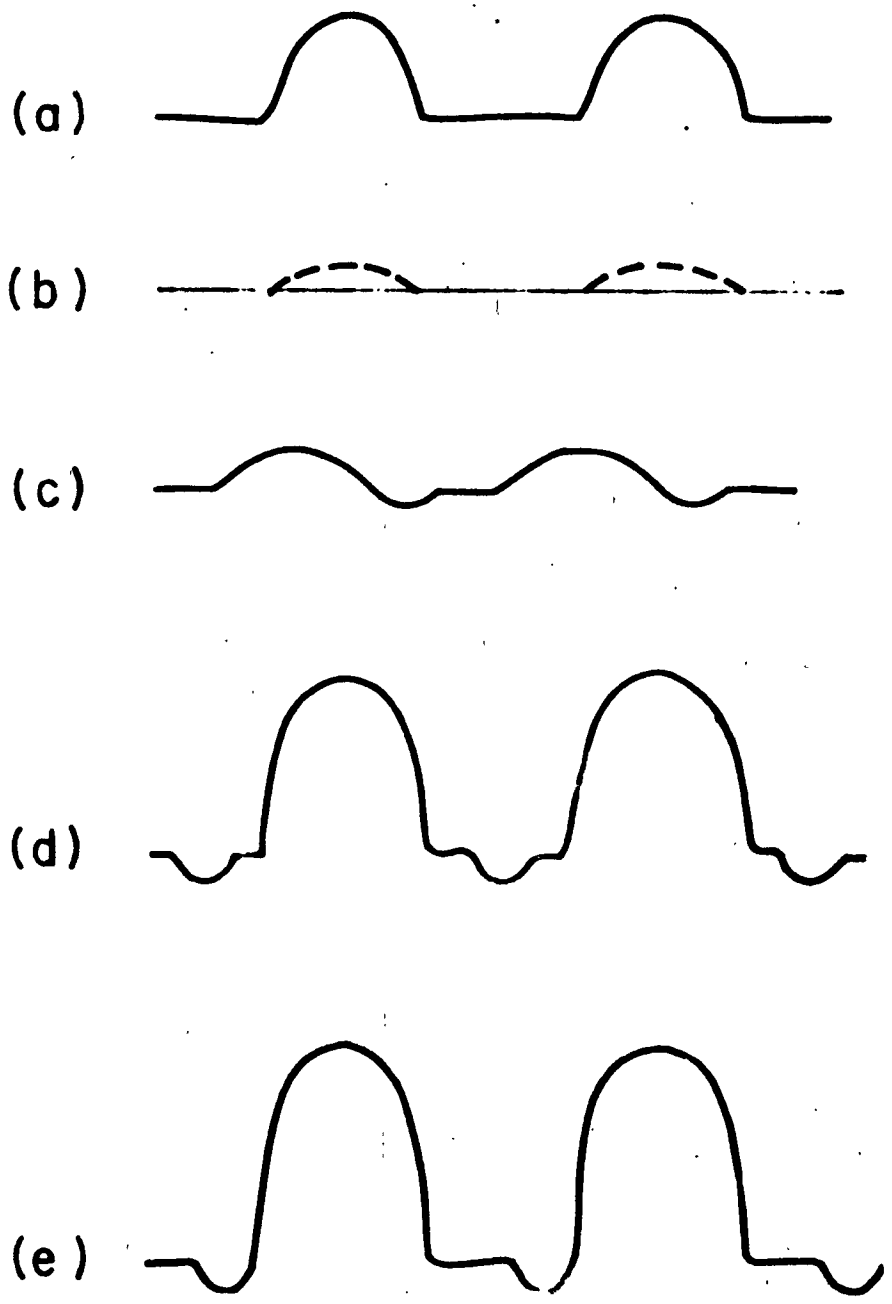

Figure 43. Wave forms observed on CRO at various steps in phase matching (see text, Appendix II).